



**Universidad de Valladolid**



**ESCUELA DE INGENIERÍAS  
INDUSTRIALES**

**UNIVERSIDAD DE VALLADOLID  
ESCUELA DE INGENIERÍAS INDUSTRIALES**

**Máster en Ingeniería Industrial**

**NUMERICAL SIMULATION OF  
RADIATION AND CONDUCTION  
HEAT TRANSFER IN A  
PARTICLE LADEN AREA**

**Autor:**

**Muñoz Mínguez, Marta**

**Responsable de Intercambio en la Uva:**

**Parra Santos, M<sup>o</sup> Teresa**

**Universidad de destino:**

**San Diego State University**

Valladolid, enero de 2018.

TFM REALIZADO EN PROGRAMA DE INTERCAMBIO

---

TÍTULO: Numerical Simulation of Radiation and Conduction Heat Transfer in a Particle Laden Area

ALUMNO: Marta Muñoz Mínguez

FECHA: 5 de diciembre de 2017

CENTRO: Universidad Estatal de San Diego, Departamento de Ingeniería Aeroespacial

TUTOR: Gustaaf B. Jacobs

## **RESUMEN**

Este TFM estudia el proceso transitorio del calentamiento de partículas en el interior de un Receptor de Partículas en Caída, una tecnología empleada para transformar la energía solar en electricidad.

La razón de ser de este TFM es el tamaño significativamente superior de estas partículas en comparación con las utilizadas en otros tipos de receptores solares, ya que puede afectar fuertemente al tiempo necesario para que las partículas alcancen las altas temperaturas deseadas.

El Método de los Elementos Finitos y el Método de Monte Carlo para el trazado de rayos se han utilizado para simular este proceso en un modelo bidimensional escrito en el programa MATLAB, donde la transferencia de calor mediante radiación y conducción se ha modelado minuciosamente.

Los resultados derivados de este estudio demuestran que, efectivamente, el tiempo necesario para que las partículas alcancen una alta temperatura no es trivial y merece una atención especial.

## **PALABRAS CLAVE**

Receptor de Partículas en Caída, Radiación, Conducción, Método de Monte Carlo, Método de los Elementos Finitos

## **ORIGINAL ABSTRACT**

This Thesis is a study of the transient heating process of the particles inside a Falling Particle Receiver, a technology used to transform the solar energy in electricity. The particles used in the Falling Particle Receivers are significantly bigger than the ones used in other solar receivers more common and studied in more depth, like the Small Particle Receivers. This important difference in particle size is the *raison d'être* of this Thesis, because it might strongly affect the time needed for the particles to reach the high temperatures desired.

The Finite Element Method and the Monte Carlo Ray Tracing Method have been used to simulate this process in a two-dimensional model written in the program MATLAB, where radiation and conduction heat transfer have been minutely modeled.

Throughout this Thesis, the governing equations of the process are explained, the model is firstly tested in simple problems with single particles, and secondly run in a set of particles located inside of the receiver.

The obtained results prove how, effectively, the time needed for the particles to reach high temperatures is not trivial, and they also show that it is very likely that recirculation of the particles is necessary in order to reach the desired temperatures.

## **KEY WORDS**

Falling Particle Receiver, Radiation, Conduction, Monte Carlo Ray Tracing Method, Finite Element Method



---

**NUMERICAL SIMULATION OF  
RADIATION AND CONDUCTION HEAT TRANSFER  
IN A PARTICLE LADEN AREA**

---

Author: Marta Muñoz Mínguez

Advisor: Dr. Gustaaf B. Jacobs

Máster en Ingeniería Industrial

Universidad de Valladolid

San Diego, December of 2017

## ABSTRACT

### NUMERICAL SIMULATION OF RADIATION AND CONDUCTION HEAT TRANSFER IN A PARTICLE LADEN AREA

Marta Muñoz Mínguez  
Universidad de Valladolid  
December of 2017

This Thesis is a study of the transient heating process of the particles inside a Falling Particle Receiver, a technology used to transform the solar energy in electricity. The particles used in the Falling Particle Receivers are significantly bigger than the ones used in other solar receivers more common and studied in more depth, like the Small Particle Receivers. This important difference in particle size is the *raison d'être* of this Thesis, because it might strongly affect the time needed for the particles to reach the high temperatures desired.

The Finite Element Method and the Monte Carlo Ray Tracing Method have been used to simulate this process in a two dimensional model written in the program MATLAB, where radiation and conduction heat transfer have been minutely modeled.

Throughout this Thesis, the governing equations of the process are explained, the model is firstly tested in simple problems with single particles, and secondly run in a set of particles located inside of the receiver.

The obtained results prove how, effectively, the time needed for the particles to reach high temperatures is not trivial. They also show that it is very likely that recirculation of the particles is necessary in order to reach the desired temperatures.

## **ACKNOWLEDGEMENTS**

To my parents, for all their help, support and effort, that has allowed me to live a very unique and especial experience in the city of San Diego.

I would also like to express my gratitude towards my advisor in San Diego State University Dr. Gustaaf B. Jacobs, without whose constant help and advice I would not have been able to complete this work, and towards Dr. Fletcher Miller for his help and input regarding the radiation phenomena.

## TABLE OF CONTENTS

	Page
ABSTRACT .....	ii
ACKNOWLEDGEMENTS .....	ii
LIST OF TABLES .....	vi
LIST OF FIGURES .....	vii
CHAPTER	
<b>1 Introduction</b> .....	1
<b>2 Governing Equations</b> .....	7
2.1 Radiation Heat Transfer .....	7
2.2 Conduction Heat Transfer .....	10
2.2.1 Initial and Boundary Conditions .....	11
<b>3 Numerical Methods</b> .....	12
3.1 The Monte Carlo Ray Tracing Method .....	12
3.1.1 Modeling of the solar rays .....	12
3.1.2 Modeling of the emitted rays .....	14
3.2 The Finite Element Method for Heat Conduction .....	15
3.2.1 Grid Refinement .....	19
<b>4 Numerical Model</b> .....	21
4.1 Single particle .....	21
4.1.1 Initial and Boundary conditions .....	22
4.1.2 Analytic solution .....	22
4.1.3 Grid Refinement study .....	23
4.1.4 Numerical solution .....	28
4.1.5 Emission from the particle. Steady-state .....	29
4.1.6 Solar rays simulation .....	30
4.2 Multiple particles .....	32
4.2.1 Generation of the particles .....	32
4.2.2 Generation of the rays .....	33



4.2.3 Simulations .....	33
<b>5 Results and Conclusions</b> .....	40
<b>6 Future Work</b> .....	41
<b>BIBLIOGRAPHY</b> .....	42
<b>APPENDIX</b>	
A - Manual of the code .....	45
B - Main script of the MATLAB code .....	75
.....	

**LIST OF TABLES**

	Page
4.1 Comparison of the characteristics of the three candidate grids. ....	23
4.2 Comparison of the characteristics of the four candidate grids. ....	25
4.3 Comparison of the characteristics of the five candidate grids. ....	26

## LIST OF FIGURES

		Page
1.1	Schemes of different CSP technologies [1] .....	2
1.2	Scheme of a Free-Falling Particle Receiver [2].....	3
1.3	Comparison of particle sizes in SPR and FPR .....	5
2.1	Part of the electromagnetic spectrum that reaches the surface of the Earth [3] .....	7
2.2	Different types of reflection [4] .....	8
2.3	Schematic representation of a two band model, with bands defined by their wavelength.....	10
3.1	Heat flux in the simulated solar rays .....	13
3.2	Scheme of the reflections of a ray along its path .....	13
3.3	Scheme of the absorption of a ray .....	14
3.4	Scheme of the path of an emitted ray .....	15
3.5	Schemes to approximate a derivative.....	18
4.1	Parameters that define the location a particle. ....	21
4.2	Scheme of the distance between the contour and the center of a particle. ....	22
4.3	Graphic representation of grids 1, 2 and 3. ....	24
4.4	Graphic representation of temperature vs. radius through the particle in grids 1, 2 and 3. ....	24
4.5	Graphic representation of grids 1, 2 and 3. ....	25
4.6	Graphic representation of temperature vs. radius through the particle in grids 1, 2, 3 and 4.....	26
4.7	Graphic representation of grids 1, 2, 3, 4 and 5. ....	27
4.8	Graphic representation of temperature vs. radius through the particle in grids 1, 2, 3, 4 and 5.....	27
4.9	Evolution of heat transfer in grid 5. ....	29
4.10	Evolution of the temperature in one particle. ....	30
4.11	Evolution of the temperature in one particle with a different number rays. ....	32
4.12	Generation of particles inside the receiver with a different void ratio. ....	33
4.13	Location of the particles of study. ....	34

4.14	Close look of the area of study.....	35
4.15	Location of the particles in Simulation 1 .....	35
4.16	Temporal evolution of the average temperature of the particles .....	36
4.17	Location of the particles in Simulation 2 .....	37
4.18	Temporal evolution of the average temperature of the particles .....	37
4.19	Location of the particles in Simulation 3 .....	38
4.20	Temporal evolution of the average temperature of the particles .....	39
A.1	Example of plotted Figures 1 and 2. ....	50
A.2	Choice of the point of reflection of a ray. ....	51
A.3	Angle $\alpha$ from the reflection point.....	51
A.4	Random angle $\gamma$ . ....	52
A.5	Example of a destination point after a reflection that would be too close to the particle. ....	52
A.6	Destination point after a reflection. ....	53
A.7	Area where rays are generated. ....	64
A.8	Graphical example of the two intersection points between a ray and a particle. ....	65

## CHAPTER 1

### Introduction

In the last decades, the concern of the society for the planet's sustainability and energy resources has increased noticeably. The environmental considerations together with the growing dependency on energy have led to an urgent global need for clean and renewable energy sources. The main challenge in the development of the renewable energy technologies is its cost, which currently is not competitive with the cost of fossil fuels. Cooperation between political, economic and scientific institutions is fundamental to guarantee the healthy sustainability of mankind.

Sunlight is a major source of energy and it holds the greatest potential to meet the energy demand of the world. The total annual solar energy input into the Earth is more than 15000 times greater than the current yearly use of fossil and nuclear fuels [5]. If only a 0.1% of this solar energy was converted at an efficiency of a 10%, the electricity obtained would be four times the world's electricity generating capacity in 2013 (about 5000GW) [6].

Solar energy can currently be harnessed with two different technologies: *solar photovoltaic* and *solar thermal* technologies. *Solar photovoltaic* technologies directly transform sunlight into electricity in photovoltaic cells and are only effective during daytime, while *solar thermal* technologies concentrate sunlight to obtain heat. If said heat is directly used, the technologies are known as *active* or *passive* solar heating, and if it is indirectly used to generate electric power, the technology is known as *concentrating solar power (CSP)*. This last technology uses solar energy collectors to reach temperatures high enough to drive steam turbines that generate the mechanical work necessary to run a generator and produce electricity [5]. There are three different CSP technologies, primarily separated by their scale and operating temperatures, including *line-concentrating systems* (parabolic troughs and linear Fresnel systems), *dish concentrating systems* and *central tower systems*, also known as *solar power towers (SPT)* [7, 8]. A scheme of these different technologies is shown in Figure 1.1.

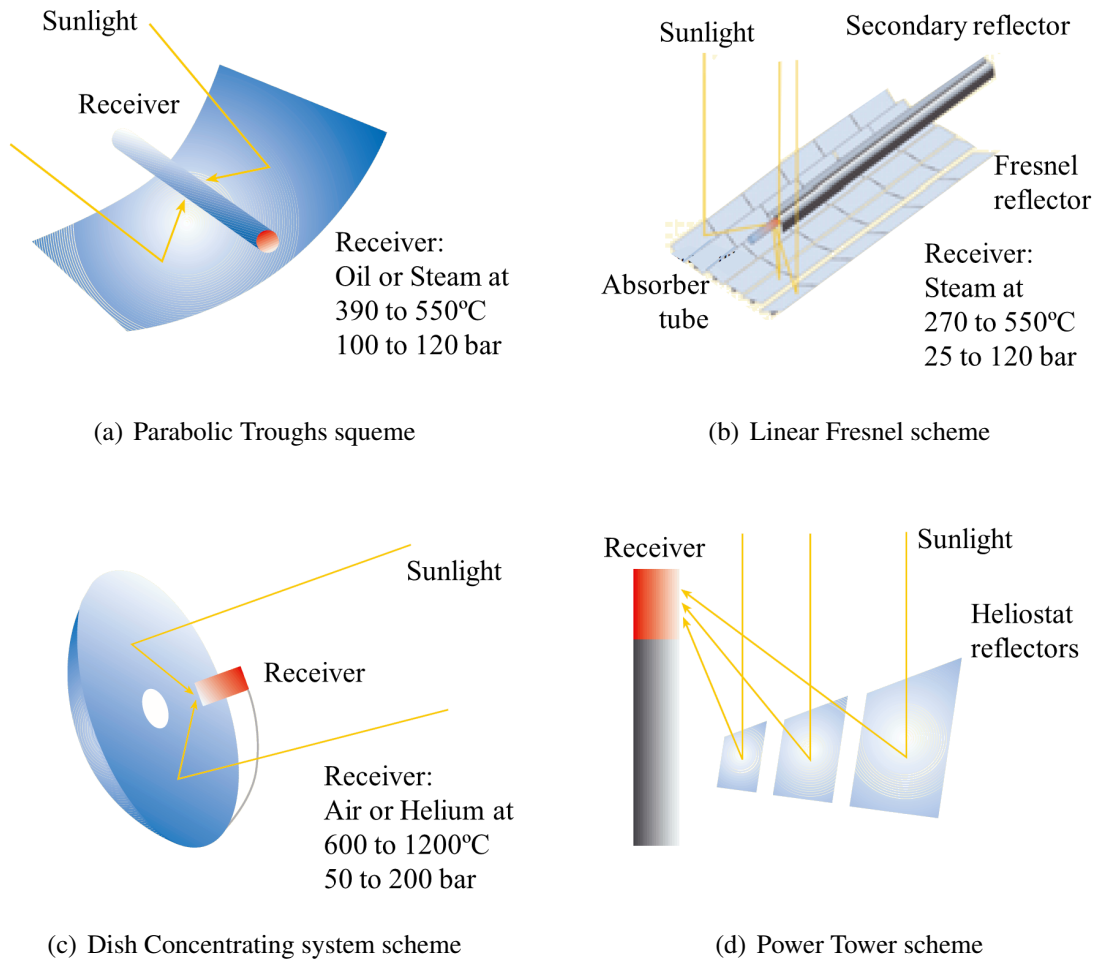


Figure 1.1: Schemes of different CSP technologies [1]

*SPT* systems use a field of distributed heliostats that individually track the sun and focus the sunlight onto a central receiver, located in the centre of the heliostat field at the top of a large solar tower. The concentrated solar energy is absorbed in the central receiver by a working medium, that then is sent to storage or to a powercycle [9, 10]. The working medium needed to transport the stored energy can be a gas, a liquid, or be made up of solid particles [11]. There is a great variety of receiver architectures, that can be divided in three main groups based on how the radiation is absorbed and transferred to the working medium [8]: *tube absorption receivers*, *volumetric receivers* and *particle receivers*. Tube absorption receivers use dark tubes to absorb solar energy and transfer it via convection to a working fluid inside, usually working with liquids such as molten salts; volumetric receivers have porous materials into which radiation penetrates and is absorbed, being air its most common working fluid; and particle receivers use dark solid particles to directly absorb sunlight.

There exist different types of particle receivers, such as Centrifugal Receivers or Falling Particle Receivers (FPR), and there are several different configurations for a FPR, being one of

them the Free-Falling Particle Receiver. A simplified scheme of this configuration is shown in Figure 1.2.

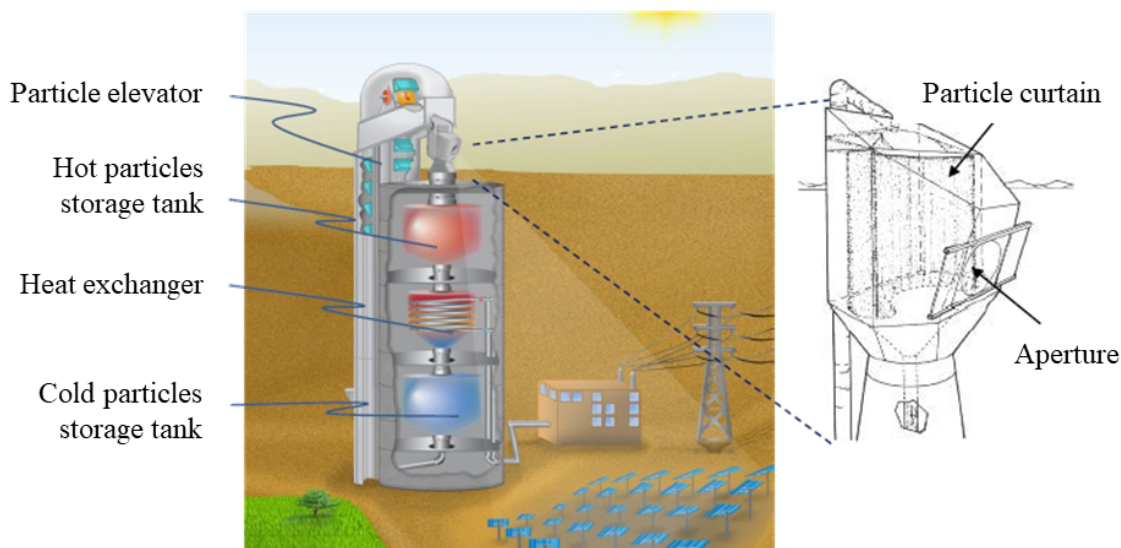


Figure 1.2: Schematic of a Free-Falling Particle Receiver [2]

The process works as follows:

- (1) Cold sand-size refractory particles fall down freely, forming a curtain after being released through a slot at the top of the receiver. There, the concentrated sunlight that comes in through a window directly irradiates them. The particles absorb part of this radiation, having a much a higher temperature by the time they exit the receiver.
- (2) These heated particles are stored in an insulated storage tank, called the “hot storage tank”.
- (3) Then they run through a heat exchanger to heat the working fluid for the power cycle [11, 12], serving as both the heat transfer fluid and thermal storage media.
- (4) The cooled particles fall into the “cold storage tank”.
- (5) Finally, the particles are brought back up by an elevator to the top receiver, and the process repeats.

The main advantages of the FPR compared to other CSP technologies are the reach of operational temperatures over of  $1000^{\circ}\text{C}$ , a higher receiver efficiency, a storage media that is chemically benign and low-cost and a reduction on the thermal stress on the plant components. However, the overall efficiency is reduced by convection heat transfer through the open aperture and by heat loss from the particles to the air [13].

Modeling CSP receivers is not an easy task. The developed models are usually specific to a concrete architecture and application, since the radiation fluxes and related heat transfer are different in every case. As the geometry of the receiver becomes more complicated, modeling the radiation between surfaces gets more complicated as well.

Simulations and experiments regarding the FPR were already done in the 1980s, mostly by Sandia National Laboratories. One of the reasons why the free-falling PR was proposed as an alternative to harness solar energy was the study made by Falcone et al. in 1985 [14], where he studied the costs of the Solid Particle Receiver (SPR) in comparison with other air receiver concepts for high-temperature applications. In 1986, Stahl and Griffin focused on identifying appropriate particle materials (Stahl and Griffin, 1986 [15]). Investigations carried out by Hruby [16] were focused on the receiver design and the particle materials, while computational models were created to simulate the receiver operation and the temperature of the particles [17, 18]. In 1988, Hruby et al. [19] developed further work in the study of flow characteristics and convective heat transfer in a falling particle curtain. In 1999, Meier [13] performed 2D CFD simulations of a chemical FPR, to study the performance of a FPR in a pilot plant, using the Monte Carlo method to model the heating of the particles by radiation. His model contemplated radiation from the gas to and from the particles but did not consider the change in the radiation field as a response to the absorption by or emission from the particles. Meier's results were extended to 3D by Chen et al. in 2007 [20], to help in the design of a prototype receiver by Sandia National Laboratories. Also in 2007, Chen et al. [21] developed a CFD model in FLUENT where a solar ray-tracing algorithm was used to predict the solar illumination energy on the walls of different receiver designs. The heating of the particles considered re-radiation from the walls, but not the direct irradiation from the heliostats.

In the following years, several FPR prototypes were built in order to gather information about distribution of particles velocity, curtain thickness, curtain opacity... and other properties, and to experimentally validate new simulation codes. In 2008, a prototype SPR was designed and tested on-sun at Sandia National Laboratories [22], and Ho et al. [23] developed a CFD model to try on it. They simulated the solar irradiation and heat transfer with a discrete-ordinates radiation model in FLUENT, without performing any ray tracing. Their model solved the radiative transfer equation (RTE) over a domain of discrete solid angles, transforming it into as many transport equations as there are solid angles. In 2009, Kim et al. [24] validated the experimental results from a prototype with the computational results of a 2D MFIX simulation model. Their work was mainly focused on particle velocity, curtain thickness and transparency, but neglected the heat transfer to the particles. In 2010, Khalsa [25] developed a program in Microsoft Excel VBA that also used the discrete-ordinates method for the radiation model. His program characterized multiple beams emanating from a surface called the solar patch, defined at the center of the receiver aperture and divided into subpatches, each of which represented irradiation from a unique section of the heliostat field. In 2011, Khalsa and Ho [26] developed a model that improved the treatment of the radiation given in [27] and [25], since it considered both the directional and spatial variability of the incoming radiance distribution. This method allowed to transform the incoming radiation from the heliostat field into a radiance boundary condition on the solid particle receiver aperture. In 2015, Wu et al. [28] developed a three-dimensional, steady-state numerical model of a centrifugal particle receiver. The cavity body was discretized with the Finite Element Method (FEM), and the discrete particles were not modeled. Instead, they considered that the receiver wall was fully covered by a single-layered, optically dense, and homogeneously moving particle film that was represented by a 1D fluid flow element.



These models focus on different aspects of a FPR: particle velocity, curtain opacity, solar irradiation... but they often do not simulate the particles themselves, but consider that the rays bounce randomly in the particle-laden area. Many models neglect the time it takes for heat transfer to happen inside the particles, considering that because of their small size, the heating process can be assumed to be instantaneous. That is only a realistic consideration when the size of the particles is similar or smaller than the wavelength of sunlight - from  $0.5 \mu m$  to  $2.5 \mu m$  approximately - which occurs, for example, in the Small Particle Receivers (SPR) that work with nanoparticles. Since the average diameter of the particles in the FPR is close to  $500 \mu m$ , the time it takes for a particle to reach the desired temperatures can be an important factor and should not be disregarded. Figure 1.3 shows a schematic comparison of the sizes of a SPR and a FPR.

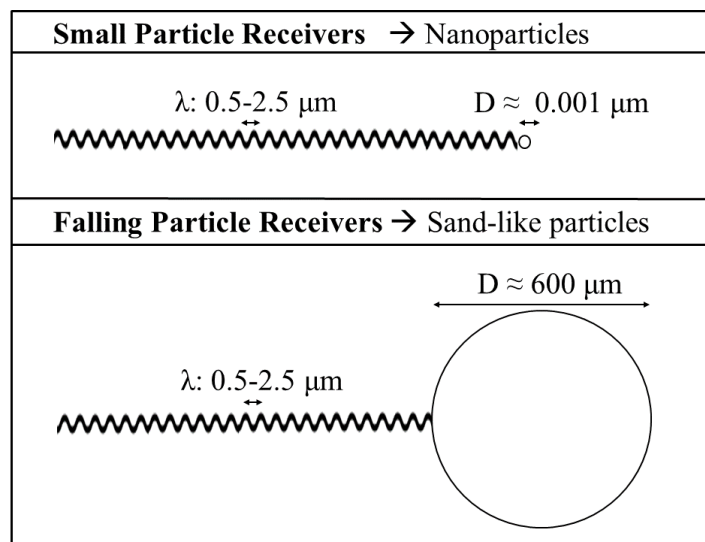


Figure 1.3: Comparison of particle sizes in SPR and FPR

In this Thesis, we simulate the interior of a FPR, using the Monte Carlo Ray Tracing Method to simulate the radiative energy and the Finite Element Method (FEM) to model the transient heat transfer in two-dimensional circular particles. Solar irradiation is modeled by a set of rays that come through the receiver window in random directions and circular two-dimensional bodies of different sizes are generated in random positions inside the receiver, in order to simulate a small sample of falling particles. The rays are partially absorbed and reflected by the particles located in their path or by the receiver walls, bouncing in random directions until their energy is negligible or until they go out through the window. Absorption, reflection and emission from the particles is minutely simulated. Every time a ray reaches a particle a Neumann boundary condition is implemented in it, that depends on the energy of the ray in that instant and the properties of the particle material. The radiative energy emitted by the particles is also simulated by a set of rays, that act in the same way as the solar rays. However, the gas-particle interaction is neglected and the gas and particle flows are not considered. The program has been implemented in MATLAB and tested in a single particle initially, and run in multiple particles secondly to imitate the functioning of a set of particles.

Chapter 2 of this Thesis introduces the governing equations of radiation and conduction of the process. Chapter 3 presents the numerical methods used, which are a Monte Carlo ray tracing method for the solar irradiation and emission from the particles, and the Finite Element Method (FEM) for the heat transfer through the particles. Chapter 4 introduces the numerical model developed, applied to simple cases of study and to the complete model. Chapter 5 presents the most important results and the corresponding conclusions. Finally in Chapter 6, propositions of future work in this model are presented. A detailed explanation of the computational model can be found on Appendix A, and the developed MATLAB code has been attached in Appendix B.

## CHAPTER 2

### Governing Equations

#### 2.1 Radiation Heat Transfer

Radiation Heat Transfer consists on the transfer of thermal energy by an electromagnetic wave. The electromagnetic radiation spectrum ranges from cosmic rays with wavelengths smaller than  $10^{-8}\mu\text{m}$  to radio waves with wavelengths up to  $10^{10}\mu\text{m}$ , where thermal radiation occupies the portion between  $10^{-1}\mu\text{m}$  and  $10^3\mu\text{m}$  that is detected as heat or light. Radiation Heat Transfer does not require a physical medium to take place, which is why sunlight can travel all the way from the Sun to the Earth. However, the Earth's atmosphere acts as a filter and only a fraction of the spectrum reaches the surface. As stated in Chapter 1, the part of the thermal radiation that does has a wavelength approximately between  $0.5$  and  $2.5\mu\text{m}$ , as can be seen in Figure 2.1.

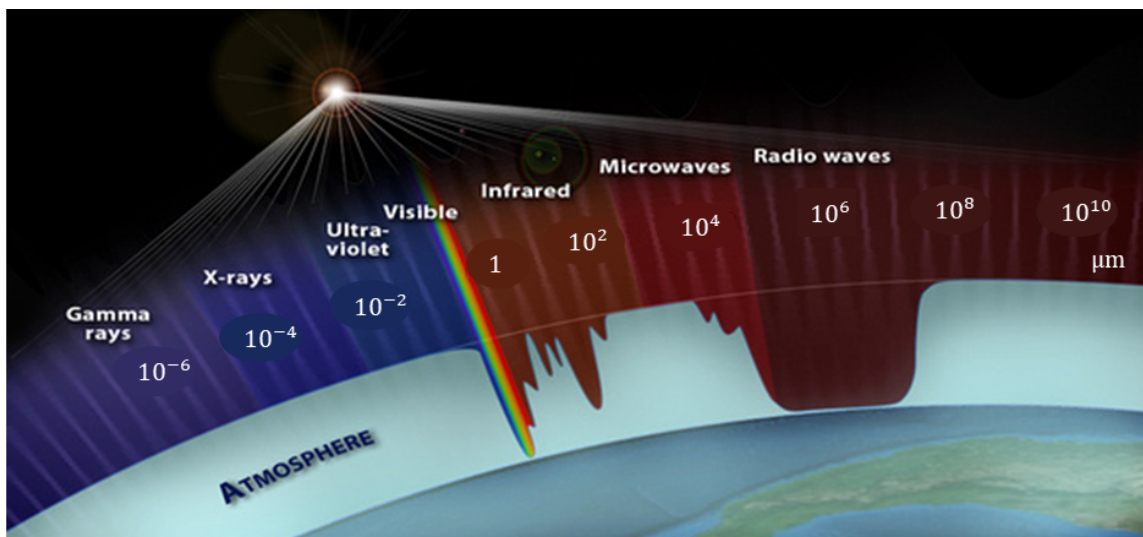


Figure 2.1: Part of the electromagnetic spectrum that reaches the surface of the Earth [3]

When radiation incides on the surface of a body, different phenomena can occur: *reflection*, if all or part of the energy is reflected by the surface, *absorption*, if all or part of the energy penetrates the body and is absorbed by it, or *transmission*, if all or part of the energy penetrates the body, is transmitted and emerges from it. If the medium is *opaque* (as are the particles in a FPR), all the radiation that penetrates into the medium is absorbed, and therefore transmission does not occur. The fraction of the incident energy that is reflected, absorbed or

transmitted by a surface is defined by its reflectivity  $\rho$ , absorptivity  $\alpha$  and transmissivity  $\tau$ , which are properties of the material and have a value between 0 and 1.

The reflectivity of a surface depends on the direction of the incident rays and on the direction of the reflected rays. In real surfaces, the reflected rays usually form an irregular shape, but modeling reflection this way is very complicated. Therefore, different assumptions are often made for simplification purposes. Surfaces can be classified as smooth or rough depending their smoothness, which is defined relatively to the wavelength of the incident radiation. If the height of the surface roughness is bigger than said wavelength, the surface is rough, and otherwise it is smooth. In rough surfaces reflection is assumed to be perfectly *diffuse*, being the radiation equally reflected in all directions, and in smooth surfaces it is considered to be *specular*, where the angles of incidence and reflection are equal. A schematic representation of these different types of reflection is shown in Figure 2.2.

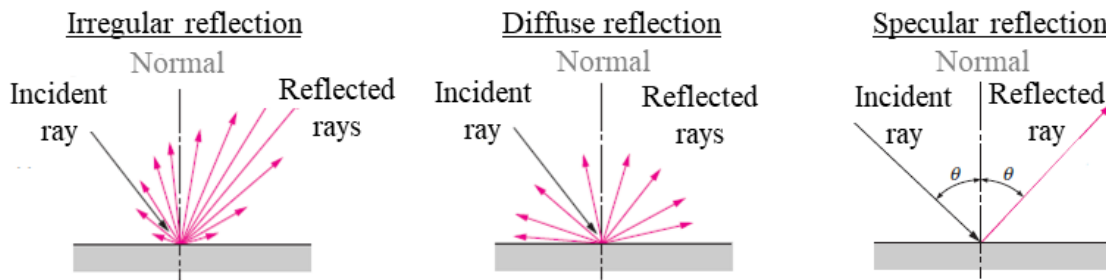


Figure 2.2: Different types of reflection [4]

Besides the three phenomena explained before, any body with a temperature higher than the absolute zero emits radiation, so the phenomenon of *emission* must also be taken into account when studying Radiative Heat Transfer. The wavelength of the emitted radiation is in the range of infrared or visible light depending on the body's absolute temperature.

In order to properly understand the study of Radiation Heat Transfer it is necessary to introduce the concept of a *black body*, which is a theoretical physical body that absorbs all the energy that it receives (perfect absorber), in every wavelength and from every direction, and emits more energy than any other body. The *Stefan-Boltzmann law* expresses the *total emissive power* ( $e_b$ ) of a *black body* as

$$e_b = \int_0^{\infty} e_{b\lambda} d\lambda = \sigma T^4, \quad (2.1)$$

where  $e_{b\lambda}$  is the emissive power of the black body at a specific wavelength  $\lambda$  in  $\frac{W}{m^2}$ ,  $\sigma$  is Stefan-Boltzmann constant ( $\sigma = 5.6704 \cdot 10^8 \frac{W}{m^2 K^4}$ ) and  $T$  is the absolute temperature of the body in  $K$ . The emissive power of a real surface is expressed as a fraction of the blackbody emissive power as

$$e_\lambda = \epsilon_\lambda e_b, \quad (2.2)$$

being  $\epsilon_\lambda$  the monochromatic hemispherical emissivity of the surface. The emissivity of a body expresses how well it emits compared to a black body, and it depends on the radiation wavelength, and the surface material, temperature and roughness.

For simplifications purposes, in most engineering applications it is assumed that emissivities of real surfaces are independent of the radiation wavelength. Bodies with this property are called *gray bodies*, and their emissive power is expressed as

$$e = \epsilon(T)e_b = \epsilon(T)\sigma T^4 . \quad (2.3)$$

If their emissivity is independent of temperature, then

$$e = \epsilon e_b = \epsilon \sigma T^4 . \quad (2.4)$$

Real bodies can absorb a fraction of the energy that they receive, determined by their *absorptivity* ( $\alpha$ ). According to *Kirchoff's law*, for a specific wavelength the monochromatic *absorptivity* ( $\alpha$ ) and *emissivity* ( $\epsilon$ ) of a surface at a given temperature are equal

$$\alpha_\lambda(T) = \epsilon_\lambda(T) . \quad (2.5)$$

For a *gray body* with properties independent of temperature, it is expressed as

$$\alpha = \epsilon . \quad (2.6)$$

The *reflectivity* ( $\rho$ ) of a surface is the portion of the incident energy that is reflected back. Considering that for an opaque medium the total energy is either absorbed or reflected, the *reflectivity* ( $\rho$ ) of a surface with properties independent of temperature can be expressed as

$$\rho = 1 - \alpha , \quad (2.7)$$

or, from Equation (2.6)

$$\rho = 1 - \epsilon . \quad (2.8)$$

An intermediate solution between the consideration of real or gray bodies is the use of a *multiband model*, where the spectrum is discretized into bands of finite width and it is assumed that radiation quantities are uniform in them. These bands are defined by radiation properties such as wavelength, frequency...

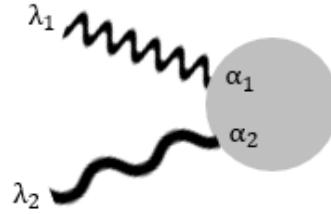


Figure 2.3: Schematic representation of a two band model, with bands defined by their wavelength

## 2.2 Conduction Heat Transfer

Fourier's law describes the conduction of thermal energy through a solid due to a temperature gradient. For an isotropic medium it takes the form

$$q = -k \frac{\partial T}{\partial n}, \quad (2.9)$$

where  $q$  is the rate of heat flow per unit area in the  $n$  direction,  $k$  is thermal conductivity and  $n$  is the normal direction, being the temperature gradient negative in the direction of positive heat flow. The law of conservation of energy for an isotropic 2D solid with temperature dependent on the thermal conductivity is

$$-\left( \frac{\partial q_x}{\partial x} + \frac{\partial q_y}{\partial y} \right) + Q = \rho C_p \frac{\partial T}{\partial t}, \quad (2.10)$$

where  $Q$ ,  $\rho$ ,  $C_p$  and  $t$  are the internal heat generation rate per unit volume, the density, the specific heat and the time, respectively.

The substitution of Equation (2.9) in Equation (2.10) leads to the heat conduction equation, which for an isotropic material with constant thermal properties, is expressed as

$$k \frac{\partial^2 T}{\partial x^2} + k \frac{\partial^2 T}{\partial y^2} + Q = \rho C_p \frac{\partial T}{\partial t}. \quad (2.11)$$

Dividing by  $k$  and regrouping  $\rho$ ,  $C_p$  and  $k$  in this manner  $\alpha = \frac{k}{\rho c_p}$ , the thermal diffusivity  $\alpha$  of the solid is obtained and, if the thermal properties are constant and there is no internal heat generation, the heat conduction equation is reduced to the diffusion equation

$$\frac{\partial^2 T}{\partial x^2} + \frac{\partial^2 T}{\partial y^2} = \frac{1}{\alpha} \frac{\partial T}{\partial t}. \quad (2.12)$$

### 2.2.1 Initial and Boundary Conditions

In order to solve Equation (2.12), an initial condition and several boundary conditions must be specified. The initial condition establishes the temperature of the solid at an initial time. In a two dimensional solid, it is expressed as

$$T = T_0(x, y) . \quad (2.13)$$

There are different kinds of boundary conditions, but the only kind of interest for the problem of study is the Neumann boundary condition, that specifies a heat flow across a boundary. It takes the form

$$-k \frac{\partial T}{\partial n} = q_n , \quad (2.14)$$

where  $q_n$  is the rate of the surface heat flow per area.

## CHAPTER 3

### Numerical Methods

#### 3.1 The Monte Carlo Ray Tracing Method

A Monte Carlo Ray Tracing Method (MCRTM) has been developed to simulate the rays inside the receiver of the FPR. Instead of directly solving the Radiative Transfer Equation (RTE), the MCRT methods use a statistical approach to model the phenomena involved in the radiation heat transfer. The MCRT method used in this Thesis traces a statistically significant number of rays that simulate the behaviour of sunlight along their path inside the receiver: from their beginning in the window until their remaining energy is negligible or they are reflected back outside the window, considering their interaction with the particles (absorption and reflection) and the back wall (reflection). Following the path of a single ray does not give any significant information; it is the information obtained after the simulation of a large number of rays what gives a real idea of the way the Radiation Heat Transfer works. Thereby, after a great number of simulations, reliable estimations of the parameters involved in the process are obtained. One of the downsides of this method is that, due to its statistical nature, in order to obtain accurate results a large number of rays must be simulated, which usually results in large computation time [29].

##### 3.1.1 Modeling of the solar rays

The total energy transmitted to the interior of the receiver can be estimated as the heat flux  $q$  that reaches the window times the length  $l$  of the window section studied. In two dimensions:

$$Q_{total}(W) = q \left( \frac{W}{m} \right) \cdot l(m) . \quad (3.1)$$

This energy is then divided by the number of simulated rays, being the results more realistic when more rays are modeled.

$$Q_{ray}(W) = \frac{Q_{total}(W)}{n_{rays}} \quad (3.2)$$

Figure 3.1 squematizes this process.



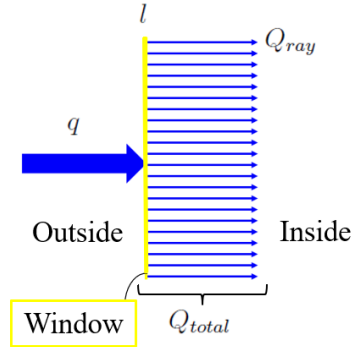


Figure 3.1: Heat flux in the simulated solar rays

The path of the rays is considered to start in the window, from where they follow a random direction (generated by a Random Number Generator (RNG)) inside the receiver, being reflected on the particles in random directions if they are located in their established path, or in the back wall otherwise. When a particle is hit by a ray, it absorbs a percentage of its energy, defined by the particle's material absorptivity  $\alpha$

$$Q_{absorbed} = Q_{incident} \cdot \alpha, \quad (3.3)$$

and the remaining energy  $Q_{reflected} = Q_{incident} \cdot (1 - \alpha)$  is redirected in a random direction and might hit other particles on its way. If the ray hits the back wall of the receiver, it is reflected in a random direction and it is considered that none of its energy is absorbed. The ray will continue being reflected, and its energy being absorbed by the particles until its path leads it to leave the receiver through the window. Along the path of a ray, a counter  $n$  stores the number of times that it has been reflected on any particle, as can be seen in Figure 3.2

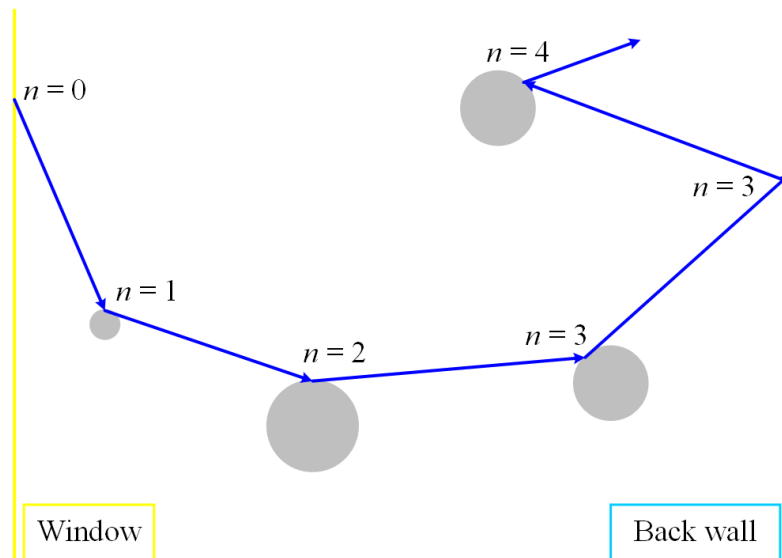


Figure 3.2: Scheme of the reflections of a ray along its path

This value of  $n$  allows to know the ray's energy at any moment. It depends on its initial energy, on  $n$ , and on the absorptivity of the particles  $\alpha$ , and can be calculated as

$$Q_{ray} = Q_{initial} \cdot (1 - \alpha)^n . \quad (3.4)$$

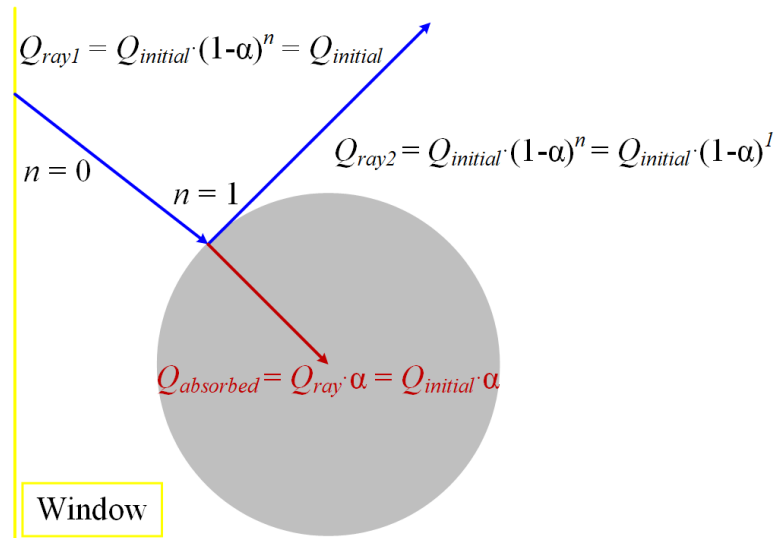


Figure 3.3: Scheme of the absorption of a ray

### 3.1.2 Modeling of the emitted rays

The particles emit an amount of energy that depends on their absolute temperature, following the Stefan-Boltzmann law for a gray body (Equation (2.4)). This energy is also emitted in the form of rays and modeled by straight lines that, as the solar rays do, follow a path that changes its direction when they are reflected and partially absorbed by the particles they find on their way or by the walls, until they are almost completely absorbed or go out the window.

The percentage of the energy emitted by a particle that is absorbed by another particle depends on the emissivity  $\epsilon$  of the particle that absorbs it, being

$$Q_{absorbed} = Q_{incident} \cdot \epsilon, \quad (3.5)$$

as can be seen in the following scheme

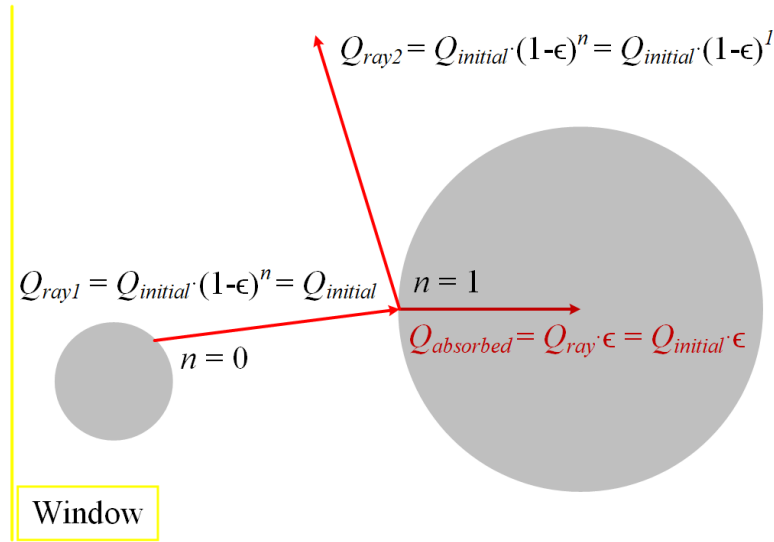


Figure 3.4: Scheme of the path of an emitted ray

The energy of a ray in any instant can therefore be calculated as

$$Q_{ray} = Q_{initial} \cdot (1 - \epsilon)^n . \quad (3.6)$$

### 3.2 The Finite Element Method for Heat Conduction

Discretization methods are commonly used to approximate the PDEs with numerical model equations, which are solved with numerical methods. One of them is the FEM, which divides the domain of study into  $E$  elements of  $n$  nodes each, being the analytical solution for the temperature approximated by a numerical solution ( $\mathbf{T} \approx T$ ). When applied to a two dimensional transient Heat Conduction problem, the temperature and temperature gradients for each element can be estimated as

$$T^{(e)}(x, y, t) = \sum_{i=1}^n N_i(x, y)T_i(t) , \quad (3.7)$$

$$\frac{\partial T^{(e)}}{\partial x}(x, y, t) = \sum_{i=1}^n \frac{\partial N_i}{\partial x}(x, y)T_i(t) \text{ and} \quad (3.8)$$

$$\frac{\partial T^{(e)}}{\partial y}(x, y, t) = \sum_{i=1}^n \frac{\partial N_i}{\partial y}(x, y)T_i(t) , \quad (3.9)$$

being  $T_i(t)$  and  $N_i(x, y)$  the value of the temperature and the interpolation function at each node, respectively. In matrix notation

$$T^{(e)}(x, y, t) = [N(x, y)]\{T(t)\}, \quad (3.10)$$

$$\begin{Bmatrix} \frac{\partial T^{(e)}}{\partial x}(x, y, t) \\ \frac{\partial T^{(e)}}{\partial y}(x, y, t) \end{Bmatrix} = [B(x, y)]\{T(t)\},$$

being

$$[N(x, y)] = [N_1 N_2 \dots N_n], \quad (3.11)$$

$$[B(x, y)] = \begin{bmatrix} \frac{\partial N_1}{\partial x} & \frac{\partial N_2}{\partial x} & \dots & \frac{\partial N_n}{\partial x} \\ \frac{\partial N_1}{\partial y} & \frac{\partial N_2}{\partial y} & \dots & \frac{\partial N_n}{\partial y} \end{bmatrix}, \quad (3.12)$$

$\{T(t)\}$  the vector of the elements nodal temperature,  $[N]$  the temperature interpolation matrix and  $[B]$  the temperature gradients interpolation matrix.

The element equations are derived using Galerkin's Weighted Residual Method, that minimizes the residual with the interpolation function.

Equation (2.12) governs heat conduction in the problem of study, and can be rewritten as

$$\frac{\partial}{\partial x} \left( k \frac{\partial T}{\partial x} \right) + \frac{\partial}{\partial y} \left( k \frac{\partial T}{\partial y} \right) - \rho C_p \frac{\partial T}{\partial t} = 0, \quad (3.13)$$

with initial and boundary conditions

$$T = T_0(x, y) \quad \text{in } \Omega, \quad t = 0 \quad (3.14)$$

$$k \frac{\partial T}{\partial x} n_x + k \frac{\partial T}{\partial y} n_y = q \quad \text{on } S_1. \quad (3.15)$$

To derive the element equations from Equations (3.13), (3.14) and (3.15), the approximate behaviour of the temperature within each element must be expressed as in Equation (3.7). Now *Galerkin's Weighted Residual Method* is applied in order to minimize the residual with the interpolation function:

$$\iint_{\Omega^{(e)}} N_i \left[ \frac{\partial}{\partial x} \left( k \frac{\partial T^{(e)}}{\partial x} \right) + \frac{\partial}{\partial y} \left( k \frac{\partial T^{(e)}}{\partial y} \right) - \rho C_p \frac{\partial T^{(e)}}{\partial t} \right] dx dy = 0. \quad (3.16)$$

To reduce the order of the derivatives and introduce the influence of the natural boundary conditions, the previous equation is integrated by parts. Focusing the attention on its first two terms, and according to

$$\int_a^b u dv = uv \Big|_a^b - \int_a^b v du, \quad (3.17)$$

where  $u = N_i$  and  $v = k \frac{\partial T^{(e)}}{\partial x} \hat{i} + k \frac{\partial T^{(e)}}{\partial y} \hat{j}$ .

The obtained result is the *symmetric weak form*

$$\begin{aligned}
 & - \iint_{\Omega^{(e)}} \left( k \frac{\partial T^{(e)}}{\partial x} \frac{\partial N_i}{\partial x} + k \frac{\partial T^{(e)}}{\partial y} \frac{\partial N_i}{\partial y} \right) dx dy - \int_{\Omega^{(e)}} N_i \rho C_p \frac{\partial T^{(e)}}{\partial t} dx dy + \\
 & \int_{S_1^{(e)}} \left( k \frac{\partial T^{(e)}}{\partial x} n_x + k \frac{\partial T^{(e)}}{\partial y} n_y \right) N_i d\Gamma = 0.
 \end{aligned} \tag{3.18}$$

The surface integral in the previous equation introduces the natural boundary conditions of Equation (3.15) for the elements on the boundary of  $\Omega$

$$k \frac{\partial T^{(e)}}{\partial x} n_x + k \frac{\partial T^{(e)}}{\partial y} n_y = q^{(e)}. \tag{3.19}$$

Substituting Equations (3.7), (3.8) and (3.9), the result takes the form

$$[K]^{(e)} \{T\}^{(e)} + [M]^{(e)} \left\{ \frac{dT}{dt} \right\}^{(e)} = \{q\}^{(e)}, \tag{3.20}$$

being

$$\begin{aligned}
 K_{ij} &= \iint_{\Omega^{(e)}} \left( k \frac{\partial N_i}{\partial x} \frac{\partial N_j}{\partial x} + k \frac{\partial N_i}{\partial y} \frac{\partial N_j}{\partial y} \right) dx dy, \\
 M_{ij} &= \int_{\Omega^{(e)}} \rho C_p N_i N_j dx dy \text{ and} \\
 q_i &= \int_{S_1^{(e)}} q N_i d\Gamma.
 \end{aligned}$$

Globally, the equation becomes

$$[K] \{T\} + [M] \left\{ \frac{dT}{dt} \right\} = \{q\}, \tag{3.21}$$

where  $[K_c]$ ,  $[M]$  and  $\{q\}$  are the global conductivity matrix, the global mass matrix and the heat flux stated by the Neumann boundary conditions [30].

Equation (3.21) can be solved with different resolution schemes, that differ in the way they approximate the value of the derivatives. The first derivative at a point in a curve  $\phi(x)$  is the slope of the tangent line to the function at that specific point, and it can be expressed as

$$\left( \frac{\partial \phi}{\partial x} \right)_{x_i} = \lim_{\Delta x \rightarrow 0} \frac{\phi(x_i + \Delta x) - \phi(x_i)}{\Delta x}. \tag{3.22}$$

Its value can be approximated by the slope of a line that passes through two nearby points on the curve. Depending on which these two points are, there are different resolution schemes: the explicit or forward difference solution if the two points are  $x_i$  and  $x_i + \Delta x$ , the implicit or backward difference solution when the points are  $x_i - \Delta x$  and  $x_i$ , the central difference solution when the two points lie on opposite sides of  $x_i$ ... and many other types. Figure 3.5 shows a graphic example of these schemes.

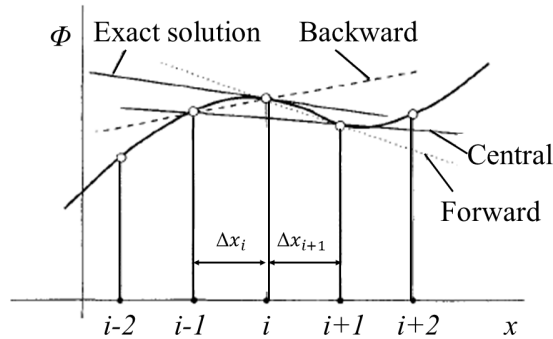


Figure 3.5: Schemes to approximate a derivative.

The approximation improves as the points get closer to each other, which is why grid refinement is an important step in numerical resolutions. Continuous differentiable functions  $\phi(x)$  can be expressed as a Taylor series in the proximity of  $x_i$  as

$$\begin{aligned} \phi(x) = & \phi(x_i) + (x - x_i) \left( \frac{\partial \phi}{\partial x} \right)_i + \frac{(x - x_i)^2}{2!} \left( \frac{\partial^2 \phi}{\partial x^2} \right)_i + \\ & \frac{(x - x_i)^3}{3!} \left( \frac{\partial^3 \phi}{\partial x^3} \right)_i + \dots + \frac{(x - x_i)^n}{n!} \left( \frac{\partial^n \phi}{\partial x^n} \right)_i + h.o.t., \end{aligned} \quad (3.23)$$

where *h.o.t.* stands for higher-order terms. Approximate expressions for the derivatives at point  $x_i$  can be obtained depending on the function values at the points nearby. For example, at  $x_{i+1}$ :

$$\left( \frac{\partial \phi}{\partial x} \right)_i = \frac{\phi_{i+1} - \phi_i}{x_{i+1} - x_i} - \frac{x_{i+1} - x_i}{2} \left( \frac{\partial^2 \phi}{\partial x^2} \right)_i - \frac{(x_{i+1} - x_i)^2}{6} \left( \frac{\partial^3 \phi}{\partial x^3} \right)_i + h.o.t., \quad (3.24)$$

at  $x_{i-1}$ :

$$\left( \frac{\partial \phi}{\partial x} \right)_i = \frac{\phi_i - \phi_{i-1}}{x_i - x_{i-1}} + \frac{x_i - x_{i-1}}{2} \left( \frac{\partial^2 \phi}{\partial x^2} \right)_i - \frac{(x_i - x_{i-1})^2}{6} \left( \frac{\partial^3 \phi}{\partial x^3} \right)_i + h.o.t., \quad (3.25)$$

and for both  $x_{i-1}$  and  $x_{i+1}$ :

$$\begin{aligned} \left( \frac{\partial \phi}{\partial x} \right)_i = & \frac{\phi_{i+1} - \phi_{i-1}}{x_{i+1} - x_{i-1}} - \frac{(x_{i+1} - x_i)^2 - (x_i - x_{i-1})^2}{2(x_{i+1} - x_{i-1})} \left( \frac{\partial^2 \phi}{\partial x^2} \right)_i - \\ & \frac{(x_{i+1} - x_i)^3 + (x_i - x_{i-1})^3}{6(x_{i+1} - x_{i-1})} \left( \frac{\partial^3 \phi}{\partial x^3} \right)_i + h.o.t.. \end{aligned} \quad (3.26)$$

If the distance between the grid points is small, the higher-order terms will be small in most cases, and the derivatives can be approximated truncating each of the series after the first terms

$$\left(\frac{\partial\phi}{\partial x}\right)_i \approx \frac{\phi_{i+1} - \phi_i}{x_{i+1} - x_i}, \quad (3.27)$$

$$\left(\frac{\partial\phi}{\partial x}\right)_i \approx \frac{\phi_i - \phi_{i-1}}{x_i - x_{i-1}}, \quad (3.28)$$

$$\left(\frac{\partial\phi}{\partial x}\right)_i \approx \frac{\phi_{i+1} - \phi_{i-1}}{x_{i+1} - x_{i-1}}, \quad (3.29)$$

being these the forward or explicit, backward or implicit, and central-difference schemes. The deleted terms from the right hand sides are the truncation errors, which measure the precision of the approximation and affect how the error is reduced as the spacing between points decreases. The first truncated term is usually the main source of error.

### 3.2.1 Grid Refinement

If the grids are fine enough, the truncation error is proportional to the leading term in the Taylor series, and can be expressed as

$$E \approx C(h)^p + h.o.t., \quad (3.30)$$

where  $C$  is a constant, dependent on the derivatives at the given point,  $h$  is a measure of grid spacing and  $p$  is the order of convergence. A second-order solution has a value of  $p = 2$ .

The initial step in a grid refinement study consists on creating three grids with a different level of refinement and a constant refinement ratio  $r$  between them. The difference between the solutions on these three grids can be used to estimate the order of convergence  $p$ . If the grid 1 has a spacing of  $4h$ , the grid 2 of  $2h$  and the grid 3 of  $h$ , since the exact solution may be expressed as

$$\phi = \phi_h + C(h)^p + h.o.t. = \phi_{2h} + C(2h)^p + h.o.t. = \phi_{4h} + C(4h)^p + h.o.t., \quad (3.31)$$

where  $\phi$  is exact solution of the partial differential equation,  $\phi_h$  is the solution in a node in grid 3,  $\phi_{2h}$  is the solution in the same node in grid 2 and  $\phi_{4h}$  is the solution in the same node in grid 1, the order of convergence  $p$  can be estimated as

$$p = \frac{\ln\left(\frac{\phi_{2h} - \phi_{4h}}{\phi_h - \phi_{2h}}\right)}{\ln(r)} \quad (3.32)$$

[31]. Since the error dependence on grid size is usually irregular when the grid is coarse, the grids considered must be sufficiently refined such that the solution is in the *Asymptotic Range of Convergence*, where errors decrease at a rate defined by the order of convergence  $p$ . In this range, the grid spacings  $h$  and the errors  $E$  result in a constant value  $C = \frac{E}{h^p}$  [32]. The estimated value of  $p$  shows if the studied grids are in said range. For this to be true,  $p$  must be approximately the same as order of the scheme.



## CHAPTER 4

### Numerical Model

#### 4.1 Single particle

As a first step in the creation of the model, the FEM has been used to simulate heat transfer in a single particle. We have considered a simple problem that allows us to create a good model and test it easily.

Since we are working in two dimensions, the particle is modeled by a circle. This circle and its location in space are defined by its centre (determined by its coordinates  $X$  and  $Y$ ), its radius  $R$  and the properties of its material. One specific point  $P$  in said circle can be defined by its distance from the center  $r$  and an angle  $\theta$ , or simply by its coordinates  $X$  and  $Y$ .

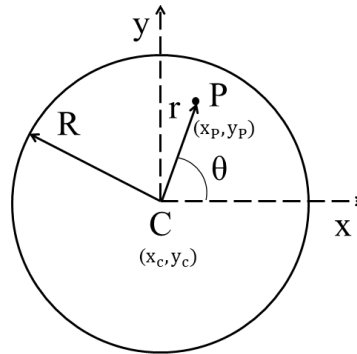


Figure 4.1: Parameters that define the location a particle.

In order to start with a simple model where results can easily be tested, one particle of a generic  $R = 1 \text{ mm}$  has been considered. This particle size has been chosen because most particles used in FPR have a size in the range of millimeters. One grid will be created for this particle, that will be properly scaled when working with a different particle size. The material of the particle of study is a kind of sintered bauxite called CARBOHSP, has the following main properties: thermal diffusivity  $\alpha = \frac{k}{\rho C_p} = 7.41310^{-7} \frac{\text{m}^2}{\text{s}}$  (where the conductivity is  $k = 2 \frac{\text{W}}{\text{mK}}$ , the density is  $\rho = 3550 \frac{\text{kg}}{\text{m}^3}$  and the specific heat is  $C_p = 760 \frac{\text{J}}{\text{kg}^\circ\text{C}}$ ) [33], absorptivity  $\alpha = 0.934$  and emissivity  $\epsilon = 0.843$  [2].

The time required for the heat to diffuse through the particle (from the contour of the particle to its center) can be calculated from the diffusion equation (2.9) applied to the line that separates said points, squematically represented in Figure 4.2

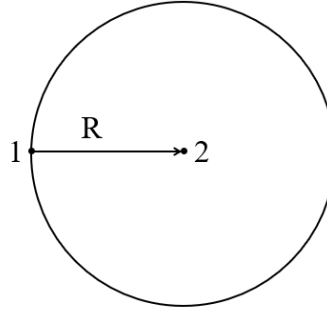


Figure 4.2: Scheme of the distance between the contour and the center of a particle.

$$\frac{\partial^2 T}{\partial x^2} = \frac{1}{\alpha} \frac{\partial T}{\partial t} \rightarrow \frac{T_2 - T_1}{R^2} = \frac{1}{\alpha} \frac{T_2 - T_1}{t_s} \rightarrow t_s = \frac{R^2}{\alpha} \rightarrow t_s = \frac{(1 \cdot 10^{-3} m)^2}{7.413 \cdot 10^{-7} \frac{m^2}{s}} = 1.349 s$$

### 4.1.1 Initial and Boundary conditions

The initial condition in this specific problem establishes that the initial temperature in every node is  $20^\circ C$ , and the boundary conditions, that the particle is being heated by a uniform heat flux  $q$  of  $600000 \frac{W}{m^2}$  along all its contour.

### 4.1.2 Analytic solution

The simulation is run during  $1.349 s$ , and considering the heat flux that is transmitted to the contour of the particle, the length of said contour and the duration of the transmission, the total heat that the particle receives can be estimated as

$$Q = q \cdot 2\pi r \cdot t = 600000 \frac{W}{m^2} \cdot 2\pi(1 \cdot 10^{-3})m \cdot 1.349s = 5085 \frac{J}{m} . \quad (4.1)$$

The specific heat is a property of the material that defines the amount of heat per unit mass necessary to raise the temperature by one degree Celsius. If no change of phase takes place, the relation between heat and temperature change can be expressed as

$$Q = C_p m \Delta T , \quad (4.2)$$

being  $m$  the mass of the body and  $\Delta T$  the increment of temperature. Reordering the previous equation,

$$\Delta T = \frac{Q}{C_p m} . \quad (4.3)$$

Finally, considering that  $m = \rho A$  (being  $A$  the area),  $\Delta T$  can be estimated as

$$\Delta T = \frac{Q}{C_p \rho A} = \frac{Q}{C_p \rho \pi r^2} = \frac{5085 \frac{J}{m}}{760 \frac{J}{kg^\circ C} 3550 \frac{kg}{m^3} \pi (1 \cdot 10^{-3} m)^2} = 600^\circ C . \quad (4.4)$$

$$T_{final} = T_{initial} + \Delta T = 20^\circ C + 600^\circ C = 620^\circ C \quad (4.5)$$

The temperature reached after applying the heat flux for 1.349 s must be approximately 620°C, so the average temperature obtained with the model must be close to this value.

### 4.1.3 Grid Refinement study

The particle is divided into  $E$  elements of  $n$  nodes each with the grid generator Gmsh. The grid created is made up triangular elements of  $n = 3$  nodes in the interior, and linear elements of  $n = 2$  nodes on the countour. Grid refinement is carried out to ensure that the results are valid and accurate enough for the purpose of this Thesis and the simulations take as little time as possible.

The procedure explained on section 3.1 of this paper is followed. To start the grid refinement study, three different grids have been generated with Gmsh: grid 1 is the least refined one, and to get grids 2 and 3 a constant refinement ratio  $r = 2$  is used between them. The next table sums up the main characteristics of said grids:

	<b>Number of nodes</b>	<b>Number of triangular elements</b>
Grid 1	468	868
Grid 2	1801	3472
Grid 3	7073	13888

Table 4.1: Comparison of the characteristics of the three candidate grids.

And figure 4.3 shows a graphic representation of them:

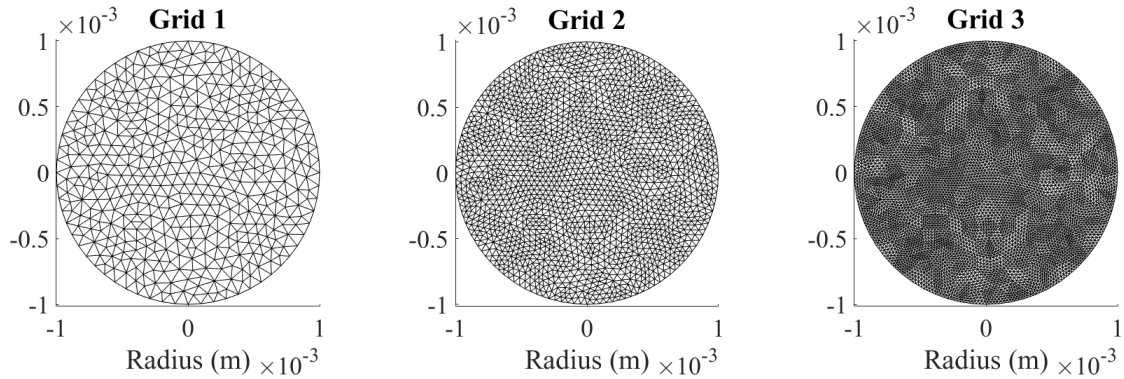


Figure 4.3: Graphic representation of grids 1, 2 and 3.

The program is run in the same conditions for each of the grids, being the value of the temperature in the nodes the parameter of interest to study the grid convergence. Using Equation (3.32) to estimate  $p$  in every node shared by the three grids, the obtained values are very close to 2 (the order of the scheme) being its average value for all the nodes 2.0352, which shows that the grids are indeed in the *Asymptotic Range of Convergence*. This can be graphically checked by plotting the results of the temperature in a straight line that crosses the particle going through its center for each of the grids, as shown in Figure 4.4

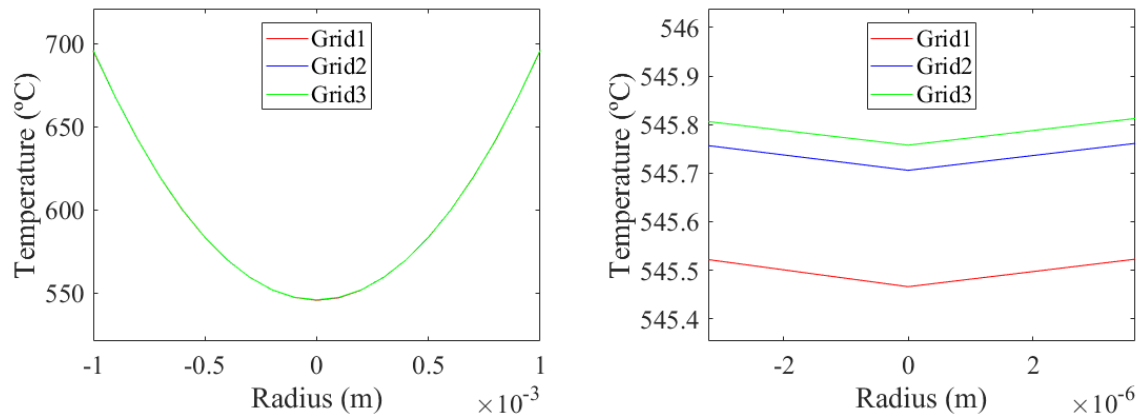


Figure 4.4: Graphic representation of temperature vs. radius through the particle in grids 1, 2 and 3.

It can be easily seen that these solutions do not differ much, especially for the most refined grids: for a temperature increment of approximately  $526^{\circ}C$  in the center of the particle, the solution in grid 1 only varies  $0.302^{\circ}C$  compared to the solution in grid 3 (the most refined one). This is a variation of a 0.000574 %, that can be considered negligible for the purpose of this Thesis. Now that we know approximately what the solution must be, it is important to check if a similar solution can be obtained with a coarser grid, in order to reduce the computational

cost. Grid 4 is therefore generated:

	<b>Number of nodes</b>	<b>Number of triangular elements</b>
Grid 1	468	868
Grid 2	1801	3472
Grid 3	7073	13888
Grid 4	130	224

Table 4.2: Comparison of the characteristics of the four candidate grids.

In Figure 4.5, the new grid is graphically compared to the previous ones

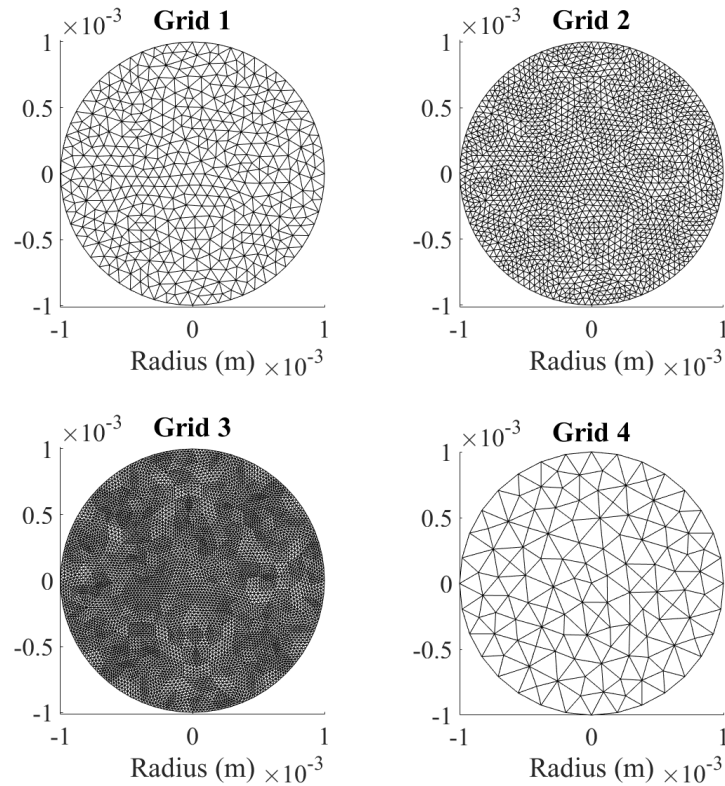


Figure 4.5: Graphic representation of grids 1, 2 and 3.

The results of the temperature in the points of a line that crosses the particle going through its center for this grid and the previous ones are shown in Figure 4.6

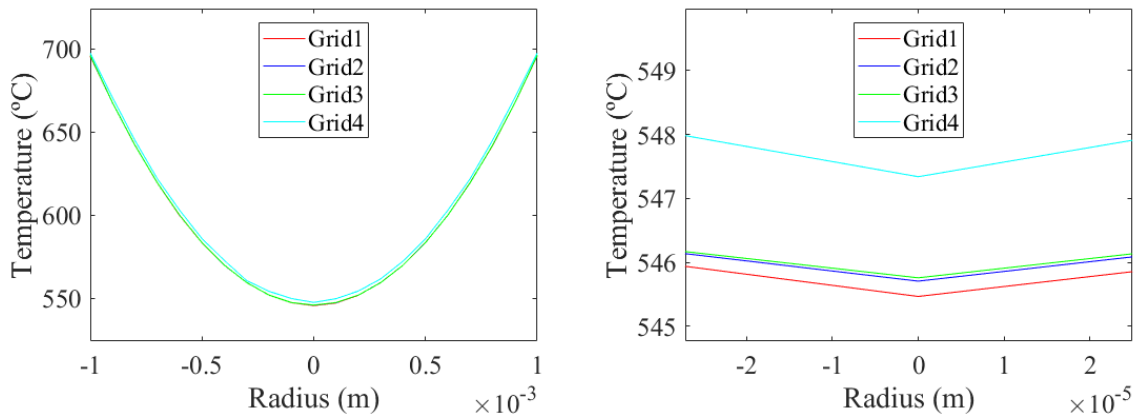


Figure 4.6: Graphic representation of temperature vs. radius through the particlein grids 1, 2, 3 and 4.

This solution differs much more from the solution in grid 3 than grid 1 did, up to  $1.572^{\circ}C$  at some points. That is a difference of a 0.00298 %, a variation 5 times bigger than the obtained when working with grid 1.

Therefore, a new grid is generated to see if it is possible to find greater accuracy with another grid that is still coarser than grid 1. Grid 5 has more nodes than grid 4 but less than grid 1, and its main properties are shown in the following table

	<b>Number of nodes</b>	<b>Number of triangular elements</b>
Grid 1	468	868
Grid 2	1801	3472
Grid 3	7073	13888
Grid 4	130	224
Grid 5	314	572

Table 4.3: Comparison of the characteristics of the five candidate grids.

Figure 4.7 shows a graphical comparison of all the grids:

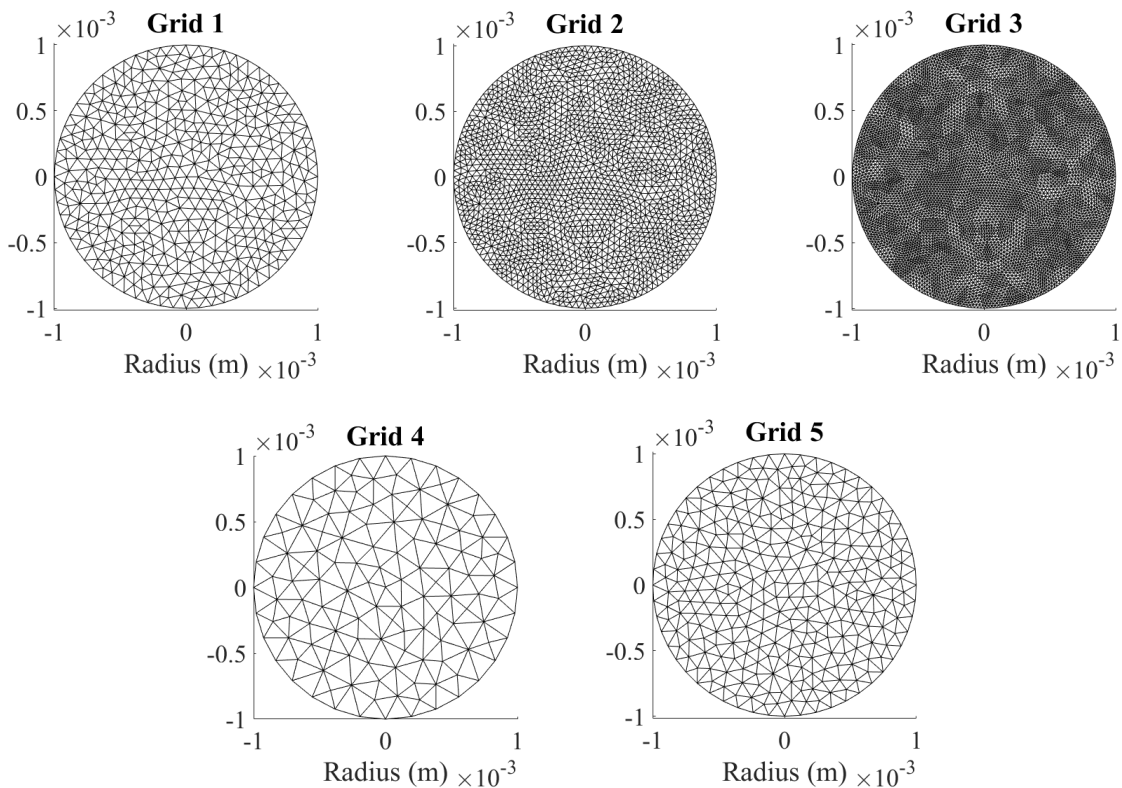


Figure 4.7: Graphic representation of grids 1, 2, 3, 4 and 5.

The temperature obtained in the points of a line that crosses the particle going through its center for all the studied grids is shown in Figure 4.8

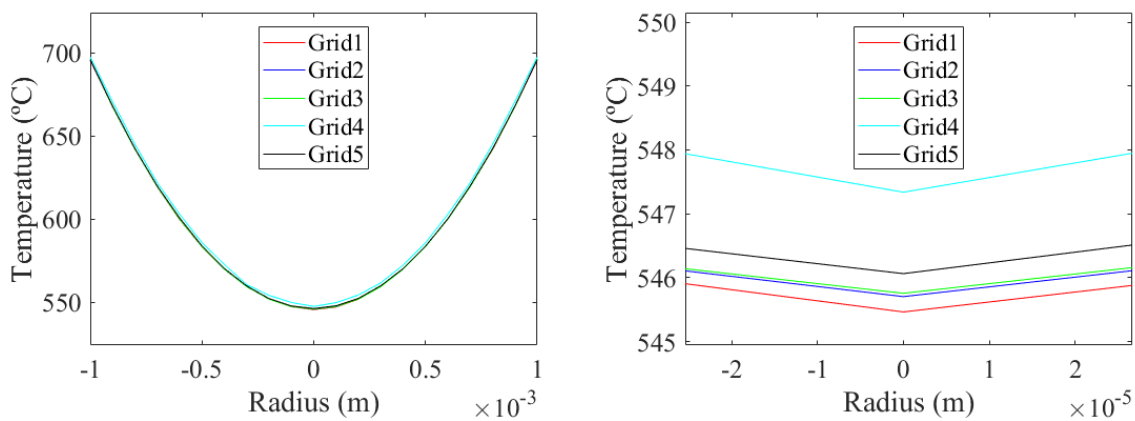


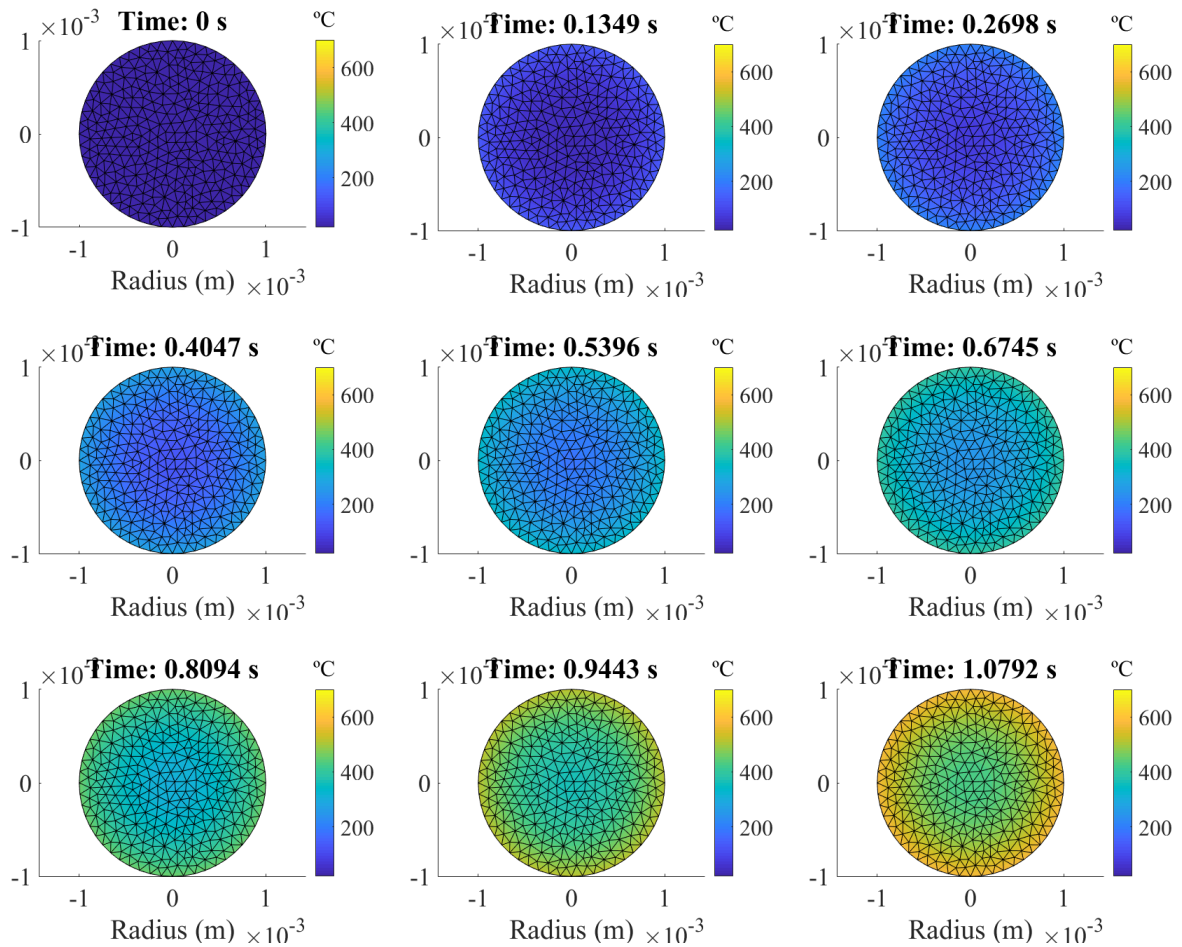
Figure 4.8: Graphic representation of temperature vs. radius through the particle in grids 1, 2, 3, 4 and 5.

The values of the temperature obtained with grid 5 do not differ as much as the previous ones: for a temperature increment of approximately  $526^{\circ}\text{C}$  in the center of the particle, the solution in grid 5 only varies  $0.297^{\circ}\text{C}$  compared to the solution in the most refined grid. This is a variation of a  $0.000564\%$ , that can be considered small enough for the purpose of this Thesis. The computation time has been reduced compared to grid 1: from  $1.406672\text{ s}$  to  $1.339610\text{ s}$  in this simulation, which is a reduction of a  $5.006\%$ .

#### 4.1.4 Numerical solution

The average temperature of the particle obtained with grid 5 in this experiment is  $628.4^{\circ}\text{C}$ , which is close enough to the solution calculated analytically.

Figure 4.9 shows the evolution of heat transfer in the chosen grid, calculated with the FEM.





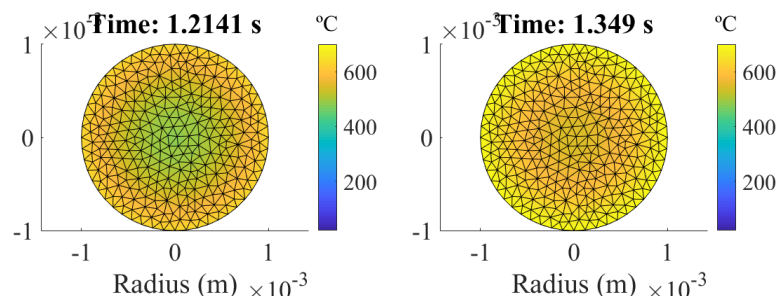


Figure 4.9: Evolution of heat transfer in grid 5.

#### 4.1.5 Emission from the particle. Steady-state

The previous situation was proposed to verify how the FEM model simulates heat transfer, therefore in order to simplify analytical resolution, emission from the particle was not considered. Taking emission into account would have complicated the analytical calculations of the increment of the energy in the particle, and the scope of the experiment was not to have a realistic result but to find an adequate grid to work with and demonstrate the proper functioning of the FEM on heat transfer. However, to obtain a realistic model of heat transfer it is absolutely necessary to consider the energy emission from the particles, which follows the *Stefan-Boltzmann Law* for a *gray body*, previously expressed on Equation (2.4). As the temperature in the particle increases, its emitted energy increases as well and at some point, a condition of equilibrium is reached. This equilibrium state is called *steady-state*, and it should be properly simulated by the model.

Furthermore, instead of considering a generic particle size of  $R = 1 \text{ mm}$ , this example is run with the estimated average size of CARBOHSP  $R = 0.3495 \text{ mm}$ .

The temperature evolution is obtained after running a simulation for  $8 \text{ s}$ , in the same conditions of the previous experiment but adding emission from the particle, is shown in Figure 4.10.

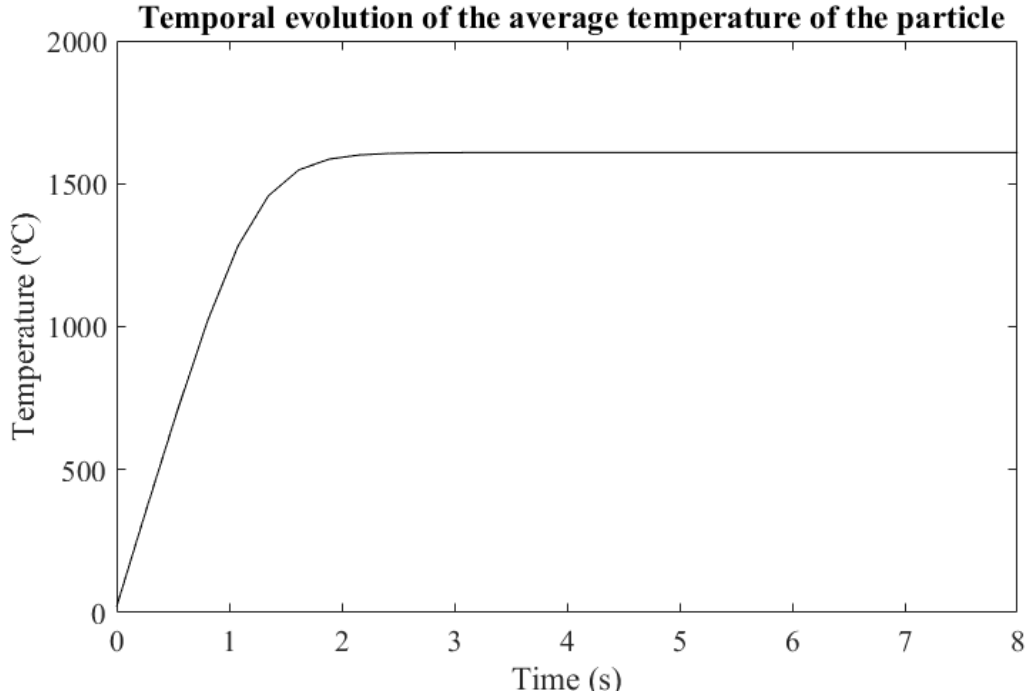


Figure 4.10: Evolution of the temperature in one particle.

This result proves that the program successfully simulates the reach of the steady-state by the particle.

#### 4.1.6 Solar rays simulation

Now that the working grid has been chosen and it has been demonstrated that the FEM works correctly, the interaction with the modeled rays must be tested. Again, in this first experiment the emission from the particles is not considered, since that would make more difficult to estimate the increment of the temperature in the particle. The simulation is run during 2.69799 s, the total incoming heat flux from the heliostats is considered to be  $600000 \frac{W}{m^2}$  (2D), and the section of the window receiver studied has a length of 0.697mm. According to Equation (3.1), the total energy transmitted to the studied domain is

$$Q_{window} = q \cdot l = 600000 \frac{W}{m^2} \cdot 0.697 \cdot 10^{-3} m = 418.2 \frac{W}{m} = 418.2 \frac{J}{m \cdot s} . \quad (4.6)$$

Considering the duration of this heat transfer, the total energy that reaches the particle is

$$Q_{particle} = Q_{window} \cdot t = 418.2 \frac{J}{m \cdot s} \cdot 0.65534 s = 274.06 \frac{J}{m} , \quad (4.7)$$

and the increment in the temperature of the particle can be estimated as

$$\Delta T = \frac{Q}{\rho C_p \pi r^2} = \frac{274.06 \frac{J}{m}}{3550 \frac{kg}{m^3} 760 \frac{J}{kg^\circ C} \pi (0.3485 \cdot 10^{-3} m)^2} = 266.23^\circ C . \quad (4.8)$$

$$T_{final} = T_{initial} + \Delta T = 20 + 266.23 = 286.23^\circ C \quad (4.9)$$

Since the initial temperature of the particle is  $20^\circ C$ , the temperature reached after  $0.65534 s$  must be approximately  $286.23^\circ C$ . The average temperature obtained in the model must be close to this value.

Three different simulations have been run, modeling a different number of rays in each one of them.

### **Simulation 1 - 3 rays**

In the first simulation, one ray has been considered for every  $0.3495 mm$  of window. Since the section of the window of interest in this experiment is  $0.697 mm$  long, only 3 rays have been simulated. Since the model is two dimensional, these rays must transmit a total of  $274.06 J$ , which means that each one of them transmits  $91.35 J$ . The final average temperature reached by the particle in this particular case is  $287^\circ C$ . This result can be seen in the subfigure (a) of Figure 4.11.

### **Simulation 2 - 21 rays**

One ray has been simulated for every  $0.03495 mm$  of window, which means that in the correspondig section of the window, 21 rays have been simulated, each one of them transmitting  $13.05J$ . The final average temperature reached by the particle is  $287.12^\circ C$ . The resut of this simulation is graphically represented in the subfigure (b) of Figure 4.11.

### **Simulation 3 - 201 rays**

One ray has been simulated for every  $0.003495 mm$  of window. In the correspondig section of the window, 201 rays have been simulated, each one of them transmitting  $1.36J$ . The final average temperature reached is  $287.13^\circ C$ , and the result can be graphically seen in the subfigure(c) of Figure 4.11.

As expected, these three results are close enough to the estimated final temperature for the particle. Figure 4.11 shows a comparison of the heat transfer in these three cases, where the grid lines have been erased for a smoother appearance. It can be seen that, even though the final average temperature is similar in all the cases, the temperature distribution is more realistic when a higher number of rays is simulated.

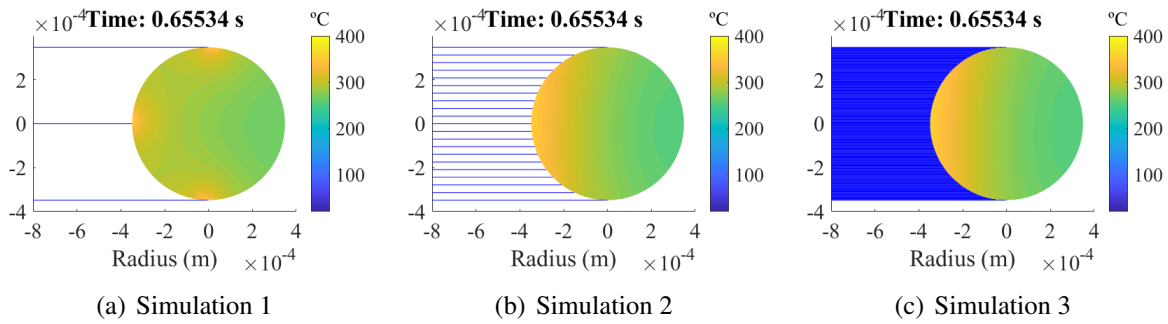


Figure 4.11: Evolution of the temperature in one particle with a different number rays.

## 4.2 Multiple particles

Now that the code has been tried out in simpler situations, it can be developed for the main problem of study in this Thesis: a sample of particles falling inside a FPR that are heated by sunlight. The code created has been divided in six different parts: parts 1 and 2 generate randomly located particles in the computational domain, parts 3 and 4 generate a grid inside each of these particles, part 5 initializes the heat transfer according to the Initial Conditions and part 6 generates a set of rays and uses the FEM to model the heat transfer. A much more detailed explanation of the code can be found on Appendix A.

### 4.2.1 Generation of the particles

The user of the program must choose the material of the particles of study. According to said material, the values of conductivity  $k$ , density  $\rho$  specific heat  $C_p$ , absorptivity  $\alpha$  and emissivity  $\epsilon$  of the particles must be introduced.

A two band model has been used to model the absorptivity of the particles. The bands are defined by the wavelength of the incident radiation: if it is shorter than  $2.5 \mu m$  (solar radiation) the absorptivity of the particle is the one defined by the material properties, and if it is longer than  $2.5 \mu m$  (radiation emitted by other particles) the absorptivity is equal to the particle emissivity.

The user of the program is able to choose the area of the receiver where the particles are created, the void ratio of that area, the distance between the window and the curtain of particles and the location of the back wall of the receiver.

Figure 4.12 shows the particles generated in an area of  $15 \text{ cm}^2$  – being the length of the window section simulated  $5 \text{ cm}$  and the depth of the receiver simulated  $3 \text{ cm}$  –, with a distance of  $0 \text{ mm}$  from the window to the curtain of particles, the back wall at a distance of  $3 \text{ cm}$  from the window and a void ratio of a 99 %, 90 % and 80 %, respectively.

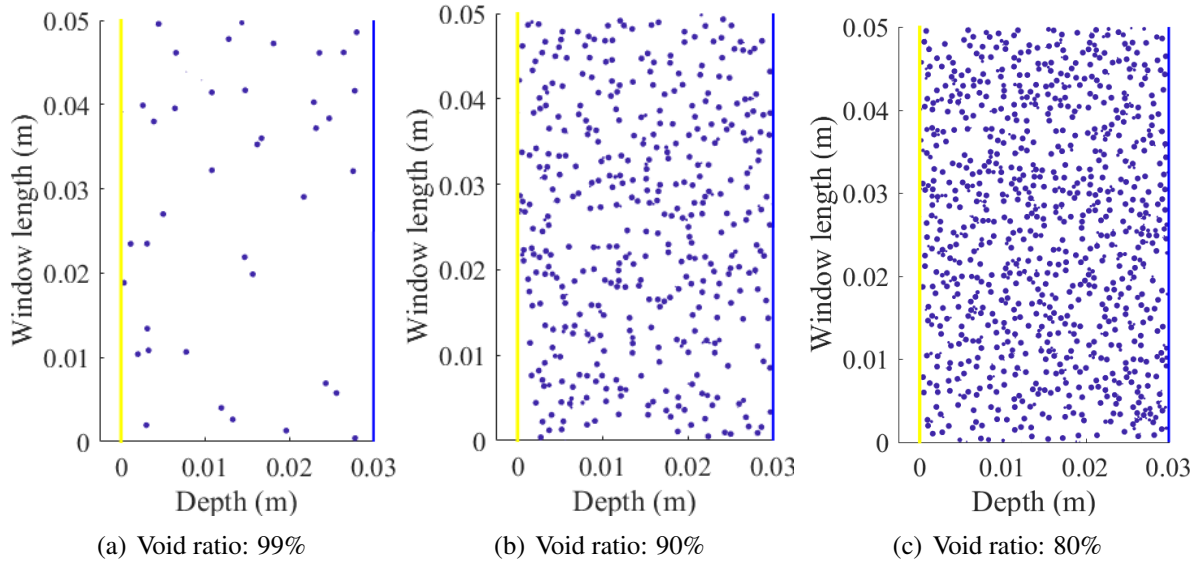


Figure 4.12: Generation of particles inside the receiver with a different void ratio.

## 4.2.2 Generation of the rays

Solar rays are simulated as explained in subsection 3.1.1.

## 4.2.3 Simulations

Running a simulation for a group of particles as numerous as the ones showed above would take too much time. In order to get some initial results for the developed code in less time, a smaller section of the receiver is modeled. The particles are located in an area of  $25 \text{ mm}^2$  – being the length of the window section of said area  $5 \text{ mm}$  and the depth of the receiver  $5 \text{ mm}$  as well –. Three simulations have been run for three groups of particles with a different number of particles, size and spatial distribution.

The group of particles is irradiated with solar rays, that instead of coming only from the section of the window of  $5 \text{ mm}$  in front of which the particles are located, are coming also from from  $10 \text{ mm}$  above and  $10 \text{ mm}$  below. This has been modeled this way because it is realistic to assume that these particles will receive sunlight coming from different parts of the window.

The total energy coming from these  $25 \text{ mm}$  of window is

$$Q_{window} = q \cdot l = 600000 \frac{W}{m^2} \cdot 2.5 \cdot 10^{-3} m = 1500 \frac{W}{m} = 1500 \frac{J}{m \cdot s} . \quad (4.10)$$

The energy emitted by the particles due to their temperature is also simulated in the way explained in subsection 3.1.2.

It is important to highlight that in this models the particles do not move, which might lead to unrealistic results in some particles if they are surrounded by others and do not receive enough sunlight.

#### 4.2.3.1 Simulation 1 - Same sized particles

In this case, four particles have been simulated, all of them with a radius of  $0.3495 \text{ mm}$ , the average value for CARBOHSP particles. The simulation has been run during  $8.1 \text{ s}$ , where 2500 rays have been used to model sunlight (1 ray every  $0.01 \text{ mm}$  of window).

The location of the particles of study can be seen in Figure 4.13.

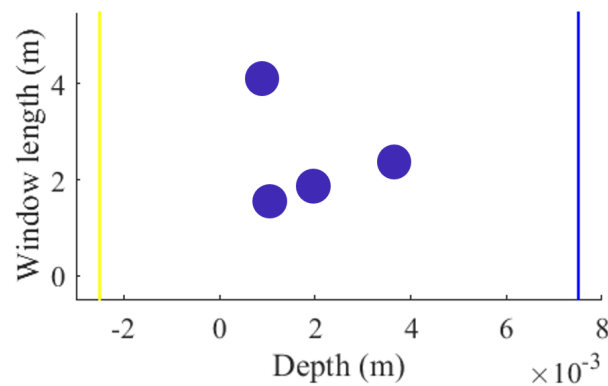


Figure 4.13: Location of the particles of study.

The solar rays are represented by blue lines, as seen in Figure 4.14, which shows a close look of the area of study so that it is possible to appreciate the different lines.

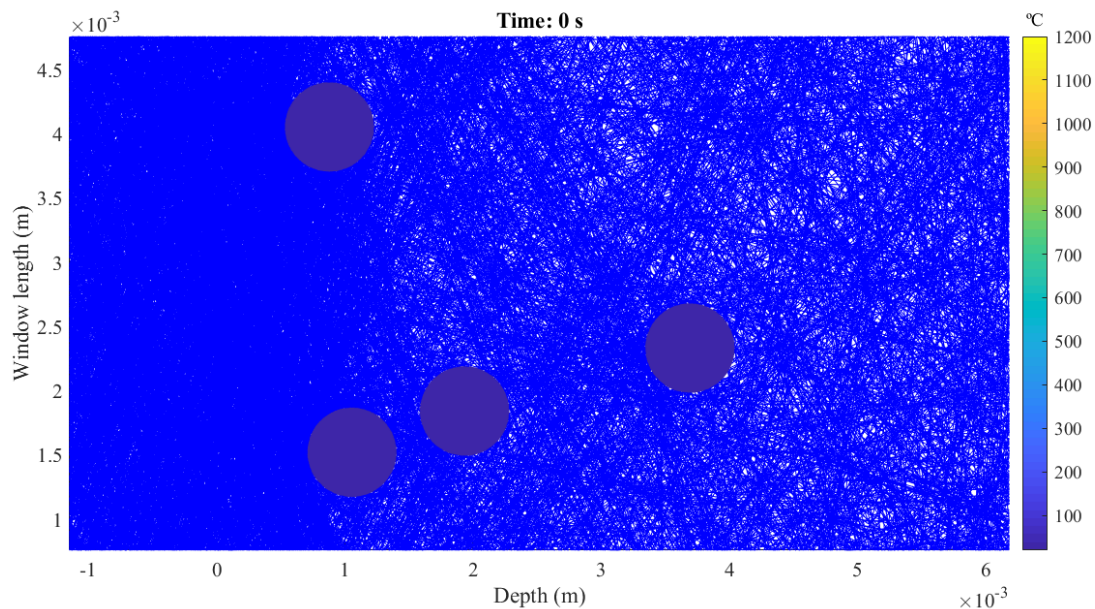


Figure 4.14: Close look of the area of study.

The rays emitted by the particles are represented by red lines, as shown in Figure 4.15.

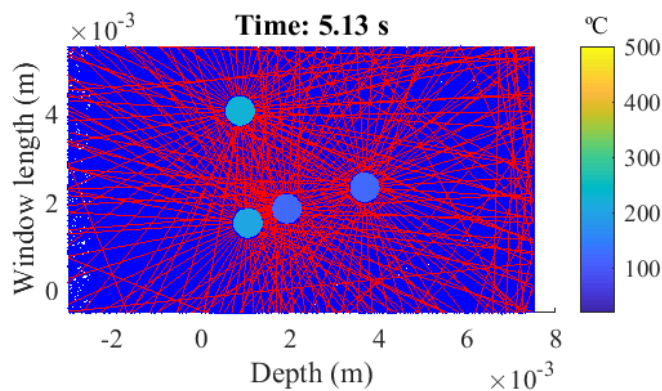


Figure 4.15: Location of the particles in Simulation 1

Both Figures 4.14 and 4.15 show the rays at a specific moment in time. These are not static, but change their paths in every timestep.

Figure 4.16 shows the evolution of the temperature of the particles after the simulation of 8.1 s. The two particles that are closer to the window are heated faster than the other two, which makes sense because they receive more solar rays. However, it looks like the particles begin to reach the steady state at around 240 °C, a temperature way below the one that is desired to reach.

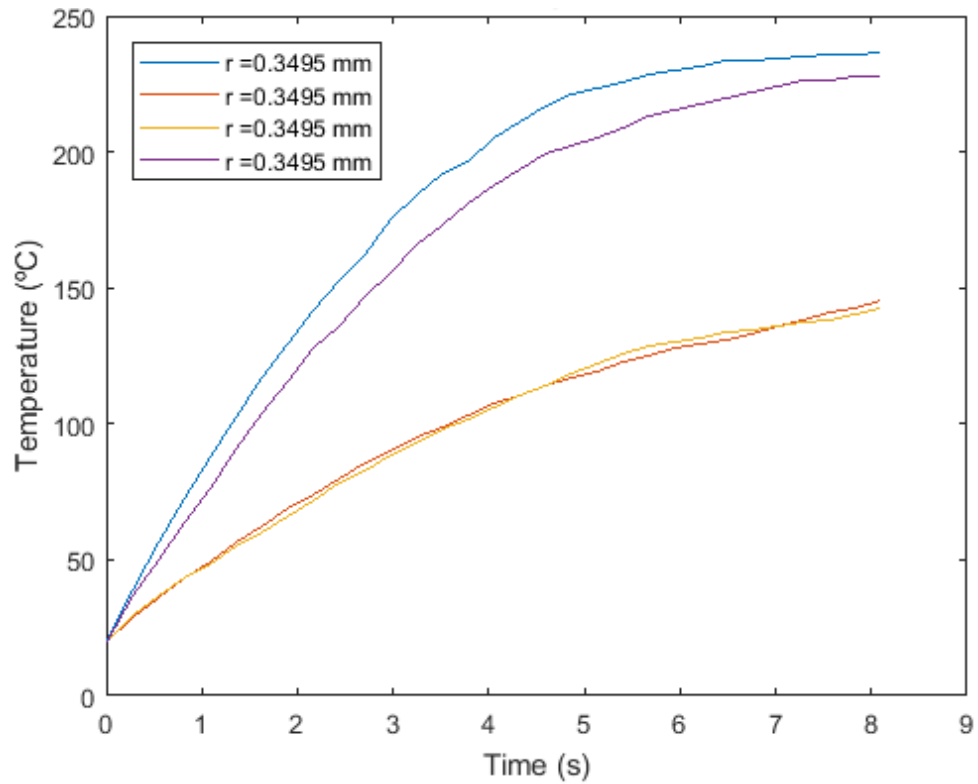


Figure 4.16: Temporal evolution of the average temperature of the particles

### 4.2.3.2 Simulation 2 - Different sized particles

Seven particles of various sizes have been simulated. The simulation has been run during 13.8 s and, as in the previous case, 2500 rays have been used to model sunlight (1 ray every 0.01 mm of window).

The location of the particles is shown in Figure 4.17 and the evolution of their temperature, in Figure 4.18.



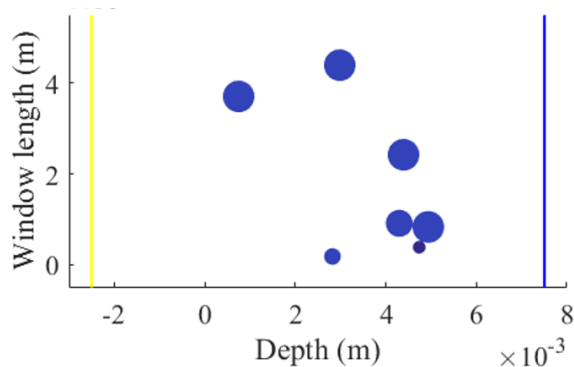


Figure 4.17: Location of the particles in Simulation 2

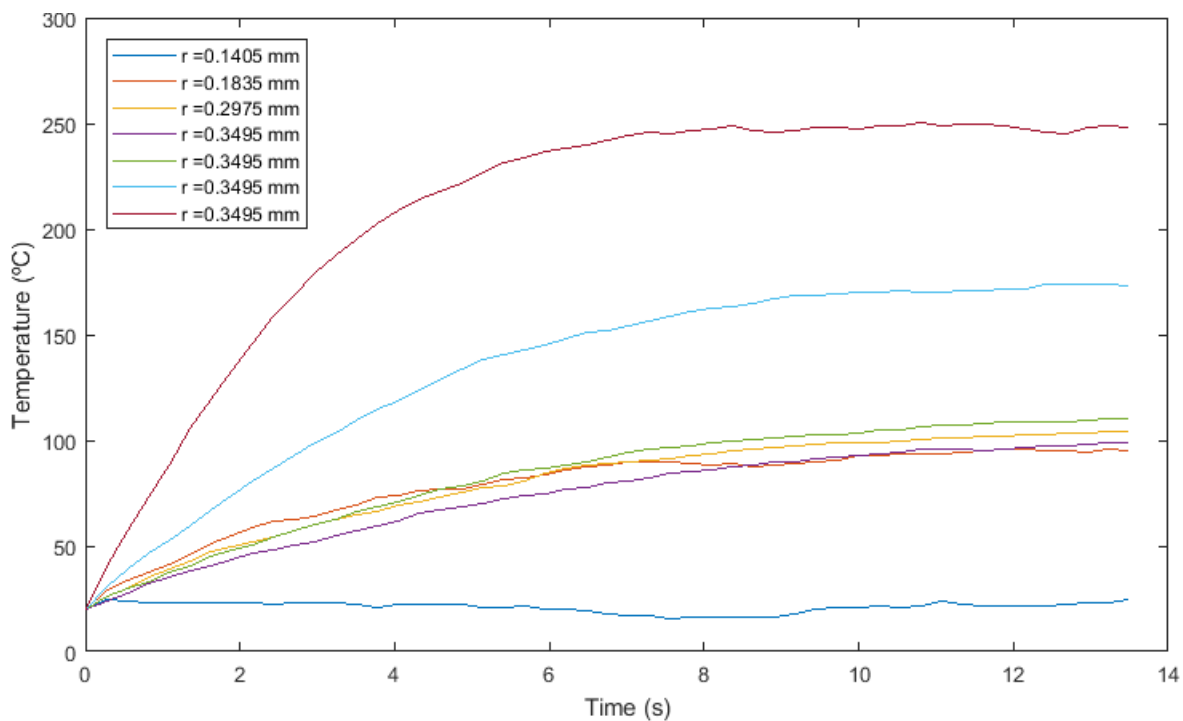


Figure 4.18: Temporal evolution of the average temperature of the particles

The result obtained in the particle of  $R = 0.1405 \text{ mm}$  (the dark blue line in Figure 4.18) stands out, since the temperature of the particle does not increase, but remains almost stable. This is due to its location: since it is surrounded by other particles, it does not get enough sunlight to increase its temperature. It emits radiation due to its temperature and absorbs radiation emitted by other particles and some sunlight, which allows it to keep a temperature somehow stable. This would not occur if particle flow had been simulated, because the particle would not have been surrounded by other particles all the time.

### 4.2.3.3 Simulation 3 - One particle smaller than the others

Four particles have been created, being one of them slightly smaller than the others. The simulation has been run during 8.1 s and in this last case, 5001 rays have been used to model sunlight (1 ray every 0.005 mm of window). This is two times more rays than in the previous simulations to model the same amount of energy, which will lead to a more accurate result but at the expense of more computational time.

The location of the particles is shown in Figure 4.19 and the evolution of their temperature, in Figure 4.20.

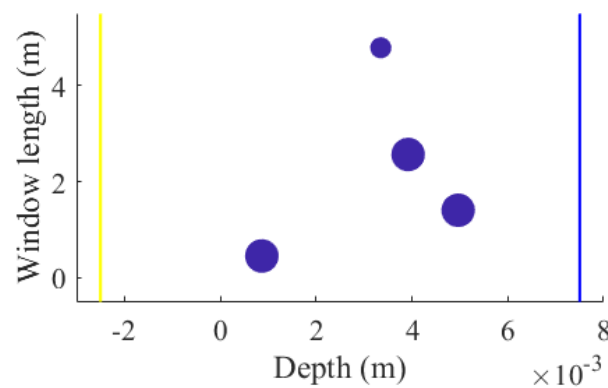


Figure 4.19: Location of the particles in Simulation 3

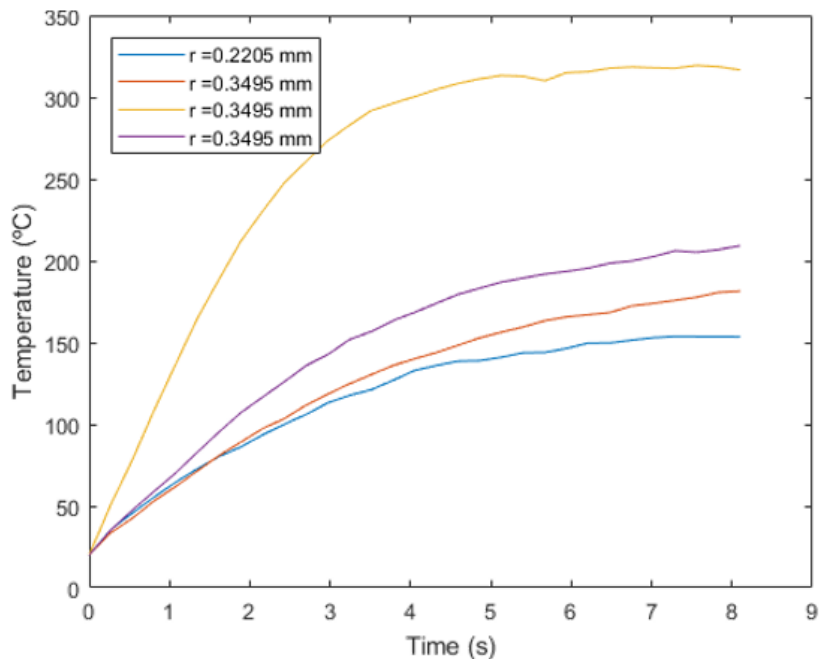


Figure 4.20: Temporal evolution of the average temperature of the particles

These last results show how all the particles are uniformly heated and how they start reaching the steady state at, as was said when discussing simulation 1, temperatures way below what is desired in a FPR. These results present how the smallest particle is heated in a similar manner as the other three particles, which serves to prove that in simulation 2 the results in the smallest particle were not due to its size, but to its location.

## CHAPTER 5

### Results and Conclusions

The transient heating process of small particles inside a FPR has been simulated, and the results obtained show that the time necessary for the particles to increase their temperature is not negligible.

Also, according to the results the particles will not reach the desired temperatures in the time it takes for them to fall in the curtain, and might need recirculation in the receiver to reach said temperatures. The particles have the capacity to reach them, as was proven in subsection 4.1.5 when modeling an ideal situation where a single particle is uniformly heated in all its contour (Figure 4.10), but do not get enough sunlight when being irradiated only from one side as they fall.

The program created consists on two different parts: the radiation model and the conduction model, and both of them can be individually used to model different problems or technologies.

## **CHAPTER 6**

### **Future Work**

The following improvements to the model are proposed:

- The addition of particle flow, so that the location of the particles changes and the results obtained are more realistic.
- The consideration of heat losses in the back wall, since in this model it has been assumed that the wall was ideal and did not absorb any of the radiation.
- The limitation of the direction of the incoming rays with an appropriate study of the angles of incidence of the concentrated rays from the heliostat field.
- The simulation with different particle materials.
- And finally, the extension of the model to three dimensions.

## BIBLIOGRAPHY

- [1] German Aerospace Center. Concentrating solar power now. clean energy for sustainable development. The Federal Ministry for the Environment, Nature Conservation and Nuclear Safety (BMU), 2002.
- [2] C. Ho, J. Christian, D. Gill, A. Moya, S. Jeter, S. Abdel-Khalik, D. Sadowski, N. Siegel, H. Al-Ansary, L. Amsbeck, B. Gobereit, and R. Buck. Technology Advancements for Next Generation Falling Particle Receivers. *Energy Procedia*, 49:398–407, 2014.
- [3] Zina Deretsky Website.
- [4] Y. A. Cengel, R. H. Turner, and J. M. Cimbala. *Fundamentals of Thermal-Fluid Sciences*. McGraw-Hill Higher Education, 2001.
- [5] M.F. Hordeski. *New Technologies for Energy Efficiency*. Marcel Dekker Inc., 2003.
- [6] World energy resources: A summary. Technical report, World Energy Council, 2013.
- [7] G. Gereffi and K. Dubay. Concentrating solar power clean energy for the electric grid. Technical report, Center on Globalization, Governance and Competitiveness, 2008.
- [8] A. Oles. *Modeling of Falling-Particle Solar Receivers for Hydrogen Production and Thermochemical Energy Storage*. PhD thesis, University of Maryland, 2014.
- [9] GE Renewable Energy. *Molten Salt Central Receiver*, 2016.
- [10] H. Müller-Steinhagen and F. Trieb. Concentrating solar power - A review of the technology. *Quarterly of the Royal Academy of Engineering*, 18:43–50, 2004.
- [11] T. Tan and Y. Chen. Review of study on solid particle solar receivers. *Renewable and Sustainable Energy Reviews*, 14(1):265–276, 2010.
- [12] K.Ho. Clifford. A Review of High-Temperature Particle Receivers for Concentrating Solar Power. *Applied Thermal Engineering*, 109:958969, 2016.
- [13] A. Meier. A predictive CFD model for a falling particle receiver/reactor exposed to concentrated sunlight. *Chemical Engineering Science*, 54(13-14):2899–2905, 1999.
- [14] P.K. Falcone, J.E. Noring, and J.M. Hruby. Assessment of a Solid Particle Receiver for a High Temperature Solar Central Receiver System. Technical Report SAND85-8208, Sandia National Laboratories, 1985.
- [15] J.W. Griffin and K.A. Stahl. Optical Properties of Solid Particle Receiver Materials: Angular Scattering and Extinction Characteristics of Norton Masterbeads ®. *Solar Energy Materials*, 14:395–416, 1986.
- [16] J.M. Hruby. A Technical Feasibility Study of a Solid Particle Solar Central Receiver for High Temperature Applications. Technical Report SAND86-8211, Sandia National Laboratories, 1986.

- [17] G. Evans, W. Houf, R. Grief, and C. Crowe. Numerical Modelling of a Solid Particle Solar Central Receiver. *Sandia National Laboratories*, 1985.
- [18] G. Evans, W. Houf, R. Greif, and C. Crowe. Gas-Particle Flow Within a High Temperature Solar Cavity Receiver Including Radiation Heat Transfer. *Journal of Solar Energy Engineering*, 109:134142., 1987.
- [19] J. Hruby, R. Steeper, G. Evans, and C. Crowe. An experimental and numerical study of flow and convective heat transfer in a freely falling curtain of particles. *Journal of Fluids Engineering*, 110:172181, 1988.
- [20] H. Chen, Y. Chen, H-T. Hsieh, G. Kolb, and N. Siegel. Numerical investigation on optimal design of solid particle solar receiver. *Proceedings of ASME Energy Sustainability*, (ES2007-36134):971–979, 2007.
- [21] H. Chen, Y. Chen, H-T. Hsieh, and N. Siegel. Computational fluid dynamics modeling of gas-particle flow within a solid particle solar receiver. *Journal Solar Ener*, 120(2):160170, 2007.
- [22] N. Siegel and G. Kolb. Design and On-Sun Testing of a Solid Particle Receiver Prototype. *Proceedings of ASME 2nd International Conference on Energy Sustainability*, (ES2008-54090):329–334, 2008.
- [23] C.K. Ho, S.S. Khalsa, and N.P. Siegel. Modeling On-Sun Tests Of A Prototype Solid Particle Receiver for Concentrating Solar Power Processes and Storage. *Proceedings of ASME*, pages ES2009–90035, 2009.
- [24] K. Kim, N. Siegel, G. Kolb, V. Rangaswamy, , and S.F Moujaes. A Study of Solid Particle Flow Characterization in Solar Particle Receiver. *Solar Energy*, 83(10):1784–1793, 2009.
- [25] S.S. Khalsa and C.K. Ho. Development of a solar patch calculator to evaluate heliostat-field irradiance as a boundary condition in cfd models. *Proceedings of the ASME 2010 4th International Conference on Energy Sustainability*, 2(ES2010-90052):483490, 2010.
- [26] C.K. Ho S.S. Khalsa. Radiation Boundary Conditions for Computational Fluid Dynamics Models of High-Temperature Cavity Receivers. *Journal of Solar Energy Engineering*, 133(3):031020, 2011.
- [27] N. Siegel, C. Ho, S. Khalsa, and G. Kolb. Development and Evaluation of a Prototype Solid Particle Receiver: On-Sun Testing and Model Validation. *Journal of Solar Energy Engineering*, 132:021008, 2010.
- [28] W. Wu, R. Uhlig, R. Buck, and R. Pitz-Paal. Numerical Simulation of a Centrifugal Particle Receiver for High-Temperature Concentrating Solar Applications. *Numerical Heat Transfer Part A*, 68(2):133–149, 2015.
- [29] Pablo Fernandez del Campo. Numerical-Stochastic Modeling, Simulation and Design Optimization of Small Particle Solar Receivers for Concentrated Solar Power Plants. Master’s thesis, University of Valladolid and San Diego State University, 2013.
- [30] K.H. Huebner, D.L. Dewhirst, D.E. Smith, and T.G. Byrom. *The Finite Element Method*

*for Engineers*. John Wiley & Sons Inc., 3rd edition, 2001.

- [31] M. Peric J.H. Ferziger. *Computational Methods for Fluid Dynamics*. Springer, 3rd edition, 2002.
- [32] NPARC alliance CFD verification and validation Web Site - Tutorial on CFD Verification and Validation. NASA.
- [33] C.ho J. Christian. Alternative designs of a high efficiency, north-facing, solid particle receiver. *Energy Procedia*, 49:314–323, 2014.



## **APPENDIX**

### **A - Manual of the code**

## A - Manual of the code

The following code simulates the heat transfer in a sample of particles inside a FPR. It has been divided in five parts:

Part 1: Generation of randomly located particles with different radii

Part 2: Relocation of the generated particles to the axes of interest

Part 3: Generation of a mesh inside the particles

Part 4: Initial Solution

Part 5: Heat transfer in the particles

Part 5.1: Generation of random rays and their reflections

Part 5.2: Heat Transfer resolution with the FEM

### A.1 Explanation of the different parts

#### Part 1: Generation of randomly located particles with different radii

The original version of this part of the code was developed by Andrea Chiarelli, Andrew Dawson, Alvaro Garcia from The University of Nottingham (The MIT License).

Its purpose is to generate particles randomly located in a two-dimensional area, that do not overlap each other and have a random radius inside a chosen range. The code has been slightly modified, and the parameters have been chosen to meet the requirements of the present Thesis. The process of generation of particles in the desired area is a little complicated, since there are some limitations derived from the use of an already existing code. It has been decided that the easiest way to go is to, first, generate the particles in an area that does not lead to any problems in the original code and, secondly, relocate said particles in the real area of interest.

Thereby, the particles are initially generated in a area of  $3 \times 5 \text{ m}$ , and have a radius in the range of  $\text{cm}$ . Since this dimensions are obviously way too big for the area and particles that we want to study, everything must be scaled and relocated, which is later done in Part 2.

It is important to highlight that the user can choose the maximum and minimum radii that desires for the particles, introducing said values in the parameters *max\_radius* and *min\_radius* in  $\text{mm}$ . In order to generate and study a manageable number of particles, the target planar void ratio used in the example simulations has been between 99% and 90% (*target\_planar\_void\_ratio* from 99 to 90), a parameter that can easily be changed by the user according to his needs if desired.

#### Part 2: Relocation of the generated particles to the axes of interest

The first step in this part of the code is the definition of the parameter *scale* = 0.01. Multiplying the dimensions obtained in Part 1 by this parameter, we obtain the units that we desired: the unit  $\text{m}$  becomes  $\text{cm}$  and the unit  $\text{cm}$  becomes  $0.1 \text{ mm}$ . This means that the area where particles

are generated is now a rectangle of  $3 \times 5 \text{ cm}$ , and the radii of the particles is in the range of  $0.1 \text{ mm}$ . The process carried out in this part is simply a relocation of the centers of the particles in the area of  $3 \times 5 \text{ cm}$ , taking into account geometric considerations.

### Part 3: Generation of a mesh inside the particles

This section of the code has been developed in combination with a code created by Emmanuel Lefrançois from the Université de Technologie de Compiègne for the resolution of conduction heat transfer using the FEM.

With the mesh generator Gmsh, a default grid has been created for a generic circle of  $R = 1 \text{ mm}$ , as was explained in section 4.1.3 of this report. This same grid is implemented in every particle studied, but the position of the nodes and elements must be properly relocated for each of them, according to their particular radii.

The program reads a file named *circle.msh* created with Gmsh generator that has a specific format, and then the process followed is just a relocation of the grids considering the centers of the particles, and of the position of the nodes considering the radii of the particles (scaling). If the user wants to work with another grid, he must provide a file named *circle.msh* created with Gmsh generator, and in order for it to have the correct format he must make some modifications to it.

First, the user must check if the number of nodes is written in the 5th row of the file and followed by the number and coordinates that correspond to all the nodes, like this:

```

1 $MeshFormat
2 2.2 0 8
3 $EndMeshFormat
4 $Nodes
5 314
6 1 0 0 0
7 2 0.001 0 0
8 3 0 0.001 0
9 4 0.001 0 0
10 5 0 0.001 0
11 ...

```

If there are more lines above, the user must change the file *get\_mesh.m* so that it ignores all those lines and the first thing it reads is the number of nodes.

If the file *circle.msh* has the number of nodes in the 5th row as said above, the file *get\_mesh.m* ignores the lines above this way:

```

1 fid = fopen(filename);
2
3 % Lecture of the first 4 useless lines
4 for i = 1:4
5     s = fgetl(fid);
6 end
7 ...

```

So if, for example, the number of nodes was written in the 15th row of the file *circle.msh*, the file *get\_mesh.m* should be:

```

1 fid = fopen(filename);
2
3 % Lecture of the fist 14 useless lines
4 for i = 1:14
5     s = fgetl(fid);
6 end
7 ...

```

Secondly, the user must change the numbers of the file that correspond to the elements, so that they have this format:

```

1 $Elements
2 624
3 1 1 2 11 1 2 6
4 2 1 2 11 1 6 7
5 3 1 2 11 1 7 8
6 4 1 2 11 1 8 9
7 5 1 2 11 1 9 10
8 6 1 2 11 1 10 11
9 7 1 2 11 1 11 12
10 8 1 2 11 1 12 13
11 9 1 2 11 1 13 14
12 10 1 2 11 1 14 15
13 ...
14 ...
15 ...
16 53 2 2 31 6 235 79 148
17 54 2 2 31 6 128 235 148
18 55 2 2 31 6 74 128 148
19 56 2 2 31 6 94 193 139
20 57 2 2 31 6 95 194 138
21 58 2 2 31 6 79 235 150
22 59 2 2 31 6 108 150 235
23 60 2 2 31 6 66 112 184
24 61 2 2 31 6 87 184 112
25 62 2 2 31 6 66 282 228
26 63 2 2 31 6 113 254 175
27 64 2 2 31 6 115 174 255
28 ...

```

The explanation of this format is, reading the rows of numbers from the left to the right:

The first number is the element number.

The second number is a 1 if the element is a line with  $n = 2$  nodes and a 2 if the element is a triangle with  $n = 3$  nodes, and will directly come out like this from Gmsh generator.

The third number must be a 2 and will be ignored by the program.

The fourth number must be changed by the user. He must write 11 for the linear elements (being 11 the initial condition that means that no ray has hit the boundary line that surrounds that element), and 31 for the triangular elements (a number later used to obtain the material properties stored in other part of the program). Once the program is run, everytime a ray hits a

linear element the number 11 will be change to a 12.

The next numbers must not be changed, being the last two or three the numbers of the nodes that make up each element.

#### Part 4: Initial Solution

The initial value of the temperature in every node of every particle is the one introduced by the user as *initial\_temperature*, in °C. In all the examples presented in this paper, *initial\_temperature* = 20. In this part of the program all the particles generated in Parts 1 and 2 will be plotted in their positions – in Figure 1 –, and the smaller area of particles that has been chosen to use for the heat transfer resolution will be plotted too – in Figure 2 –. In both cases, the particles will be shown in the color corresponding to their initial temperature according to the colorbar located on the side of the figures. The vertical yellow line represents the window where rays come from, and the vertical blue line represents the back wall of the receiver cavity, where rays are reflected every time they reach it. The position of the window is established when the user defines the distance between the curtain of falling particles and the window, with the parameter *distance\_window\_curtain*. The curtain of falling particles starts at X=0, so the distance chosen will set the window in a negative position of the coordinate X. The positions of both the window and the back wall are chosen by the user. The position of the back wall in Figures 1 and 2 does not have to be the same. It may be convenient to simulate it closer to the window than it is in reality, since we are working with a reduced model. This position of the back wall in Figure 2 is defined by the user with the parameter *xdest*.

A simulation has been run to exemplify what has been explained above, with the following values for the parameters of interest:

*initial\_temperature* = 20

*distance\_window\_curtain* = 0

*target\_planar\_void\_ratio* = 90

Area where particles are created (not chosen by the user):

*xorigmin\_part* = 0

*xorigmax\_part* = 0.030

*yorigmin\_part* = *xorigmin\_part*

*yorigmax\_part* = 0.050

Area where the particles will be studied:

*xmin\_area* = 0

*xmax\_area* = 0.005

*ymin\_area* = 0

*ymax\_area* = 0.005

Area that will be plotted, slightly bigger than the previous one:

*xaxismin\_area* = -0.0030

*xaxismax\_area* = 0.008

*yaxismin\_area* = -0.0005

*yaxismax\_area* = 0.0055

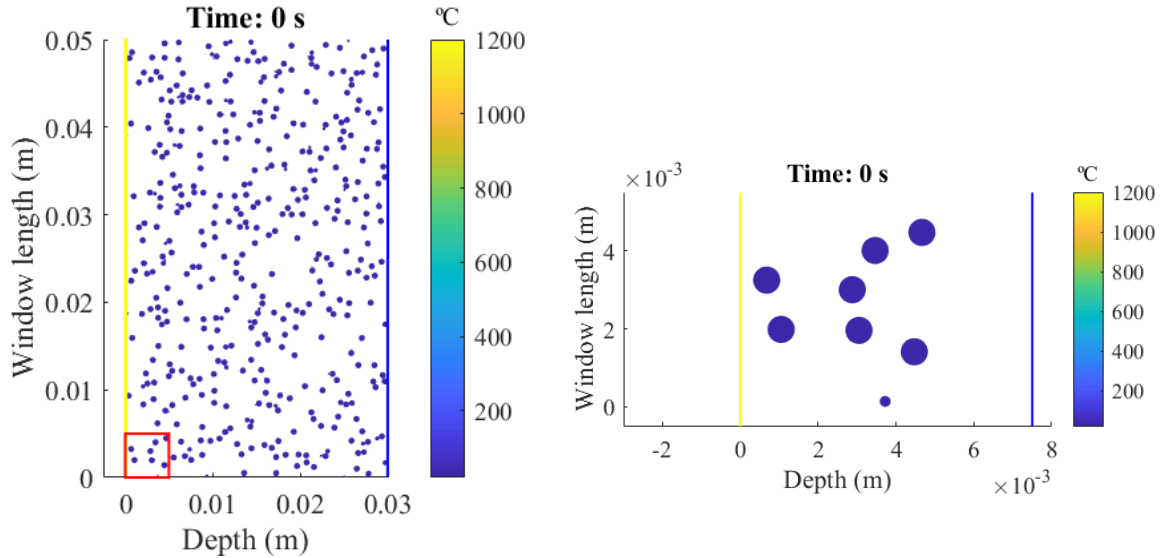


Figure A.1: Example of plotted Figures 1 and 2.

## Part 5: Heat transfer in the particles

In this last part of the code, the rays are created and the simulation of radiation and conduction heat transfer takes place. It has been divided in two parts, the first one for the generation of the rays and the second one for the heat transfer modeling.

### Part 5.1: Generation of random rays and their reflections

This section is also separated in two parts: one for the solar rays, and one for the rays emitted by the particles because of their temperature.

#### Solar rays

The solar rays are considered start at the window, and are separated between them a uniform distance  $dy$  defined by the user. This means that the origin point of all the solar rays has the same X coordinate, and the Y coordinate of the origin point of every ray varies a distance  $dy$  with the previous ray.

The destination point of every ray is a has the same X coordinate as the back wall, and a random Y coordinate inside the range  $[y_{destmin}, y_{destmax}]$  defined by the user, that also has a distance of  $dy$  between every possible point in said range.

The code has been written in a way that runs ray by ray in a big loop. Inside it, there is another loop that runs every section of the studied ray, being a section the straight line the ray describes between reflection consecutives points. In order to calculate the point where the ray will be reflected, the code equalizes the equation of a line of the studied section of the ray ( $y = m \cdot x + n$ ) with the equation of a circle of every particle ( $r = (x - a)^2 + (y - b)^2$ ). If there are points of the line of the ray that coincide with any points of the circumferences of

the particles, the code chooses the closest point found in this calculation as the next reflection point. This is graphically exemplified in the following Figure A.2, where, after finding four possible intersection points of the ray with the circumferences, the code chooses the closest one and ignores the rest. Then the ray is redirected in a random direction and the process continues.

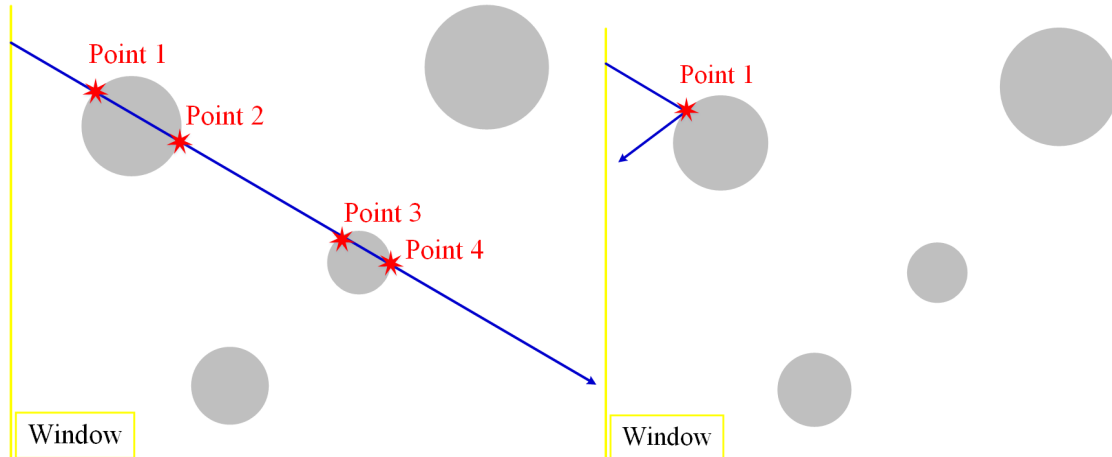


Figure A.2: Choice of the point of reflection of a ray.

If the ray does not find any particle in its way and reaches the back wall, it will be reflected by it. However, if it reaches the window it will not be reflected back into the receiver but will go out of the area of study. The choice of the new direction followed by a ray after being reflected by a particle takes various steps. First, an angle  $\alpha$  is calculated, in a range from  $0^\circ$  to  $360^\circ$  as shown in Figure A.4.

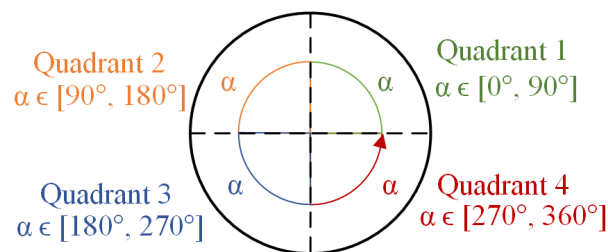
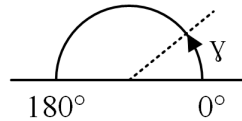


Figure A.3: Angle  $\alpha$  from the reflection point.

Secondly, a random angle  $\gamma$  is generated in a range from  $0^\circ$  to  $180^\circ$ .

Figure A.4: Random angle  $\gamma$ .

We want to find a destination point for the ray that is realistic. We can combine  $\gamma$  and  $\alpha$  in the following manner to obtain a new direction for the ray:

$$x_{destinationpoint} = x_{reflectionpoint} + \cos(\gamma + \alpha - 90^\circ)$$

$$y_{destinationpoint} = y_{reflectionpoint} + \sin(\gamma + \alpha - 90^\circ)$$

However, the destination point obtained this way will be too close to the particle and inside the area of study. This can be graphically seen in the example Figure A.5.

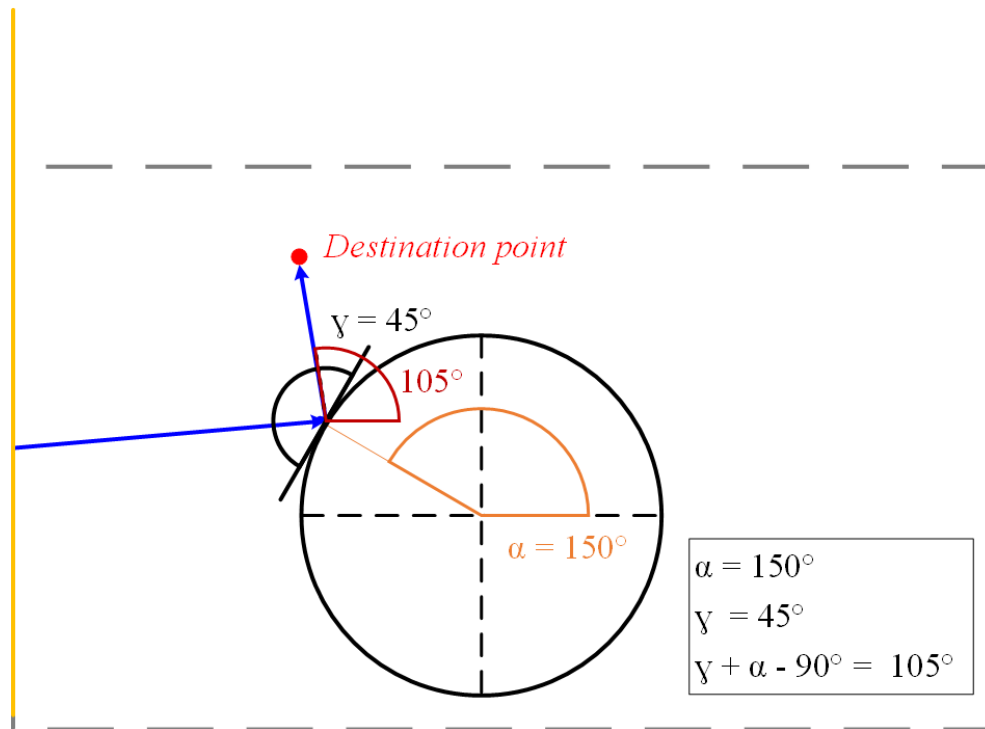


Figure A.5: Example of a destination point after a reflection that would be too close to the particle.

To solve this small problem we multiply by a constant  $K$  (named  $k\_length$  in the code), so that the destination point is further from the particle and outside of the area of study:

$$x_{destinationpoint} = x_{reflectionpoint} + K \cdot \cos(\gamma + \alpha - 90^\circ)$$

$$y_{destinationpoint} = y_{reflectionpoint} + K \cdot \sin(\gamma + \alpha - 90^\circ)$$

This final solution is seen in Figure A.6.



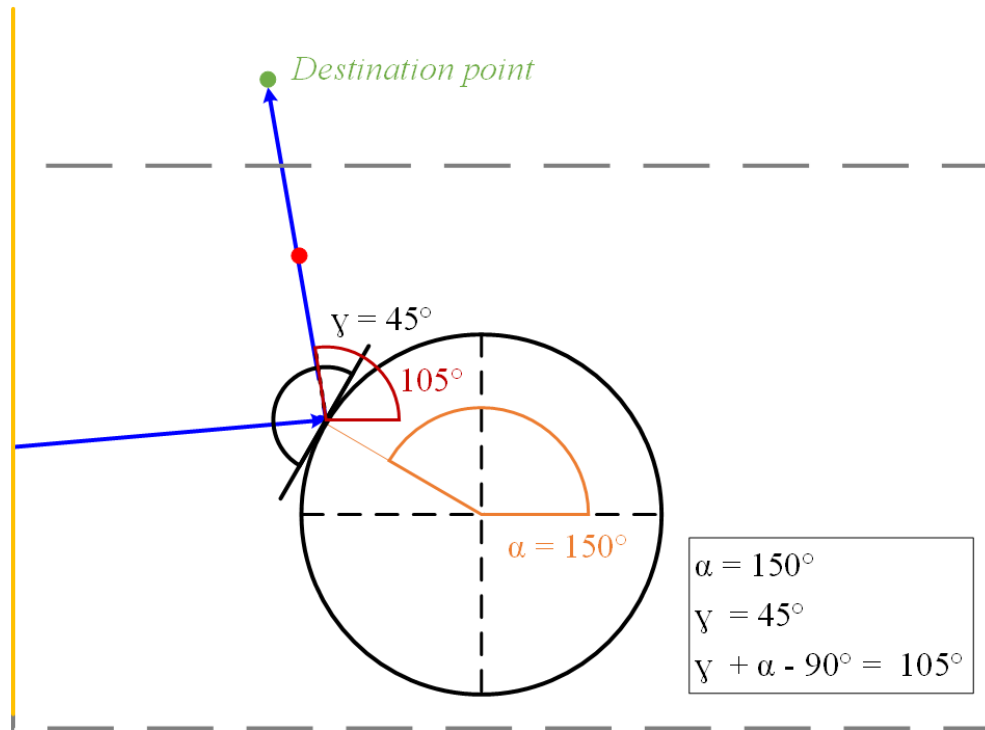


Figure A.6: Destination point after a reflection.

The rays can be reflected as many times as the user desires. Since every time that they are reflected by a particle a big part of their energy is absorbed by it, after a few reflections its energy can be considered negligible. The maximum number of sections allowed for each solar ray is then decided by the user with the parameter *n\_sections\_ray*.

Information about every reflection that has been experimented by a solar ray along its path is stored in the matrix *ray\_intersections*, and information about every reflection of solar rays that has happened in the surface of a particle is stored in the matrix *particle\_intersections*.

### Emitted rays

As was explained in section 4.1.3, a grid has been used in every particle to model the conduction heat transfer. The contour of the circular grid is made up of a number of linear elements of  $n = 2$  nodes each, while the interior of the particles is made up of triangular elements of  $n = 3$  nodes each. In order to model the emission of radiation by the particles, it has been considered that every linear element of the boundary of the particles (that we often refer to as *boundary lines*) emits one ray. Since the chosen grid has 52 linear elements in the contour of the circle (parameter *n\_bars* in the code), every particle will emit 52 rays due to its temperature.

The energy of these emitted rays is calculated with the Stefan-Boltzmann law for gray bodies (Equation (2.4)), using for the value of the temperature the mean between the temperature of the two nodes of each element.

From this point, the emitted rays are modeled just like the solar rays: as straight lines that are reflected and absorbed by other particles, also reflected on the back wall or that go out through

the receiver window. The maximum number of sections allowed for each emitted ray is the same as for the solar rays:  $n\_sections\_ray$ . Information about every reflection that has been experimented by an emitted ray along its path is stored in the matrix  $ray\_intersections\_em$ , and information about every reflection of rays emitted by other particles that has happened in the surface of a concrete particle is stored in the matrix  $particle\_intersections\_em$ .

## Part 5.2: Heat Transfer resolution with the FEM

This part of the code models the heat transfer as a result from the interaction between the rays and the particles. Every time that a solar ray hits a particle, information about this fact is stored in  $particle\_intersections$  and  $ray\_intersections$ , and every time that a ray emitted by one particle hits another particle, the information is stored in  $particle\_intersections\_em$  and  $ray\_intersections\_em$ . The information about all the rays emitted by the particles is stored in  $emission\_radiation$ .

These interactions between rays and particles generate a heat transfer that is modeled with the Finite Element Method. A very important part of this code consists on the treatment on the boundary conditions implemented in the boundary lines of every particle, that change in every time step, due to the impact of rays and the emission of rays. This treatment is explained step by step in the following paragraphs.

The energy absorbed by a particle when it is hit by the first section of one solar ray (which means that it just came from the window and has all the energy) is (representing the initial energy of the ray as  $E_{solar}$ ):

$$E_{solar}(W) \cdot \alpha$$

The energy absorbed by a particle when it is hit by the second section of one solar ray is the initial energy that the ray had minus the energy that it has lost when it was absorbed in its first reflection times the absorptivity  $\alpha$ :

$$(E_{solar}(W) - E_{solar}(W) \cdot \alpha) \cdot \alpha = E_{solar}(W) \cdot (1 - \alpha) \cdot \alpha$$

The energy absorbed by a particle when it is hit by the third section of one solar ray is the initial energy that the ray had minus the energy that it has lost when it was absorbed in its first and second reflections times the absorptivity  $\alpha$ :

$$(E_{solar}(W) - E_{solar}(W) \cdot (1 - \alpha) \cdot \alpha) \cdot \alpha = E_{solar}(W) \cdot (1 - \alpha)^2 \cdot \alpha$$

The energy absorbed by a particle when it is hit by the fourth section of one solar ray is the initial energy that the ray had minus the energy that it has lost when it was absorbed in its first, second and third reflections times the absorptivity  $\alpha$ :

$$(E_{solar}(W) \cdot (1 - \alpha)^2 \cdot \alpha) \cdot \alpha = E_{solar}(W) \cdot (1 - \alpha)^3 \cdot \alpha$$

... and so on.

This way, the energy that one boundary line absorbs can be easily calculated if it is known how many rays in each section hit it. For example, if one specific boundary line is hit by 5

solar rays that are in their first section, 7 solar rays that are in their second section and 2 solar rays that are in their fifth section, the total absorbed energy:

$$E_{solar}(W) \cdot \alpha \cdot [5 \cdot (1 - \alpha)^0 + 7 \cdot (1 - \alpha)^1 + 0 \cdot (1 - \alpha)^2 + 0 \cdot (1 - \alpha)^3 + 2 \cdot (1 - \alpha)^4 + 0 \dots]$$

In our code, this absorption is calculated when the Neumann boundary conditions are applied on the boundary lines (in the file *data\_boundaryconditions\_lines.m*).

It is necessary to highlight that the code does not work with  $E_{solar}(W)$ , but with

$$\frac{\text{Flux}\left(\frac{W}{m^2}\right)}{\text{arc\_length}(m^2)} = E_{solar}(W).$$

The exact appearance found in the file *data\_boundaryconditions\_lines.m* of the energy absorbed by a boundary line is

```
1 flux*absp/arc_length(p,1)*incident_sun(ie,1,p)
```

being *incident\_sun* a summation in the style of one shown in the example above. The program will make this calculation for every boundary line of every particle.

The calculation of the energy from rays emitted by other particles that is absorbed by one boundary line when it is hit by them follows the same logic. For every ray in every boundary line, the code calculates the energy absorbed as

$$E_{emission}(W) \cdot (1 - \epsilon)^n \cdot \epsilon = \frac{\text{Flux}\left(\frac{W}{m^2}\right)}{\text{arc\_length}(m^2)} \cdot (1 - \epsilon)^n \cdot \epsilon$$

being *n* the number of times that the ray has been reflected and absorbed by other particles (without including the times that it has been reflected on the wall).

The exact appearance of this calculation in the code is:

```
1 (particle_intersections_em(row(j,1),4,p)/arc_length(p,1))*e*((1-e)^n);
```

In order to calculate the total energy that comes in or goes out of a specific boundary line, the code sums the energy absorbed from solar rays and the rays emitted by other particles, and subtracts the energy that the boundary line emits because of its temperature:

Total energy absorbed = Energy absorbed from solar rays + energy absorbed from emitted rays  
- energy emitted

The appearance of this calculation in the file *data\_boundaryconditions\_lines.m* is:

```
1 (flux*absp/arc_length(p,1))*incident_sun(ie,1,p) + emission_radiation(ie,p)
2 emission_radiation_incident(ie,p)
```

## A.2 Parameters and Matrices

### General parameters

*solar\_flux*: Input value. Concentrated solar flux considered in watts.  
*n\_reflections*: Input value. Number of sections that will be simulated for each ray.  
*s\_b*: StefanBoltzmann constant.  
*e*: Emissivity of the particles.  
*absp*: Absorptivity of the particles.  
*k*: Conductivity of the particles in  $\frac{W}{m \cdot K}$ .  
*dens*: Density of the particles in  $\frac{kg}{m^3}$ .  
*cp*: Specific heat of the particles in  $\frac{J}{kg \cdot K}$ .

## Part 1: Generation of randomly located particles with different radii

### Parameters

*xaxismin*: Input value. Minimum value for the axis of the X-coordinate.  
*xaxismax*: Input value. Maximum value for the axis of the X-coordinate.  
*yaxismin*: Input value. Minimum value for the axis of the Y-coordinate.  
*yaxismax*: Input value. Maximum value for the axis of the Y-coordinate.  
*target\_planar\_void\_ratio*: Input value. Planar void content as a percentage.  
*max\_radius*: Input value. Maximum value desired for the radius of the particles in *mm*.  
*min\_radius*: Input value. Minimum value desired for the radius of the particles in *mm*.  
*origin\_of\_cartesian\_axes*: Input value. Origin of the cartesian axes for the rectangular domain where particles are created (*m*).  
*rectangle\_width*: Rectangle width (*m*).  
*rectangle\_height*: Rectangle height (*m*).  
*number\_of\_domains*: Number of packed domains to generate.  
*number\_of\_particles*: Input value. Number of particles in the first generation seeded.  
*new\_particles\_per\_generation*: Number of particles added in each new generation.  
*maximum\_radius*: Minimum radius of the generated particles in *m*, directly derived from the value introduced by the user in *max\_radius*.  
*minimum\_radius\_seeded*: Maximum radius the generated particles in *m*, directly derived from the value introduced by the user in *min\_radius*.  
*counter*: Counter of the number of particles in each iteration.  
*can\_it\_grow*: Logical condition that will indicate if a particle is allowed to grow.  
*squared\_sum\_of\_radii*: Squared sum of the radii of the particles, later used to obtain the total area of the circles.  
*n\_particles*: Number of particles that have been generated. This number will change when a smaller number of particles is chosen for the heat transfer study.  
*n\_particles\_initial*: Number of particles that were generated initially.

**Matrices**

*radius*: Radii of the particles (*m*).

Particle number	Radius
1	$(radius_1)$
2	$(radius_2)$
...	...
...	...
n_particles	$(radius_n)$

*centre*: X and Y coordinates of the particles' centers.

Particle number	X-coordinate	Y-coordinate
1	$(X_1)$	$(Y_1)$
2	$(X_2)$	$(Y_2)$
...	...	...
...	...	...
n_particles	$(X_n)$	$(Y_n)$

*angles\_for\_parametric\_circle*: Angles for the equation for parametric circumferences.

*x\_coordinates\_circles*: X-coordinates of the particles.

*y\_coordinates\_circles*: Y-coordinates of the particles.

## Part 2: Relocation of the generated particles to the axes of interest

### Parameters

*xorig*: Input value. Value of the X-coordinate for the origin of the rays.

*xdest*: Input value. Value of the X-coordinate for the destination of the rays.

*yorigmin*: Input value. Minimum value of the Y-coordinate for the origin of the rays.

*yorigmax*: Input value. Maximum value of the Y-coordinate for the origin of the rays.

*ydestmax*: Input value. Minimum value of the Y-coordinate for the destination of the rays.

*ydestmin*: Input value. Maximum value of the Y-coordinate for the destination of the rays.

*dy*: Input value. Separation between rays in the Y-axis ( $m$ ).

*yorigmin\_part*: Input value. Lower limit of the Y-coordinate to relocate the particles ( $m$ ).

*yorigmax\_part*: Input value. Upper limit of the Y-coordinate to relocate the particles ( $m$ ).

*r\_standard*: Input value. Desired value for the average radius ( $m$ ).

*scale*: rstandard times 10.

*xmed*: Middle point in the studied range of the X-coordinate.

*ymed*: Middle point in the studied range of the Y-coordinate.

*x1*: X-coordinates of the rays' origins. Constant value.

*y1*: Range for the Y-coordinates of the rays' origins. Equally spaced values.

*n\_rays*: Number of rays.

*x2*: X-coordinates of the rays' destinations. Constant value.

*y2*: Range for the Y-coordinates of the rays' destination. Random value in this range.

## Matrices

*centre\_initial*: Coordinates of the centers of the particles generated in the part 1 of the program.

*radius\_initial*: Radii of the particles generated in the part 1 of the program ( $m$ ).

<b>Particle number</b>	<b>Radius</b>
1	$(radius_1)$
2	$(radius_2)$
...	...
...	...
n_particles	$(radius_n)$

*radius*: Scaled radii of the particles ( $m$ ).

<b>Particle number</b>	<b>Radius</b>
1	$(radius_1)$
2	$(radius_2)$
...	...
...	...
n_particles	$(radius_n)$

## Part 3: Generation of a mesh inside the particles

### Parameters

*nnt*: Total number of nodes.

*n\_bn*: Number of boundary nodes.

*n\_bars*: Number of boundary lines (elements with  $n = 2$  nodes where the boundary conditions are applied).

### Matrices

*vcorg\_stored*: Correct coordinates of the nodes.

<b>Node number</b>	<b>X-coordinate</b>	<b>Y-coordinate</b>
1	$X_1$	$Y_1$
2	$X_2$	$Y_2$
...	...	...
...	...	...
nnt	$X_n$	$Y_n$

*vcorg\_original*: Coordinates of the nodes before they were moved to its right location for each particle.

Particle number	X-coordinate	Y-coordinate
1	$X_1$	$Y_1$
2	$X_2$	$Y_2$
...	...	...
...	...	...
n_particles	$X_n$	$Y_n$

*r\_1*: Distance between the corresponding node and the center of the corresponding particle ( $m$ ).

Node number	Distance
1	$(distance_1)$
2	$(distance_2)$
...	...
...	...
nnt	$(distance_n)$

*r\_2*: *r\_1* correctly scaled ( $m$ ).

Node number	Distance
1	$(distance_1)$
2	$(distance_2)$
...	...
...	...
nnt	$(distance_n)$

*vcorg\_scaled*: Coordinates of every particle's nodes.

Node number	X-coordinate	Y-coordinate
1	$X_1$	$Y_1$
2	$X_2$	$Y_2$
...	...	...
...	...	...
nnt	$X_n$	$Y_n$

*boundary\_nodes*: Number of the boundary nodes that form every boundary line.

<b>Boundary line number</b>	<b>Node number 1</b>	<b>Node number 2</b>
1	$Nodenumber$	$Nodenumber$
2	$Nodenumber$	$Nodenumber$
...	...	...
...	...	...
n_bars	...	...

*boundary\_nodes\_vector*: List of the numbers of the boundary nodes.

<b>Node number</b>
1
2
...
...
$n_{bn}$

*vcorg\_scaled\_boundary*: Coordinates of the boundary nodes of every particle.

<b>Node number</b>	<b>X-coordinate</b>	<b>Y-coordinate</b>
1	$X_1$	$Y_1$
2	$X_2$	$Y_2$
...	...	...
...	...	...
n_bn	$X_n$	$Y_n$

*arc\_length*: Length of the boundary lines of every particle ( $m$ ).

<b>Particle number</b>	<b>Arc length</b>
1	$arclength$
2	$arclength$
...	...
...	...
n_particles_initial	$arclength$

## Part 4: Initial Solution

### Parameters

Region where particles will be initially generated, plotted in Figure 1:

*xorigmin\_part*: Minimum value of the X- coordinate.



*xorigmax\_part*: Maximum value of the X- coordinate.

*yorigmin\_part*: Minimum value of the Y- coordinate.

*yorigmax\_part*: Maximum value of the Y- coordinate.

Choice of smallest region inside the previous one where heat transfer will be studied in the particles:

*xmin\_area*: Input value. Minimum value of the X- coordinate.

*xmax\_area*: Input value. Maximum value of the X- coordinate.

*ymin\_area*: Input value. Minimum value of the Y- coordinate.

*ymax\_area*: Input value. Maximum value of the Y- coordinate.

Choice of the region that will be plotted in the study of heat transfer, plotted in Figure 2. It is recommended to choose an area slightly bigger than the one defined above.

*xaxismin\_area*: Input value. Minimum value of the X- coordinate.

*xaxismax\_area*: Input value. Maximum value of the X- coordinate.

*yaxismin\_area*: Input value. Minimum value of the Y- coordinate.

*yaxismax\_area*: Input value. Maximum value of the Y- coordinate.

*initial\_temperature*: Input value. Initial temperature of the particles.

*distance\_window\_curtain*: Input value. Distance in *m* between the window and the curtain of falling particles. This value directly establishes the position of the window, which is the X-coordinate for the origin of the solar rays.

*count\_fig*: Counts the number of figures plotted.

*time\_previous\_iteration*: Time when the previous iteration ended (*s*).

## Matrices

*area\_study\_1*: Checking the centers of every particle, writes a 1 if the coordinates of their centers are bigger than the minimum of the area of interest, and a 0 otherwise.

<b>Particle number</b>	<b>Value correspondent to the X-coordinate of the center</b>	<b>Value correspondent to the Y-coordinate of the center</b>
1	0 – 1	0 – 1
2	0 – 1	0 – 1
...	...	...
...	...	...
n_particles_initial	0 – 1	0 – 1

*area\_study\_2*: Checking the centers of every particle, writes a 1 if the coordinates of their centers are smaller than the maximum of the area of interest, and a 0 otherwise.

Particle number	Value correspondent to the X-coordinate of the center	Value correspondent to the Y-coordinate of the center
1	0 - 1	0 - 1
2	0 - 1	0 - 1
...	...	...
...	...	...
n_particles_initial	0 - 1	0 - 1

*area\_study\_3*: Sums the numbers (0 or 1) obtained in *area\_study\_1* and *area\_study\_2* for the X coordinates of the centers, and the numbers obtained for the Y coordinates of the centers. The results can be 0, 1 or 2.

Particle number	Value correspondent to the X-coordinate of the center	Value correspondent to the Y-coordinate of the center
1	0 - 1 - 2	0 - 1 - 2
2	0 - 1 - 2	0 - 1 - 2
...	...	...
...	...	...
n_particles_initial	0 - 1 - 2	0 - 1 - 2

*area\_study\_4*: Sums the numbers obtained in *area\_study\_3* for both the X coordinates and the Y coordinates. The results can be 0, 1, 2, 3 or 4, being the particles where a 4 is obtained inside the area of interest. *particles\_area\_study*: numbers of the particles that have been found inside the area of interest.

Particle number	Value correspondent to the center
1	0 - 1 - 2 - 3 - 4
2	0 - 1 - 2 - 3 - 4
...	...
...	...
n_particles_initial	0 - 1 - 2 - 3 - 4

*vsol*: Temperature of the nodes ( $^{\circ}C$ ).

Node number	Temperature
1	$(temperature_1)$
2	$(temperature_2)$
...	...
...	...
nnt	$(temperature_n)$

## Part 5: Heat transfer in the particles

### Parameters

*flux*: Thermal flux in every solar ray ( $W$ ).

*n\_rays\_em* : number of rays emitted by a particle.

*DV1*: Input value. Default value for the number of rows in the matrices: *rays*, *unions*, *tangents*, *true\_xint*, *true\_int*.

*DV2*: Input value. Default value for the number of rows in the matrices: *xint*, *XX*, *YY*, *DD*.

*DV3*: Input value. Default value for the number of rows in the matrix: *particle\_intersections\_em*.

*DV4*: Input value. Default value for the number of rows in the matrix: *particle\_intersections*.

### Matrices

*average\_temp*: stores the average temperature of the nodes of every particle every 10 timesteps.

*time\_axis*: stores the time every 10 timesteps.

## Part 5.1: Generation of random rays and its reflections

### Parameters

*xorig*: X- coordinate where the window is located, which is also the X-coordinate of the origin of the rays.

*xdest*: X- coordinate where the back wall is located, which is also the X-coordinate of the destination of the rays.

*yorigmin*: minimum value of the Y-coordinate of the window from where the solar rays will be originated.

*yorigmax*: maximum value of the Y-coordinate of the window from where the solar rays will be originated.

*dy*: distance between consecutive rays that come from the window ( $m$ ).

The parameters *yorigmin* and *yorigmax* are respectively lower and higher than the area where heat transfer is studied in the particles. This is due to the fact that it is realistic to assume that the particles will not only be irradiated by rays coming from the section on the window located exactly at their height (Y-coordinate), but also by rays coming from lower and higher parts of the window.

*ydestmax*: maximum value of the Y-coordinate of the back wall towards where the solar rays will be directed.

*ydestmin*: minimum value of the Y-coordinate of the back wall towards where the solar rays will be directed.

These parameters can be schematically seen in Figure [A.7](#).

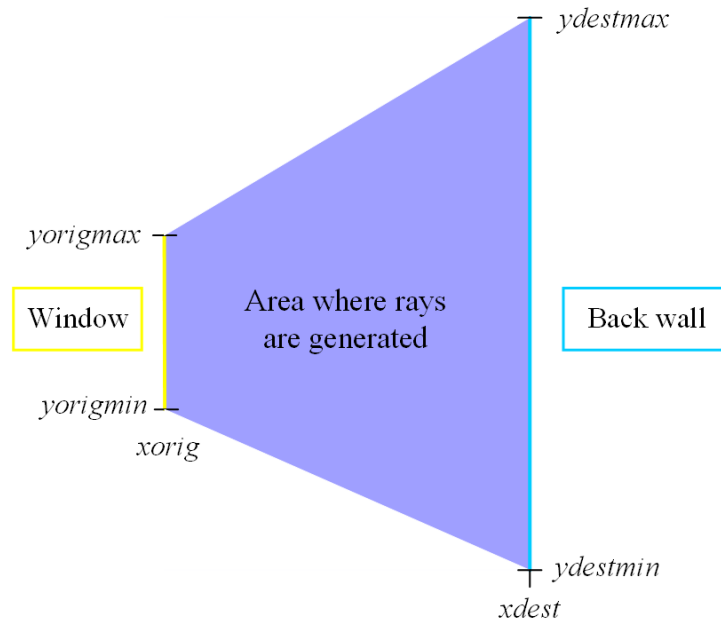


Figure A.7: Area where rays are generated.

$x1$ :  $x_{orig}$ .

$y1$ : vector that contains all the Y-coordinates of the origin points of the solar rays.

$n_{rays}$ : number of solar rays.

$x2$ :  $x_{dest}$ .

$y2$ : vector that contains all the possible Y-coordinates of the destination points of the solar rays.

$a$ : X-coordinate of the center of the studied particle.

$b$ : Y-coordinate of the center of the studied particle.

$r$ : Radius of the studied particle.

$prev_{ref\_in\_part}$ : Indicates if the ray's previous reflection was on a particle (1: Yes, 0: No).

$n_{wall\_refl}$ : Number of times the ray has been reflected on the back wall.

Mathematically speaking, when a line intersects with a circle, there are two intersection points. In reality, rays cannot go through the particles, which is why there is only one intersection point, where reflection happens (reflection point). The other point calculated has been called impossible point. This has been graphically exemplified in Figure A.8.

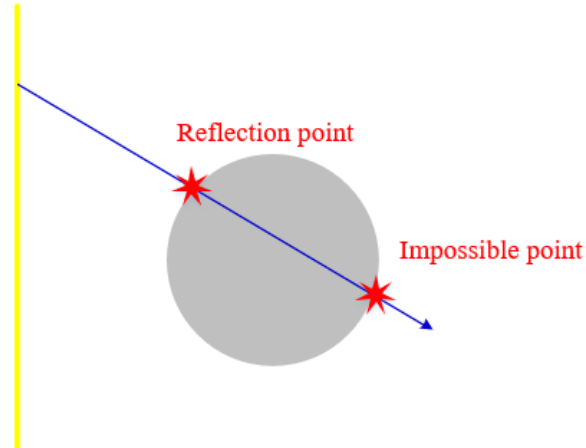


Figure A.8: Graphical example of the two intersection points between a ray and a particle.

The equation of a line is  $y = mx + n$ , being:

$m$ : Intersection point of the line with the ordinate axis (value of Y when X=0).

$n$ : Slope of the line.

$m1$ : m for the studied ray.

$n1$ : n for the studied ray.

$xreflection\_point$ : X-coordinate of the reflection point.

$yreflection\_point$ : Y-coordinate of the reflection point.

$ximpossible\_point$ : X-coordinate of the impossible point.

$yimpossible\_point$ : Y-coordinate of the impossible point.

$C$ : Indicates if there has been an intersection (1:Yes, 0:No).

$shortest\_d$ : Shortest distance in matrix DD.

$row\_previous$ : Number of the particle that reflects the studied ray.

$xint\_true$ : X-coordinate of the intersection point.

$yint$ : Y-coordinate of the intersection point.

$x\_or$ : X-coordinate of the origin of the studied ray.

$y\_or$ : Y-coordinate of the origin of the studied ray.

$gamma$ : Random angle in the range  $[0, \pi]$  (rad).

$alpha$ : Angle between the reflection point and the horizontal line of the first quadrant of the circle (rad). See Figure A.4.

$beta$ : Angle necessary to get the right reflection direction for the ray (rad).  $beta = alpha - 90^\circ$ .

$k\_length$ : Input value. Number high enough to make sure the destination point of the ray is out of the studied boundary.

$xor\_c0$ : X-coordinate of the origin of the ray.

$yor\_c0$ : Y-coordinate of the origin of the ray.

$xdest\_c0$ : X-coordinate of the initial destination of the ray.

$ydest\_c0$ : Y-coordinate of the initial destination of the ray.

$x\_wall$ : X-coordinate of the back wall.

$y\_wall$ : Y-coordinate of the reflection of the ray on the back wall.

*gamma1*: Random angle in the range  $[0, \pi]$  (*rad*).  
*beta1*: Input value. Angle necessary to get the right reflection direction for the ray (*rad*).  
*x\_r*: X-coordinate of the final random point that the ray will be reflected towards.  
*y\_r*: Y-coordinate of the final random point that the ray will be reflected towards.  
*m2*: m for reflected ray.  
*n2*: n for the reflected ray.  
*prev\_ref\_in\_part\_em*: Indicates if the emitted ray's previous reflection was on a particle (1:Yes,0:No).  
*n\_wall\_refl\_em*: Number of times the emitted ray has been reflected on the back wall.  
*xor\_c0\_em*: X-coordinate of the origin of the ray.  
*yor\_c0\_em*: Y-coordinate of the origin of the ray.  
*xdest\_c0\_em*: X-coordinate of the initial destination of the ray.  
*ydest\_c0\_em*: Y-coordinate of the initial destination of the ray.  
*position*: Keeps the count of the number of reflections in a particle.  
*n\_times*: Number of times that the studied ray is reflected on the studied particle.  
*node1*: First node of the studied boundary line.  
*node2*: Second node of the studied boundary line.  
*x\_node1*: X-coordinate of node1.  
*y\_node1*: Y-coordinate of node1.  
*x\_node2*: X-coordinate of node2.  
*y\_node2*: Y-coordinate of node2.  
*x\_orig*: X-coordinate of the origin of the emitted ray.  
*y\_orig*: Y-coordinate of the origin of the emitted ray.  
*x\_dest*: X-coordinate of the initial destination of the emitted ray.  
*y\_dest*: Y-coordinate of the initial destination of the emitted ray.  
*temp\_node1*: Temperature of the node1.  
*temp\_node2*: Temperature of the node2.  
*temp\_med\_line*: Average temperature between *temp\_node1* and *temp\_node2*.  
*reps*: Number of times that the studied ray is reflected on the studied particle .  
*repetitions*: Number of rays that are reflected on the studied boundary line of the studied particle.  
*total\_abs\_em*: Total energy is that is absorbed by the studied boundary line of the studied particle coming from other particles' emission (*W*).  
*ray\_n*: Ray that hits the studied boundary line of the particle.  
*part\_n*: Number of the particle that emitted said ray.  
*n*: Number that helps calculate the energy of said ray when it hits the studied boundary line.  
*abs\_energy*: Energy of that ray that is absorbed by the studied boundary line.  
*n\_rays\_em*: Number of rays emitted by every particle.

## Matrices

*points\_origin*: Coordinates of the solar rays' origins.

<b>Ray number</b>	<b>X-coordinate</b>	<b>Y-coordinate</b>
1	$X_1$	$Y_1$
2	$X_2$	$Y_2$
...	...	...
...	...	...
n_rays	$X_n$	$Y_n$

*points\_destination*: Coordinates of the solar ray's initial destinations (they will change if the ray is reflected).

<b>Ray number</b>	<b>X-coordinate</b>	<b>Y-coordinate</b>
1	$X_1$	$Y_1$
2	$X_2$	$Y_2$
...	...	...
...	...	...
n_rays	$X_n$	$Y_n$

*rays*: Stores the values  $m_1$  and  $n_1$  for every ray.

<b>Ray number</b>	<b>m</b>	<b>n</b>
1	$m_1$	$n_1$
2	$m_2$	$n_2$
...	...	...
...	...	...
n_rays	$m_n$	$n_n$

*true\_xint*: X-coordinate of every reflection point.

<b>Reflection number</b>	<b>Ray 1 X-coordinate</b>	<b>Ray 2 X-coordinate</b>	...	<b>Ray n X-coordinate</b>
1	$X_1$	$X_1$	...	$X_1$
2	$X_2$	$X_2$	...	$X_2$
...	...	...	...	...
...	...	...	...	...
n_sections_ray	$X_n$	$X_n$	...	$X_n$

*true\_yint*: Y-coordinate of every reflection point.

Reflection number	Ray 1 Y-coordinate	Ray 2 Y-coordinate	...	Ray n Y-coordinate
1	$Y_1$	$Y_1$	...	$Y_1$
2	$Y_2$	$Y_2$	...	$Y_2$
...	...	...	...	...
...	...	...	...	...
n_sections_ray	$Y_n$	$Y_n$	...	$Y_n$

*ray\_intersections*: For every solar ray, it stores the number of the particle where it has been reflected, the X and Y coordinates of the reflection point, the section of the ray in that reflection, the total number of times that the ray has been reflected on the back wall in that moment and the number of times that the ray has been reflected on the particles on that moment (which is the difference between the two previous values).

Ray number	Particle number	X-coordinate of the reflection point	Y-coordinate of the reflection point	Section number of the ray	Number of reflections on the wall	Number of reflections on the particles
1	$p.number$	$X_1$	$Y_1$	1	$refl.number$	$refl.number$
2	$p.number$	$X_2$	$Y_2$	2	$refl.number$	$refl.number$
...	$p.number$	...	...	...	$refl.number$	$refl.number$
...	$p.number$	...	...	...	$refl.number$	$refl.number$
n_rays	$p.number$	$X_n$	$Y_n$	$n\_sections\_ray$	$refl.number$	$refl.number$

*xint*: Values of the X-coordinates of all the mathematical intersection points of the studied ray with each particle.

Particle number	X-coordinate 1	X-coordinate 1
1	$X_1$	$X_1$
2	$X_1$	$X_1$
...	...	...
...	...	...
n_particles	$X_1$	$X_1$

*XX*: Stores the real values of the X-coordinate of the possible reflection points, and DV2 in the remaining points.



Particle number	X-coordinate 1 or DV2	X-coordinate 2 or DV2
1	...	...
2	...	...
...	...	...
...	...	...
n_particles	...	...

*YY*: Stores the real values of the Y-coordinate of the possible reflection points, and DV2 in the remaining points.

Particle number	Y-coordinate 1 or DV2	Y-coordinate 2 or DV2
1	...	...
2	...	...
...	...	...
...	...	...
n_particles	...	...

*DD*: Stores the distance between the origin of the ray and the possible reflection point and DV2 in the remaining points.

Particle number	Distance or DV2	Distance or DV2
1	...	...
2	...	...
...	...	...
...	...	...
n_particles	...	...

*particle\_intersections*: Stores the number of the solar ray reflected by the particle at one moment, the X and Y coordinates of that reflection point, the number of the section of the solar ray that is reflected, the number of the boundary line of the particle where said reflection happens and the number of times that the solar ray has been reflected on the particles at that moment. Since it is not possible to know a priori how many solar rays are going to be reflected on the surface of a particle, a big default value *DV4* defined by the user is used to establish the size of the matrix. This way, the matrix *particle\_intersections* will be able to store a total of *DV4* reflections of solar rays on the surface of every particle.

	<b>Ray number</b>	<b>X-coordinate of the reflection point</b>	<b>Y-coordinate of the reflection point</b>	<b>Section number of the ray</b>	<b>Affected boundary line number</b>	<b>Number of reflections of the ray on the particles</b>
1	$r.number$	$X_1$	$Y_1$	$s.number$	$b.l.number$	$refl.number$
2	$r.number$	$X_2$	$Y_2$	$s.number$	$b.l.number$	$refl.number$
...	$r.number$	...	...	$s.number$	$b.l.number$	$refl.number$
...	$r.number$	...	...	$s.number$	$b.l.number$	$refl.number$
DV4	$r.number$	$X_n$	$Y_n$	$s.number$	$b.l.number$	$refl.number$

*distance\_to\_intersection*: Distance from every boundary node to the studied reflection point ( $m$ ).

<b>Boundary node number</b>	<b>Distance</b>
1	...
2	...
...	...
...	...
n_bn	...

*n\_intersections*: Stores the number of rays reflected on each particle.

	<b>Number of the particle</b>			
	1	2	...	n_particles
<b>Number of rays reflected</b>	...	...	...	...

*nrays\_l\_z*: Stores the number of rays that are reflected on the same boundary line of a particle and belong to the same section of their corresponding rays.

	<b>Number of the boundary line</b>			
	b.l.1	b.l.2	...	n_lines
<b>Number of reflections</b>	...	...	...	...
1	...	...	...	...
2	...	...	...	...
...	...	...	...	...
n_reflections	...	...	...	...

*rays\_em*: Stores  $m$  and  $n$  for all the rays emitted by every particle.

*points\_origin\_em*: Coordinates of the emitted rays' origins.

Ray number	X-coordinate	Y-coordinate
1	$X_1$	$Y_1$
2	$X_2$	$Y_2$
...	...	...
...	...	...
n_rays_em	$X_n$	$Y_n$

*points\_destination\_em*: Coordinates of the emitted rays' initial destinations (they will change if the ray is reflected).

Ray number	X-coordinate	Y-coordinate
1	$X_1$	$Y_1$
2	$X_2$	$Y_2$
...	...	...
...	...	...
n_rays_em	$X_n$	$Y_n$

*ray\_intersections\_em*: Every particle emits one rays from every one of its boundary lines. Since, in the chosen grid, every particles has 52 boundary lines (n\_bars), every particle emits 52 rays. For every ray emitted by every particle, *ray\_intersections\_em* stores: the number of the particles where it has been reflected, the X and Y coordinates of said reflection points, the section of the ray in that reflection, the total number of times that the ray has been reflected on the back wall in that moment and the number of times that the ray has been reflected on the particles on that moment (which is difference between the two previous values).

Ray number	Particle number	X-coordinate of the reflection point	Y-coordinate of the reflection point	Section number of the ray	Number of reflections on the wall	Number of reflections on the particles
1	$p.number$	$X_1$	$Y_1$	1	$refl.number$	$refl.number$
2	$p.number$	$X_2$	$Y_2$	2	$refl.number$	$refl.number$
...	$p.number$	...	...	...	$refl.number$	$refl.number$
...	$p.number$	...	...	...	$refl.number$	$refl.number$
n_bars	$p.number$	$X_n$	$Y_n$	$n\_sections\_ray$	$refl.number$	$refl.number$

*true\_xint\_em*: X-coordinates of every reflection point.

<b>Reflection number</b>	<b>Ray 1 X-coordinate</b>	<b>Ray 2 X-coordinate</b>	<b>...</b>	<b>Ray n_rays_em X-coordinate</b>
1	$X_1$	$X_1$	...	$X_1$
2	$X_2$	$X_2$	...	$X_2$
...	...	...	...	...
...	...	...	...	...
n_sections_ray	$X_n$	$X_n$	...	$X_n$

*true\_yint\_em*: Y-coordinates of every reflection point.

<b>Reflection number</b>	<b>Ray 1 Y-coordinate</b>	<b>Ray 2 Y-coordinate</b>	<b>...</b>	<b>Ray n_rays_em Y-coordinate</b>
1	$Y_1$	$Y_1$	...	$Y_1$
2	$Y_2$	$Y_2$	...	$Y_2$
...	...	...	...	...
...	...	...	...	...
n_sections_ray	$Y_n$	$Y_n$	...	$Y_n$

*emission\_radiation*: Energy emitted by every boundary line of every particle ( $W$ ).

<b>Boundary line</b>	<b>Particle 1</b>	<b>Particle 2</b>	<b>...</b>	<b>Particle n_particles</b>
1	<i>emittedenergy</i>	<i>emittedenergy</i>	...	<i>emittedenergy</i>
2	<i>emittedenergy</i>	<i>emittedenergy</i>	...	<i>emittedenergy</i>
...	...	...	...	...
...	...	...	...	...
n_bars	<i>emittedenergy</i>	<i>emittedenergy</i>	...	<i>emittedenergy</i>

*particle\_intersections\_em*: For every particle, it stores: the number of the rays emitted by other particles that have been reflected on the studied particle, the number of the particles that emitted each one of said rays, the section of those rays at the moment they were reflected on the studied particle, the initial energy ( $W$ ) that those rays had when they were emitted, the boundary lines of the studied particle where they are reflected, and the number of reflections on the particles. Since it is not possible to know a priori how many rays emitted by other particles are going to be reflected on the surface of a particle, a big default value  $DV3$  defined by the user is used to establish the size of the matrix. This way, the matrix *particle\_intersections\_em* will be able to store a total of  $DV3$  reflections of rays emitted by other particles on the surface of every particle.

	<b>Ray number</b>	<b>Emitting particle number</b>	<b>Section number of the ray</b>	<b>Initial energy of the ray</b>	<b>Affected boundary line number</b>	<b>Number of reflections on the particles</b>
1	$r.number$	$p.number$	$s.number$	$energy$	$b.l.number$	$refl.number$
2	$r.number$	$p.number$	$s.number$	$energy$	$b.l.number$	$refl.number$
...	$r.number$	$p.number$	$s.number$	$energy$	$b.l.number$	$refl.number$
...	$r.number$	$p.number$	$s.number$	$energy$	$b.l.number$	$refl.number$
DV3	$r.number$	$p.number$	$s.number$	$energy$	$b.l.number$	$refl.number$

*indices*: Positions (rows) where the studied ray is reflected on the studied particle.

*emission\_radiation\_incident*: Energy absorbed by every boundary line of every particle coming from other particles' emission ( $W$ ).

<b>Boundary line</b>	<b>Particle 1</b>	<b>Particle 2</b>	<b>...</b>	<b>Particle n_particles</b>
1	$absorbedenergy$	$absorbedenergy$	...	$absorbedenergy$
2	$absorbedenergy$	$absorbedenergy$	...	$absorbedenergy$
...	...	...	...	...
...	...	...	...	...
n_bars	$absorbedenergy$	$absorbedenergy$	...	$absorbedenergy$

## Part 5.2: Heat Transfer resolution with the FEM

### Parameters

*scheme*: Input value. Number that establishes the resolution scheme used (1: Implicit, 0: Explicit, 0.5: Crank Nicholson).

*n\_ray\_sets*: Input value. Number of times that a new set of incoming solar rays is simulated.

*dt*: Input value. Time step value.

*nsteps*: Input value. Number of time steps.

*node\_number*: Boundary node closest to the reflection point.

*line\_change\_BC*: Boundary line these nodes belong to in this particle.

*ndle*: Input value. Number of nodes per triangular element.

*inel*: Input value. Number of nodes of the studied element (the default value is 2, which is the number of nodes for the line elements).

*itype*: Type of element (1:Boundary line with Neumann BC, 2:Boundary line with Cauchy BC, 3:Triangular element).

*iclass*: Number that specifies the boundary condition that will be applied (1 or 2).

*vres*: Residue for time control.

*vdu*: Incremental solution.

*nres*: Euclidean norm of vector vres.

*time*: Time of the studied iteration (s).

## Matrices

*n\_BC\_matrix*: Numbers assigned to every node in every particle that will be used to implement in them their corresponding boundary conditions. For the nodes in the boundary, 11 means that no ray has hit its surrounding boundary line, and 12 means and one or more rays have. For the nodes in the interior of the particle, this number will always be 31, and is used to obtain the material properties stored in other part of the program. The election of these numbers is due to the fact that the original code for the FEM resolution for heat transfer belongs to Emmanuel Lefrançois from the Université de Technologie de Compiègne, and he used them to assign different boundary conditions and material properties to the solids of study. To learn more information about the reasons why, the user should look for his original code.

Node number	Particle 1	Particle 2	...	Particle n_particles
1	<i>assignednumber</i>	<i>assignednumber</i>	...	<i>assignednumber</i>
2	<i>assignednumber</i>	<i>assignednumber</i>	...	<i>assignednumber</i>
...	...	...	...	...
...	...	...	...	...
nnt	<i>assignednumber</i>	<i>assignednumber</i>	...	<i>assignednumber</i>

*vkg\_particles*: Global rigidity (conductivity) matrix of every particle. Its size is  $nnt \times nnt \times n\_particles$ .

*vmg\_particles*: Global mass matrix of every particle. Its size is  $nnt \times nnt \times n\_particles$ .

*vfg\_particles*: Global sollicitation vector of every particle. Its size is  $nnt \times 1 \times n\_particles$ .

*incident\_sun*: Total solar energy that incides in every boundary line of every particle ( $W$ ).

Boundary line	Particle 1	Particle 2	...	Particle n_particles
1	<i>incidentenergy</i>	<i>incidentenergy</i>	...	<i>incidentenergy</i>
2	<i>incidentenergy</i>	<i>incidentenergy</i>	...	<i>incidentenergy</i>
...	...	...	...	...
...	...	...	...	...
n_bars	<i>incidentenergy</i>	<i>incidentenergy</i>	...	<i>incidentenergy</i>

*vkg*: Global rigidity (conductivity) matrix of the studied particle. Its size is  $nnt \times nnt$ .

*vmg*: Global mass matrix of the studied particle. Its size is  $nnt \times nnt$ .

*vfg*: Global sollicitation vector of the studied particle. Its size is  $nnt \times 1$ .

*kloce*: Localization table for the degrees of freedom of the studied element.

*vcore*: X and Y coordinates of the studied element.

*vkt*: Tangent matrix. Its size is  $nnt \times nnt \times n\_particles$ .

*vsol\_stored*: Stores the temperature of the nodes of every particle every 10 timesteps

.

## **APPENDIX**

### **B - Main script of the MATLAB code**

## B - Main script of the MATLAB code

```

1  clc
2  clear all
3  close all
4
5  % Code by:
6  % Copyright (c) 2017
7  % Marta Mu oz M nguez
8  % Volunteer Staff at SDSU, student at University of Valladolid
9
10 % This code simulates the transient heating process of the particles inside
11 % a Falling Particle Receiver. A Monte Carlo Ray Tracing Method is used to
12 % model radiation to and from a polydisperse particle phase, and a Finite
13 % Element Method is used for the simulation of conduction heat transfer
14 % inside the particles.
15
16 % The code has been divided in five parts:
17 % Part 1: Generation of randomly located particles with different radii
18 % Part 2: Relocation of the generated particles to the axes of interest
19 % Part 3: Generation of a mesh inside the particles
20 % Part 4: Initial Solution
21 % Part 5: Heat transfer in the particles
22 %   Part 5.1: Generation of random rays and their reflections
23 %   Part 5.2: Heat Transfer resolution with the FEM
24
25
26 %=====
27 % THE USER MUST DEFINE THE FOLLOWING PARAMETERS:
28 %=====
29
30 %=====
31 % GENERAL PARAMETERS
32 %=====
33
34 solar_flux      = 600000; % W/m^2
35 n_sections_ray = 1;      % Maximum number of sections allowed for each ray
36 s_b             = 5.670373*10e 8; % Stefan Boltzmann constant [W/m^2 K ^4]
37
38 % Material properties
39 e               = 0.843;   % Emissivity
40 absp            = 0.934;   % Absorptivity
41 k               = 2;      % Conductivity [W/ m K ]
42 dens           = 3550;    % Density [kg/m^3]
43 cp             = 760;     % Specific heat [J/ kg K ]
44
45 %=====
46 % INPUT PARAMETERS FOR
47 % PART 1  GENERATION OF RANDOMLY LOCATED PARTICLES WITH DIFFERENT RADII
48 %=====

```



```

49
50 % Choice of the target planar void ratio on the region of the particles
51 target_planar_void_ratio = 99;
52
53 % Choice of the maximum and minimum radius desires in the particles
54 % generated in mm
55 max_radius = 0.35; % mm
56 min_radius = 0.5e 3; % mm
57 %=====
58 % INPUT PARAMETERS FOR
59 % PART 4 INITIAL SOLUTION
60 %=====
61
62 % From all the particles initially generated in the area X:[0 0.030]
63 % Y:[0 0.050], the user can chose to model the heat transfer process only
64 % in the particles located in a smaller region of this area.
65
66 % This is recommended because solving the problem for all the particles
67 % would require too much computational time.
68
69 % Choice of the smaller region where particles will be studied , inside the
70 % area X:[0 0.030] Y:[0 0.050]
71 xmin_area = 0;
72 xmax_area = 0.005;
73 ymin_area = 0;
74 ymax_area = 0.005;
75
76 % Region that will be plotted. It is recommended to choose an area slightly
77 % bigger than the one defined above.
78 xaxismin_area = 0.0030;
79 xaxismax_area = 0.008;
80 yaxismin_area = 0.0005;
81 yaxismax_area = 0.0055;
82
83 initial_temperature = 20; %Initial temperature of the particles [ C ]
84
85 distance_window_curtain = 0; % This number determines where the position of
86 % the window in both Figures 1 and 2
87 %=====
88 % INPUT PARAMETERS FOR
89 % PART 5 HEAT TRANSFER IN THE PARTICLES
90 %=====
91
92 % PART 5.1 GENERATION OF RANDOM RAYS AND THEIR REFLECTIONS
93
94 % Section of the window where solar rays are simulated
95 % (Parameters to define the origin and destination of the rays)
96
97 xorig = 0 distance_window_curtain;
98 xdest = 0.0075; % This number determines the position of the back
99 yorigmin = 0.010; % wall in Figure 2
100 yorigmax = 0.015;
101 dy = 0.00005; % Distance between rays in the window
102 ydestmax = 0.035;

```

```

103 ydestmin      = 0.030;
104
105 % PART 5.2    HEAT TRANSFER RESOLUTION WITH THE FEM
106
107 scheme        = 1;          % Resolution squeme(1:Implicit,0:Explicit,
108 n_ray_sets    = 3;          % 0.5:Crank Nicholson)
109 dt            = 0.027;
110 nsteps        = 10;
111
112 %=====
113 % END OF INPUT PARAMETERS
114 %=====
115
116 %%
117
118 %=====
119 % PART 1     GENERATION OF RANDOMLY LOCATED PARTICLES WITH DIFFERENT RADII
120 %=====
121
122 % Code by:
123 % Copyright (c) 2017
124 % Marta Mu oz M nguez
125 % Volunteer Staff at SDSU, student at University of Valladolid
126
127 % This PART 1 is mainly based on the original code by:
128 % The MIT License (MIT)
129 % Copyright (c) 2016
130 % Andrea Chiarelli , Andrew Dawson, Alvaro Garcia
131 % The University of Nottingham
132
133 % Permission is hereby granted, free of charge, to any person obtaining a
134 % copy of this software and associated documentation files (the "Software"),
135 % to deal in the Software without restriction, including without limitation
136 % the rights to use, copy, modify, merge, publish, distribute, sublicense,
137 % and/or sell copies of the Software, and to permit persons to whom the
138 % Software is furnished to do so, subject to the following conditions:
139 % The above copyright notice and this permission notice shall be included
140 % in all copies or substantial portions of the Software.
141
142 % THE SOFTWARE IS PROVIDED "AS IS", WITHOUT WARRANTY OF ANY KIND, EXPRESS
143 % OR IMPLIED, INCLUDING BUT NOT LIMITED TO THE WARRANTIES OF
144 % MERCHANTABILITY, FITNESS FOR A PARTICULAR PURPOSE AND NONINFRINGEMENT.
145 % IN NO EVENT SHALL THE AUTHORS OR COPYRIGHT HOLDERS BE LIABLE FOR ANY
146 % CLAIM, DAMAGES OR OTHER LIABILITY, WHETHER IN AN ACTION OF CONTRACT, TORT
147 % OR OTHERWISE, ARISING FROM, OUT OF OR IN CONNECTION WITH THE SOFTWARE OR
148 % THE USE OR OTHER DEALINGS IN THE SOFTWARE.
149
150 %
151
152 % THE USER MUST NOT CHANGE THE FOLLOWING PARAMETERS:
153
154 % Region where the particles are initially generated      Figure 1
155 xorigmin_part = 0;
156 xorigmax_part = 0.030;

```

```

157 yorigmin_part = xorigmin_part;
158 yorigmax_part = 0.050;
159 % xorigmin_part and yorigmin_part must be equal
160
161 % Region plotted initially Figure 1
162 xaxismin      = 0.0025;
163 xaxismax      = 0.030; % This number also determines the position of the
164 yaxismin      = 0;      % back wall in Figure 1
165 yaxismax      = 0.050;
166
167 desired_width  = abs(xorigmax_part - xorigmin_part);
168 desired_height = abs(yorigmax_part - yorigmin_part);
169 factor         = desired_height/desired_width;
170
171 origin_of_cartesian_axes = 0;
172 rectangle_width  = 3;
173 rectangle_height = factor*rectangle_width;
174
175 xmin_generation = origin_of_cartesian_axes;
176 xmax_generation = xmin_generation + rectangle_width;
177 xmed_generation = (xmin_generation + xmax_generation)/2;
178
179 ymin_generation = origin_of_cartesian_axes;
180 ymax_generation = ymin_generation + rectangle_height;
181 ymed_generation = (ymin_generation + ymax_generation)/2;
182
183 %                INPUT VARIABLES INITIALIZATION (START)                %
184 number_of_particles      = 2;
185 new_particles_per_generation = 2;
186 maximum_radius          = max_radius/10;%This parameter is in meters
187 minimum_radius_seeded   = min_radius/10;%This parameter is in meters
188 %                INPUT VARIABLES INITIALIZATION (END)                %
189
190 % Generation of a vector of radii , one row for each particle
191 radius = minimum_radius_seeded*ones(number_of_particles,1);
192 % Generation of the centres with random positions , one row for particle
193 centre(:,1) = minimum_radius_seeded+(rectangle_width 2* ...
194             minimum_radius_seeded)*rand(number_of_particles,1);
195 centre(:,2) = minimum_radius_seeded+(rectangle_height 2* ...
196             minimum_radius_seeded)*rand(number_of_particles,1);
197 % Generation of the angle for the equation for parametric circumferences
198 angles_for_parametric_circle = 0:0.01:2*pi;
199 % Initialisation of the first generation of particles
200 x_coordinates_circles = zeros(length(angles_for_parametric_circle), ...
201                               number_of_particles);
202 y_coordinates_circles = x_coordinates_circles;
203 % Counter for later use
204 counter = number_of_particles;
205 % Beginning of the packing process
206 iteration = 2;
207 planar_void_ratio(2) = 100; % This needs to start at 2 because in the
208     %loops below it compares the current void ratio to its previous value
209
210 while planar_void_ratio(iteration)~=planar_void_ratio(iteration - 1) && ...

```

```

211         planar_void_ratio(iteration)>target_planar_void_ratio
212 iteration = iteration+1;
213 for k=1:number_of_particles
214     % Condition 1: Is the distance between particle k and all other
215     % particles smaller than the sum of their radii plus the minimum
216     % radius growth? This must return 1, because in order to grow this
217     % condition must be 0 when particle k is compared to all other
218     % particles but when it will be compared to itself the result will
219     % be 1.
220     condition(1) = sum(sqrt((centre(:,1)-centre(k,1)).^2+(centre(:,2)-
221         centre(k,2)).^2)<(radius(k)+minimum_radius_seeded+radius));
222     % Conditions 2-5: If the radius grows by 'minimum_radius_seeded',
223     % will it still be inside the rectangle defined above?
224     condition(2) = (centre(k,1)+radius(k)+minimum_radius_seeded<
225         ...
226         rectangle_width);
227     condition(3) = (centre(k,1)-radius(k)-minimum_radius_seeded>
228         ...
229         origin_of_cartesian_axes);
230     condition(4) = (centre(k,2)+radius(k)+minimum_radius_seeded<
231         ...
232         rectangle_height);
233     condition(5) = (centre(k,2)-radius(k)-minimum_radius_seeded>
234         ...
235         origin_of_cartesian_axes);
236     % Condition 6: If the radius grows by 'minimum_radius_seeded', will
237     % it still be smaller than the maximum radius allowed?
238     condition(6) = (radius(k)+minimum_radius_seeded<=maximum_radius);
239     % Logical condition: if all the conditions above are true (=1), the
240     % particle k is allowed to grow
241     can_it_grow = condition(1)==1 && condition(2)==1 &&
242         ...
243         condition(3)==1 && condition(4)==1 &&
244         ...
245         && condition(5)==1 && condition(6)==1 ;
246     % The radius of particle k is increased by 'minimum_radius_seeded'
247     if can_it_grow==1
248         radius(k)=radius(k)+minimum_radius_seeded;
249         x_coordinates_circles(:,k)=radius(k).*
250             ...
251             cos(angles_for_parametric_circle)+centre(k,1);
252         y_coordinates_circles(:,k)=radius(k).*
253             ...
254             sin(angles_for_parametric_circle)+centre(k,2);
255     end
256 end
257 % The planar void ratio is calculated for the current iteration
258 squared_sum_of_radii = sum(radius(1:number_of_particles).^2);
259 planar_void_ratio(iteration) = (rectangle_width*rectangle_height
260     ...
261     pi*squared_sum_of_radii)/(rectangle_width*rectangle_height)*100;
262 % If the planar void ratio is lower than the target the calculation
263 % must stop
264 if planar_void_ratio(iteration)<target_planar_void_ratio
265     quit_the_calculation = 1; % If this is equal to 1, the algorithm is
266     break % stopped
267 end
268 quit_the_calculation = 0;
269 end
270 % From now on, new generation of particles are created and added.
271 % When the planar void ratio drops below certain values, it is
272 % best to seed more particles per generation than the default value.
273 % This is done to have a better chance that they will fall in empty space.

```

```

265 increase_particles_per_generation = 0;
266 % In the 'if' conditions below this is increased to 1 and then 2 and 3
267 % just so that the increase in 'new_particles_per_generation' happens
268 % only once at each planar void ration mentioned
269 while planar_void_ratio(iteration)>target_planar_void_ratio && ...
270                                     quit_the_calculation==0
271     i_new_generation = counter;
272     if planar_void_ratio(iteration)<35 && ...
273         increase_particles_per_generation==0
274         new_particles_per_generation=new_particles_per_generation+1000;
275         increase_particles_per_generation = 1;
276     end
277     if planar_void_ratio(iteration)<25 && ...
278         increase_particles_per_generation==1
279         new_particles_per_generation=new_particles_per_generation+5000;
280         increase_particles_per_generation = 2;
281     end
282     if planar_void_ratio(iteration)<15 && ...
283         increase_particles_per_generation==2
284         new_particles_per_generation=new_particles_per_generation+10000;
285         increase_particles_per_generation = 3;
286     end
287 % The next condition avoids that no new generation of particles is empty
288 while counter == i_new_generation
289     for q=i_new_generation+1: ...
290         i_new_generation+new_particles_per_generation
291         % A new particle is initialised
292         centre(q,1) = minimum_radius_seeded+(rectangle_width ...
293             2*minimum_radius_seeded)*rand;
294         centre(q,2) = minimum_radius_seeded+(rectangle_height ...
295             2*minimum_radius_seeded)*rand;
296         radius(q) = minimum_radius_seeded;
297         % Is the particle acceptable? If yes, it is added to the vectors of
298         % centres and radii
299         if sum(sqrt((centre(:,1)-centre(q,1)).^2+(centre(:,2)-
300             centre(q,2)).^2)<(radius(q)+minimum_radius_seeded+radius))')==1
301             counter = counter+1;
302             centre(counter,:) = centre(q,:);
303             radius(counter) = radius(q);
304         end
305     end
306 end
307
308 % The vectors of centres and radii are cleaned from the unused values
309 centre(counter+1:end,:) = [];
310 radius(counter+1:end) = [];
311 iteration = iteration+1;
312 % This is re initialised due to the counters used below
313 planar_void_ratio(iteration) = 100;
314
315 while planar_void_ratio(iteration)~=planar_void_ratio(iteration 1) ...
316                                     && quit_the_calculation==0
317     iteration = iteration+1;
318     for k = i_new_generation+1:counter

```

```

319 % For the meaning of these conditions see above.
320 condition(1) = sum(sqrt((centre(:,1) - centre(k,1)).^2+ ...
321 (centre(:,2) - centre(k,2)).^2)<(radius(k)+ ...
322 minimum_radius_seeded+radius));
323 condition(2) = (centre(k,1)+radius(k)+minimum_radius_seeded< ...
324 rectangle_width);
325 condition(3) = (centre(k,1) - radius(k) - minimum_radius_seeded> ...
326 origin_of_cartesian_axes);
327 condition(4) = (centre(k,2)+radius(k)+minimum_radius_seeded< ...
328 rectangle_height);
329 condition(5) = (centre(k,2) - radius(k) - minimum_radius_seeded> ...
330 origin_of_cartesian_axes);
331 condition(6) = (radius(k)+minimum_radius_seeded<=maximum_radius);
332
333 can_it_grow = condition(1)==1 && condition(2)==1 && ...
334 condition(3)==1 && condition(4)==1 ...
335 && condition(5)==1 && condition(6)==1;
336 if can_it_grow == 1
337     radius(k) = radius(k)+minimum_radius_seeded;
338 end
339 end
340 % The planar void ratio is calculated for the current iteration
341 squared_sum_of_radii = sum(radius(1:counter).^2);
342 planar_void_ratio(iteration) = (rectangle_width*rectangle_height ...
343 pi*squared_sum_of_radii)/(rectangle_width*rectangle_height)*100;
344
345 % If the planar void ratio is lower than the target the calculation
346 % must stop
347 if planar_void_ratio(iteration)<target_planar_void_ratio
348     quit_the_calculation = 1; % If this is equal to 1, the algorithm is
349     break % stopped
350 end
351 end
352 planar_void_ratio(end);
353 end
354 % The planar void ratio vector is saved as a simple number
355 planar_void_ratio = planar_void_ratio(end);
356 clear x_coordinates_circles y_coordinates_circles planar_void_ratio
357
358 n_particles = counter;
359 n_particles_initial = n_particles;
360 hold on
361
362 %%
363
364 %=====
365 % PART 2 RELOCATION OF THE GENERATED PARTICLES TO THE AXES OF INTEREST
366 %=====
367 % Code by:
368 % Copyright (c) 2017
369 % Marta Mu oz M nguez
370 % Volunteer Staff at SDSU, student at University of Valladolid
371
372 scale = 0.01; % 1 m becomes 1 cm, 1 cm becomes 0.1 mm

```

```

373 xmax          = xorigmax_part;
374 xmin          = xorigmin_part;
375 ymax          = yorigmax_part;
376 ymin          = yorigmin_part;
377 xmed          = (xmax+xmin)/2;
378 ymed          = (ymax+ymin)/2;
379 centre_initial = centre;
380 radius_initial = radius;
381 radius        = radius_initial*scale;
382
383 % Scallation of the centres to the axis of interest
384 for i = 1:n_particles_initial
385     if      xmin_generation<=centre_initial(i,1) && centre_initial(i,1)    ...
386           <=xmed_generation && ...
387           ymax_generation>=centre_initial(i,2) && centre_initial(i,2)    ...
388           >ymed_generation
389         % If the particle is in the quadrant 1:
390         centre(i,1) = (((xmed -xmin)/xmed_generation)*centre_initial(i,1))+xmin;
391         centre(i,2) = (((ymax -ymed)/ymed_generation)*(centre_initial(i,2)    ...
392           ymed_generation))+ymed;
393
394     elseif  xmin_generation<=centre_initial(i,1) && centre_initial(i,1)    ...
395           <=xmed_generation && ...
396           ymed_generation>=centre_initial(i,2) && centre_initial(i,2)    ...
397           >=ymin_generation
398         % If the particle is in the quadrant 2:
399         centre(i,1) = (((xmed -xmin)/xmed_generation)*centre_initial(i,1))+xmin;
400         centre(i,2) = (((ymed -ymin)/ymed_generation)*centre_initial(i,2))+ymin;
401
402     elseif  xmax_generation>=centre_initial(i,1) && centre_initial(i,1)    ...
403           >xmed_generation && ...
404           ymed_generation>=centre_initial(i,2) && centre_initial(i,2)    ...
405           >=ymin_generation
406         % If the particle is in the quadrant 3:
407         centre(i,1) = (((xmax -xmed)/xmed_generation)*(centre_initial(i,1)    ...
408           xmed_generation))+xmed;
409         centre(i,2) = (((ymed -ymin)/ymed_generation)*centre_initial(i,2))+ymin;
410
411     elseif  xmax_generation>=centre_initial(i,1) && centre_initial(i,1)    ...
412           >xmed_generation && ...
413           ymax_generation>=centre_initial(i,2) && centre_initial(i,2)    ...
414           >ymed_generation
415         % If the particle is in the quadrant 4:
416         centre(i,1) = (((xmax -xmed)/xmed_generation)*(centre_initial(i,1)    ...
417           xmed_generation))+xmed;
418         centre(i,2) = (((ymax -ymed)/ymed_generation)*(centre_initial(i,2)    ...
419           ymed_generation))+ymed;
420     end
421 end
422
423 %%
424
425 %=====
426 % PART 3    GENERATION OF A MESH INSIDE THE PARTICLES

```

```

427 %=====
428 % Code by:
429 % Copyright (c) 2017
430 % Marta Mu oz M nguez
431 % Volunteer Staff at SDSU, student at University of Valladolid
432
433 %                Generic grid of radius R = 1 mm                %
434 % Data reading
435 datageneral_Gmsh
436
437 vcorg_stored    = zeros(nnt,2,n_particles_initial);
438 vcorg_original = vcorg;
439
440 % Relocation of the nodes considering the centers of the particles. The
441 % real size of the particles is not taken into account yet
442 for i=1:n_particles_initial
443     vcorg = [vcorg_original(:,1)+centre(i,1) vcorg_original(:,2)+centre(i,2)];
444     vcorg_stored(:, :, i) = vcorg;
445 end
446
447 % Scaling of the grid in each particle considering its real radius:
448 % relocation of the nodes to their final positions
449 r_1      = zeros(nnt,2);
450 r_2      = zeros(nnt,2);
451 vcorg_scaled = zeros(nnt,2,n_particles_initial);
452
453 for i=1:n_particles_initial
454     r_1(:,1) = vcorg_stored(:,1,i) - centre(i,1);
455     r_1(:,2) = vcorg_stored(:,2,i) - centre(i,2);
456
457     r_2      = r_1*(radius(i)/0.001);
458
459     vcorg_scaled(:,1,i) = r_2(:,1) + centre(i,1);
460     vcorg_scaled(:,2,i) = r_2(:,2) + centre(i,2);
461 end
462
463 % Plotting of the particles
464 for i=1:n_particles_initial
465     meshplot(vcorg_scaled(:, :, i),kconec)
466     hold on
467 end
468 axis ([ xaxismin xaxismax yaxismin yaxismax ])
469
470 % Information about the mesh
471 boundary_nodes      = kconec(find(kconec(:,3)==0),1:2);
472 boundary_nodes_vector = unique(boundary_nodes);
473 vcorg_scaled_boundary = zeros(max(size(boundary_nodes_vector)),2, ...
474                               n_particles_initial);
475 %Stores the coordinates of the nodes in the boundary
476 for p = 1:n_particles_initial
477     vcorg_scaled_boundary(:, :, p) = vcorg_scaled(boundary_nodes_vector, :, p);
478 end
479 n_bars      = numel(find(kconec(:,3)==0));
480 n_bn       = max(size(boundary_nodes_vector));

```



```

481 arc_length          = zeros(n_particles_initial,1);
482 for p=1:n_particles_initial
483     arc_length(p,1)=(2*pi*radius(p))/n_bars;
484 end
485
486 %%
487
488 %=====
489 % PART 4   INITIAL SOLUTION
490 %=====
491 % Code by:
492 % Copyright (c) 2017
493 % Marta Mu oz M nguez
494 % Volunteer Staff at SDSU, student at University of Valladolid
495
496 vsol = initial_temperature.*ones(ndlt,n_particles_initial);
497
498 % Plotting of the initial solution
499 % Initial solution for all the particles generated
500 figure(1)
501 for p=1:n_particles_initial
502     caxis([20 1200])
503     femplot(vcorg_scaled(:, :, p),kconec , vsol(:, p),1)
504     shading interp;
505     title_plot = ['Time: 0 s'];
506     title(title_plot)
507     colorbar
508
509 % This yellow line represents the window
510 rectangle(...
511     'Position',[0 distance_window_curtain ,yaxismin ,0.0001 ,...
512                                     abs(yaxismax yaxismin)], ...
513     'EdgeColor','y' ,...
514     'LineWidth', 1.5 ,...
515     'LineStyle',' ')
516
517 % This blue line represents the back wall
518 rectangle(...
519     'Position',[xaxismax ,yaxismin ,0.0001 ,abs(yaxismax yaxismin)] ,...
520     'EdgeColor','b' ,...
521     'LineWidth', 1.5 ,...
522     'LineStyle',' ')
523
524 % This red rectangle represents the area where heat transfer is modeled
525 rectangle(...
526     'Position',[xmin_area ,ymin_area ,abs(xmax_area xmin_area) ,...
527                                     abs(ymax_area ymin_area)] ,...
528     'EdgeColor','r' ,...
529     'LineWidth', 1.5 ,...
530     'LineStyle',' ')
531
532 set(gca , 'fontsize' ,16);
533 set(gca , 'FontName' , 'Times New Roman');
534 axis ([ xaxismin xaxismax yaxismin yaxismax ])

```

```

535 hold on
536 title(colorbar,'C')
537 xlabel('Depth (m)')
538 ylabel('Window length (m)')
539 end
540 time_previous_iteration = 0;
541
542 %           Selection of the particles inside the area of study           %
543
544 xmin_area_vector = xmin_area*ones(n_particles_initial,1);
545 xmax_area_vector = xmax_area*ones(n_particles_initial,1);
546 ymin_area_vector = ymin_area*ones(n_particles_initial,1);
547 ymax_area_vector = ymax_area*ones(n_particles_initial,1);
548
549 area_study_1      = [xmin_area_vector <= centre(:,1)  ymin_area_vector <=      ...
550                                centre(:,2)];
551 area_study_2      = [centre(:,1) <= xmax_area_vector  centre(:,2) <=      ...
552                                ymax_area_vector];
553 area_study_3      = [area_study_1(:,1)+area_study_2(:,1)      ...
554                                area_study_1(:,2)+area_study_2(:,2)];
555 area_study_4      = [area_study_3(:,1)+area_study_3(:,2)];
556
557 particles_area_study = find(area_study_4==4);
558
559 centre            = centre(particles_area_study,:);
560 n_particles        = size(centre,1);
561 radius            = radius(particles_area_study,:);
562 average_radius     = sum(radius)/n_particles;
563
564 vcorg_scaled      = vcorg_scaled(:, :, particles_area_study);
565 vsol              = initial_temperature .* ones(ndlt, n_particles);
566
567 % Initial solution only for the particles located in the area of study
568 figure(2)
569 for p=1:n_particles
570     caxis([20 1200])
571     femplot(vcorg_scaled(:, :, p), kconec, vsol(:, p), 1)
572     shading interp;
573     title_plot = ['Time: 0 s'];
574     title(title_plot)
575     colorbar
576
577 % This yellow line represents the window
578     rectangle(...
579         'Position',[xorig, yorigmin, 0.000001, abs(yorigmax - yorigmin)], ...
580         'EdgeColor','y', ...
581         'LineWidth', 1.5, ...
582         'LineStyle','')
583
584 % This blue line represents the back wall
585     rectangle(...
586         'Position',[xdest, ydestmin, 0.000001, abs(ydestmax - ydestmin)], ...
587         'EdgeColor','b', ...
588         'LineWidth', 1.5, ...

```

```

589     'LineStyle',' ')
590
591     set(gca,'fontsize',16);
592     set(gca,'FontName','Times New Roman');
593     hold on
594     title(colorbar,'C')
595     xlabel('Depth (m)')
596     ylabel('Window length (m)')
597     axis equal
598     axis ([ xaxismin_area xaxismax_area yaxismin_area yaxismax_area ])
599 end
600 time_previous_iteration = 0;
601 count_fig = 2;
602 %%
603
604 %=====
605 % PART 5   HEAT TRANSFER IN THE PARTICLES
606 %=====
607 % Code by:
608 % Copyright (c) 2017
609 % Marta Mu oz M nguez
610 % Volunteer Staff at SDSU, student at University of Valladolid
611
612 % The FEM resolution code was taken from
613 % E. Lefrancois UTC/2014
614
615 % GENERATION OF THE RAYS
616
617 % Rays' coordinates
618 % Origin points of solar rays
619 x1      = xorig;
620 y1      = yorigmax:dy:yorigmin;
621 n_rays  = length(y1);
622
623 % Destination points of solar rays
624 x2      = xdest;
625 y2      = ydestmax:dy:ydestmin;
626
627 %                               INPUT VARIABLES INITIALIZATION (START)           %
628 % Total energy emitted from the studied section of the window
629 flux_window = solar_flux*abs(yorigmax yorigmin); % W
630 flux        = flux_window/n_rays;
631 n_rays_em   = n_bn;
632
633 DV1         = 300;
634 DV2         = 500;
635 DV3         = 500;
636 DV4         = 100;
637 %                               INPUT VARIABLES INITIALIZATION (END)           %
638 average_temp = zeros(n_particles , n_ray_sets+1);
639 time_axis    = zeros(1 , n_ray_sets+1);
640 average_temp(:,1) = initial_temperature;
641 time_axis(1,1) = 0;
642

```

```

643
644 for set_rays=1:n_ray_sets
645 =====
646 % PART 5.1 GENERATION OF RANDOM RAYS AND THEIR REFLECTIONS
647 =====
648
649 % Solar rays generation (start) %
650 points_origin = zeros(n_rays,2);
651
652 for i=1:n_rays
653     points_origin(i,1) = x1;
654     points_origin(i,2) = y1(i);
655 end
656
657 points_destination = zeros(n_rays,2);
658
659 for i=1:n_rays
660     points_destination(i,1) = x2;
661     points_destination(i,2) = ydestmax (((ydestmax (ydestmin))/(1 0))* ...
662                                     (1 rand));
663 end
664
665 % Reflection of the rays in the particles
666 rays = ones(n_sections_ray,2,n_rays)*DV1;
667 true_xint = ones(n_sections_ray,n_rays)*DV1;
668 true_yint = ones(n_sections_ray,n_rays)*DV1;
669
670 ray_intersections = zeros(n_sections_ray,6,n_rays);
671
672 for i=1:n_rays % Runs ray by ray
673     prev_refl_in_part = 0;
674     n_wall_refl = 0;
675     for z=1:n_sections_ray % Runs all the reflections of one ray
676         xint = ones(n_particles,2)*DV2;
677         if z==1 %Initial section of the ray
678             % Deduction of the line equation
679             m1 = (points_destination(i,2) - points_origin(i,2))/ ...
680                 (points_destination(i,1) - points_origin(i,1));
681             n1 = (points_destination(i,1)*points_origin(i,2) ...
682                 - points_origin(i,1)*points_destination(i,2))/...
683                 (points_destination(i,1) - points_origin(i,1));
684             rays(z,1,i) = m1;
685             rays(z,2,i) = n1;
686         else
687             m1 = rays(z,1,i); % Already stored, in the previous iteration of z
688             n1 = rays(z,2,i);
689         end
690
691         for j=1:n_particles % Runs particle by particle
692             a = centre(j,1);
693             b = centre(j,2);
694             r = radius(j,1);
695             % Calculation of the intersection points with each particle
696             xint(j,1) = ( sqrt( a^2*m1^2 + 2*a*b*m1 - 2*a*m1*n1 - b^2 + ...

```

```

697         2*b*n1 + m1^2*r^2    n1^2 + r^2)+a+b*m1 m1*n1)/(m1^2+1);
698     xint(j,2) = (sqrt( a^2*m1^2 + 2*a*b*m1    2*a*m1*n1    b^2 + ...
699         2*b*n1 + m1^2*r^2    n1^2 + r^2)+a+b*m1 m1*n1)/(m1^2+1);
700     end
701
702     XX = ones(n_particles ,2)*DV2;
703
704     for h=1:n_particles
705         real_1 = isreal(xint(h,1));
706         if real_1 == 1
707             XX(h,1)= xint(h,1);
708         end
709         real_2 = isreal(xint(h,2));
710         if real_2 == 1
711             XX(h,2)= xint(h,2);
712         end
713     end
714
715     YY = ones(n_particles ,2)*DV2;
716
717     for u=1:n_particles
718         if XX(u,1)~= DV2
719             YY(u,1)= m1*XX(u,1)+n1;
720         end
721         if XX(u,2)~= DV2
722             YY(u,2)= m1*XX(u,2)+n1;
723         end
724     end
725     for p=1:n_particles
726         if YY(p,1)==DV2
727             XX(p,1)=DV2;
728         end
729         if YY(p,2)==DV2
730             XX(p,2)=DV2;
731         end
732     end
733
734     % This loop prevents the reflected rays to go through the particles
735     if prev_refl_in_part==1 && z~=1
736         if abs(XX(row_previous ,1) true_xint(z 1 ,i)) <= 0.0000000001
737             xreflection_point = XX(row_previous ,1);
738             yreflection_point = YY(row_previous ,1);
739             ximpossible_point = XX(row_previous ,2);
740             yimpossible_point = YY(row_previous ,2);
741         end
742         if abs(XX(row_previous ,2) true_xint(z 1 ,i)) <= 0.0000000001
743             xreflection_point = XX(row_previous ,2);
744             yreflection_point = YY(row_previous ,2);
745             ximpossible_point = XX(row_previous ,1);
746             yimpossible_point = YY(row_previous ,1);
747         end
748         if yreflection_point > yimpossible_point
749             % Points lower than yreflection_point are erased
750             for ii=1:n_particles

```

```

751         if YY(ii ,1) < yreflection_point
752             YY(ii ,1) = DV2;
753             XX(ii ,1) = DV2;
754         end
755         if YY(ii ,2) < yreflection_point
756             YY(ii ,2) = DV2;
757             XX(ii ,2) = DV2;
758         end
759     end
760 else % if yreflection_point < yimpossible_point
761     % Points higher than yreflection_point are erased
762     for ii=1:n_particles
763         if YY(ii ,1) > yreflection_point
764             YY(ii ,1) = DV2;
765             XX(ii ,1) = DV2;
766         end
767         if YY(ii ,2) > yreflection_point
768             YY(ii ,2) = DV2;
769             XX(ii ,2) = DV2;
770         end
771     end
772 end
773 % The intersections with the same particle that reflected the ray
774 % are erased
775 XX(row_previous ,1) = DV2;
776 XX(row_previous ,2) = DV2;
777 YY(row_previous ,1) = DV2;
778 YY(row_previous ,2) = DV2;
779 end
780
781 A = XX~=DV2;
782 B = A(:);
783 C = any(B); % If C=1: There are intersections with particles
784             % If C=0: There are no intersections , all the possible
785             %             ones were ideal
786 if C==1
787     if z==1
788         x_or = points_origin(i,1);
789         y_or = points_origin(i,2);
790     end
791     % If z>1, the origin of the ray will be the intersection point of
792     % the previous iteration of z
793     DD = ones(n_particles ,2)*DV2;
794     for s=1:n_particles
795         if XX(s,1)~= DV2
796             DD(s,1)= sqrt((abs(x_or - XX(s,1)))^2+(abs(y_or - YY(s,1)))^2);
797         end
798         if XX(s,2)~= DV2
799             DD(s,2)= sqrt((abs(x_or - XX(s,2)))^2+(abs(y_or - YY(s,2)))^2);
800         end
801     end
802
803     shortest_d = min(min(DD));
804     [row , col] = find(DD==shortest_d); % Position of the shortest

```

```

805     row_previous = row; % distance in matrix DD
806     xint_true = XX(row,col); % (row:particle intersected)
807     true_xint(z,i) = xint_true;
808     yint = m1*xint_true+n1;
809     true_yint(z,i) = yint;
810
811     ray_intersections(z,1,i) = row; % Stores the number of the
812                                     % particle intersected
813     ray_intersections(z,2,i) = xint_true; % Stores the X coordinate of
814                                     % the intersection
815     ray_intersections(z,3,i) = yint; % Stores the Y coordinate of
816                                     % the intersection
817     ray_intersections(z,4,i) = z; % Stores the number of the
818                                     % reflection
819     ray_intersections(z,5,i) = n_wall_refl;
820
821     ray_intersections(z,6,i) = ray_intersections(z,4,i) ...
822                                     ray_intersections(z,5,i);
823
824     x_or = xint_true; % This will be the origin of the ray for the
825     y_or = yint; % next iteration of z
826
827     a = centre(row,1);
828     b = centre(row,2);
829
830     % Generation of a random angle gamma in the range 0 180 degrees
831     gamma = pi*rand;
832
833     % Calculation of the angle alpha between the intersection point and
834     % a horizontal line that goes across the center of the circle
835     alpha = mod(atan2((yint - b),(xint_true - a)),2*pi);
836
837     beta = alpha - (pi/2);
838
839     % Calculation of the final random point that the ray will be
840     % reflected towards
841     k_length = 30; % This number must simply be high enough so that the
842                   % random point(x_r,y_r) is outside the area of study
843
844     x_r = xint_true + k_length*cos(gamma+beta);
845     y_r = yint + k_length*sin(gamma+beta);
846
847     % Line parameters for the equation of the reflected ray
848     m2 = (y_r - yint)/(x_r - xint_true);
849     n2 = (x_r*yint - xint_true*y_r)/(x_r - xint_true);
850
851     rays(z+1,1,i) = m2;
852     rays(z+1,2,i) = n2;
853
854     % Plotting of the rays (Postprocessing)
855     if z==1
856         plot([points_origin(i,1) true_xint(z,i)],[points_origin(i,2) ...
857                                                     true_yint(z,i)],'b')
858         hold on

```





```

913     x_or = x_wall; % This will be the origin of the ray for the
914     y_or = y_wall; % next iteration of z
915
916     gammal    = pi*rand;
917     beta1     = (pi/2);
918
919     % Calculation of the final random point that the ray will be
920     % reflected towards
921     k_length = 30; % This number must simply be high enough so that
922     % the random point(x_r,y_r) is outside the area of
923     % study
924     x_r = x_wall + k_length*cos(gammal+beta1);
925     y_r = y_wall + k_length*sin(gammal+beta1);
926
927     m2 = (y_r - y_wall)/(x_r - x_wall);
928     n2 = (x_r*y_wall - x_wall*y_r)/(x_r - x_wall);
929
930     rays(z+1,1,i) = m2;
931     rays(z+1,2,i) = n2;
932
933     plot([x_or_c0 x_wall],[y_or_c0 y_wall],'b')
934     hold on
935     prev_refl_in_part = 0;
936     elseif xdest_c0<xor_c0
937         plot([x_or_c0 xdest_c0],[y_or_c0 ydest_c0],'b')
938         hold on
939     end
940 end % from if C==1
941 if C==0 && xdest_c0<xor_c0 % If there is not a reflection , finish
942 % the corresponding ray
943     break
944 end
945 axis ([ xaxismin_area xaxismax_area yaxismin_area yaxismax_area ])
946 end
947 end
948 %                               Solar rays generation (end)                               %
949
950 % Storage of information about the solar rays reflections
951 particle_intersections = zeros(DV4,6,n_particles);
952 for p=1:n_particles
953     position = 0;
954     for j=1:n_rays
955         if find(ray_intersections(:,1,j)==p) % If the studied ray is
956 % reflected by the studied
957 % particle
958 [row,col] = find(ray_intersections(:,1,j)==p);
959 n_times = max(size(row));
960 for z = 1:max(size(row))
961     position = position+1;
962     particle_intersections(position,1,p) = j;
963     particle_intersections(position,2,p) = ...
964 % ray_intersections(row(z),2,j);
965     particle_intersections(position,3,p) = ...
966 % ray_intersections(row(z),3,j);

```

```

967     particle_intersections(position,4,p) = ...
968                                     ray_intersections(row(z),4,j);
969 % Storage of the distance from every boundary node to the
970 % intersection point
971     distance_to_intersection = zeros(n_bn,1);
972     for jj = 1:n_bn
973         distance_to_intersection(jj,1) = ...
974                                     sqrt((particle_intersections(position,2,p) ...
975                                     vcorg_scaled_boundary(jj,1,p))^2 + ...
976                                     (particle_intersections(position,3,p) ...
977                                     vcorg_scaled_boundary(jj,2,p))^2);
978     end
979 % Calculation of the two nodes closest to the reflection point:
980 % node_number1 and node_number2
981     [min_distance1, node_number1] = min(distance_to_intersection);
982     distance_to_intersection(node_number1) = Inf;
983     [min_distance2, node_number2] = min(distance_to_intersection);
984 % Finding of the boundary line where the reflection occurs
985     [roww, columnn] = find(boundary_nodes==node_number1);
986     if boundary_nodes(roww(1),columnn(2))==node_number2
987         particle_intersections(position,5,p) = roww(1);
988     elseif boundary_nodes(roww(2),columnn(1))==node_number2
989         particle_intersections(position,5,p) = roww(2);
990     end
991     particle_intersections(position,6,p) = ...
992                                     ray_intersections(row(z),6,j);
993     end
994 end
995 end
996 end
997
998 n_intersections = zeros(1,n_particles);
999
1000 for p=1:n_particles
1001     aux = size(find(particle_intersections(:,1,p)~=0));
1002     n_intersections(1,p) = aux(1,1);
1003 end
1004
1005 nrays_l_z = zeros(n_sections_ray, n_bars, n_particles);
1006
1007 for p=1:n_particles
1008     for line=1:n_bars
1009         for z=1:n_sections_ray
1010             n = z-1;
1011             %If that particle has an intersection in that line
1012             if sum(ismember(particle_intersections(:,5,p),line)~=0)
1013                 [row]=find(particle_intersections(:,5,p)==line);
1014                 contador=0;
1015                 for i=1:max(size(row))
1016                     if particle_intersections(row(i),6,p)==n
1017                         contador=contador+1;
1018                     end
1019                 end
1020                 nrays_l_z(z,line,p)=contador;

```

```

1021         end
1022     end
1023 end
1024 end
1025
1026 %                               Emitted rays generation (start)                               %
1027
1028 if set_rays ~=1
1029     rays_em          = ones(n_sections_ray ,2 ,n_rays_em , n_particles)*DVI;
1030     points_origin_em  = zeros(n_bn ,2 , n_particles);
1031     points_destination_em = zeros(n_bn ,2 , n_particles);
1032     for p=1:n_particles
1033         for i=1:n_bn
1034             node1    = boundary_nodes(i ,1);
1035             node2    = boundary_nodes(i ,2);
1036             x_node1  = vcorg_scaled(node1 ,1 ,p);
1037             y_node1  = vcorg_scaled(node1 ,2 ,p);
1038             x_node2  = vcorg_scaled(node2 ,1 ,p);
1039             y_node2  = vcorg_scaled(node2 ,2 ,p);
1040
1041             % Origin coordinates
1042             x_orig   = (x_node1+x_node2)/2;
1043             y_orig   = (y_node1+y_node2)/2;
1044
1045             points_origin_em(i ,1 ,p) = x_orig;
1046             points_origin_em(i ,2 ,p) = y_orig;
1047
1048             % Destination coordinates
1049             a = centre(p ,1);
1050             b = centre(p ,2);
1051             if x_orig > a
1052                 x_dest = xdest; %xdest=0.015
1053                 y_dest = ((x_dest - x_orig)/(a - x_orig))*(b - y_orig)+y_orig;
1054             elseif x_orig < a
1055                 x_dest = xdest;
1056                 y_dest = ((x_dest - x_orig)/(a - x_orig))*(b - y_orig)+y_orig;
1057             end
1058             if x_orig == a
1059                 if y_orig > b
1060                     y_dest = xdest;
1061                     x_dest = a;
1062                 elseif y_orig < b
1063                     y_dest = xdest;
1064                     x_dest = a;
1065                 end
1066             end
1067             points_destination_em(i ,1 ,p) = x_dest;
1068             points_destination_em(i ,2 ,p) = y_dest;
1069         end
1070     end
1071
1072     ray_intersections_em = zeros(n_sections_ray ,6 ,n_rays_em , n_particles);
1073
1074     for p=1:n_particles

```

```

1075 % Reflection of the rays in the particles
1076 true_xint_em = ones(n_sections_ray , n_rays_em)*DV1;
1077 true_yint_em = ones(n_sections_ray , n_rays_em)*DV1;
1078 for i=1:n_rays_em % Runs ray by ray from one particle
1079     prev_refl_in_part_em = 0;
1080     n_wall_refl_em = 0;
1081     for z=1:n_sections_ray % Runs all the reflections of one ray from
1082         % one particle
1083         xint = ones(n_particles ,2)*DV2; % Stores de values of all the
1084             % "intersections", real or ideal
1085         if z==1 %Initial section of the ray
1086             % Deduction of the line ecuation:
1087             m1 = (points_destination_em(i,2,p) points_origin_em(i,2,p))/...
1088                 ((points_destination_em(i,1,p) points_origin_em(i,1,p)));
1089             n1 = (points_destination_em(i,1,p)*points_origin_em(i,2,p) ...
1090                 points_origin_em(i,1,p)*points_destination_em(i,2,p))/...
1091                 (points_destination_em(i,1,p) points_origin_em(i,1,p));
1092             rays_em(z,1,i,p) = m1;
1093             rays_em(z,2,i,p) = n1;
1094         else
1095             m1 = rays_em(z,1,i,p); % Previously stored , in the previous
1096             n1 = rays_em(z,2,i,p); % iteration of z
1097         end
1098         for j=1:n_particles
1099             a = centre(j,1);
1100             b = centre(j,2);
1101             r = radius(j,1);
1102             % Calculation of the intersection points with each particle
1103             xint(j,1) = ( sqrt( a^2*m1^2 + 2*a*b*m1 2*a*m1*n1 b^2 + ...
1104                 2*b*n1 + m1^2*r^2 n1^2 + r^2)+a+b*m1 m1*n1)/(m1^2+1);
1105             xint(j,2) = ( sqrt( a^2*m1^2 + 2*a*b*m1 2*a*m1*n1 b^2 + ...
1106                 2*b*n1 + m1^2*r^2 n1^2 + r^2)+a+b*m1 m1*n1)/(m1^2+1);
1107         end
1108
1109         XX = ones(n_particles ,2)*DV2;
1110
1111         for h=1:n_particles
1112             real_1 = isreal(xint(h,1));
1113             if real_1 == 1
1114                 XX(h,1)= xint(h,1);
1115             end
1116             real_2 = isreal(xint(h,2));
1117             if real_2 == 1
1118                 XX(h,2)= xint(h,2);
1119             end
1120         end
1121
1122         YY = ones(n_particles ,2)*DV2;
1123
1124         for u=1:n_particles
1125             if XX(u,1)~= DV2
1126                 YY(u,1)= m1*XX(u,1)+n1;
1127             end
1128             if XX(u,2)~= DV2

```

```

1129         YY(u,2)= m1*XX(u,2)+n1;
1130     end
1131 end
1132 for q=1:n_particles
1133     if YY(q,1)==DV2
1134         XX(q,1)=DV2;
1135     end
1136     if YY(q,2)==DV2
1137         XX(q,2)=DV2;
1138     end
1139 end
1140 if z==1
1141     % points_origin_em(i,2,p) is Y from the origin of the emission
1142     if points_origin_em(i,2,p) > centre(p,2)
1143         % Points lower than yreflection_point are erased
1144         for ii=1:n_particles
1145             if YY(ii,1) < points_origin_em(i,2,p)
1146                 YY(ii,1) = DV2;
1147                 XX(ii,1) = DV2;
1148             end
1149             if YY(ii,2) < points_origin_em(i,2,p)
1150                 YY(ii,2) = DV2;
1151                 XX(ii,2) = DV2;
1152             end
1153         end
1154     elseif points_origin_em(i,2,p) < centre(p,2)
1155         % Points higher than yreflection_point are erased
1156         for ii=1:n_particles
1157             if YY(ii,1) > points_origin_em(i,2,p)
1158                 YY(ii,1) = DV2;
1159                 XX(ii,1) = DV2;
1160             end
1161             if YY(ii,2) > points_origin_em(i,2,p)
1162                 YY(ii,2) = DV2;
1163                 XX(ii,2) = DV2;
1164             end
1165         end
1166     end
1167     XX(p,1) = DV2; % The intersections with the particle that EMITS
1168     XX(p,2) = DV2; % the ray are erased (they are not possible)
1169     YY(p,1) = DV2;
1170     YY(p,2) = DV2;
1171 end
1172 % This loop prevents the reflected rays to go through the
1173 % particles
1174 if prev_refl_in_part_em==1 && z~=1
1175     if abs(XX(row_previous,1) true_xint_em(z 1,i)) <= 0.0000000001
1176         xreflection_point = XX(row_previous,1);
1177         yreflection_point = YY(row_previous,1);
1178         ximpossible_point = XX(row_previous,2);
1179         yimpossible_point = YY(row_previous,2);
1180     end
1181     if abs(XX(row_previous,2) true_xint_em(z 1,i)) <= 0.0000000001
1182         xreflection_point = XX(row_previous,2);

```

```

1183     yreflection_point = YY(row_previous ,2);
1184     ximpossible_point = XX(row_previous ,1);
1185     yimpossible_point = YY(row_previous ,1);
1186 end
1187 if yreflection_point > yimpossible_point
1188     % Points lower than yreflection_point are erased
1189     for ii=1:n_particles
1190         if YY(ii ,1) < yreflection_point
1191             YY(ii ,1) = DV2;
1192             XX(ii ,1) = DV2;
1193         end
1194         if YY(ii ,2) < yreflection_point
1195             YY(ii ,2) = DV2;
1196             XX(ii ,2) = DV2;
1197         end
1198     end
1199 elseif yreflection_point < yimpossible_point
1200     % Points higher than yreflection_point are erased
1201     for ii=1:n_particles
1202         if YY(ii ,1) > yreflection_point
1203             YY(ii ,1) = DV2;
1204             XX(ii ,1) = DV2;
1205         end
1206         if YY(ii ,2) > yreflection_point
1207             YY(ii ,2) = DV2;
1208             XX(ii ,2) = DV2;
1209         end
1210     end
1211 end
1212
1213     XX(row_previous ,1) = DV2; % The intersections with the particle
1214     XX(row_previous ,2) = DV2; % that reflects the ray are erased
1215     YY(row_previous ,1) = DV2; % (they are not possible)
1216     YY(row_previous ,2) = DV2;
1217 end
1218 A = XX~=DV2;
1219 B = A(:);
1220 C = any(B);
1221 if C==1
1222     if z==1
1223         x_or = points_origin_em(i ,1 ,p);
1224         y_or = points_origin_em(i ,2 ,p);
1225     end % If z>1, the origin will be the intersection point of the
1226         % previous iteration of z
1227     DD = ones(n_particles ,2)*DV2;
1228     for s=1:n_particles
1229         if XX(s ,1)~= DV2
1230             DD(s ,1)= sqrt((abs(x_or - XX(s ,1)))^2+(abs(y_or - YY(s ,1)))^2);
1231         end
1232         if XX(s ,2)~= DV2
1233             DD(s ,2)= sqrt((abs(x_or - XX(s ,2)))^2+(abs(y_or - YY(s ,2)))^2);
1234         end
1235     end
1236 end

```

```

1237     shortest_d      = min(min(DD));
1238     [row,col]       = find(DD==shortest_d);
1239     row_previous    = row;
1240
1241     xint_true       = XX(row,col);
1242     true_xint_em(z,i) = xint_true;
1243     yint            = m1*xint_true+n1;
1244     true_yint_em(z,i) = yint;
1245
1246     ray_intersections_em(z,1,i,p) = row;           % Stores the number
1247                                                    % of the particle
1248                                                    % intersected
1249     ray_intersections_em(z,2,i,p) = xint_true;     % Stores the
1250                                                    % X coordinate of
1251                                                    % the intersection
1252     ray_intersections_em(z,3,i,p) = yint;         % Stores the
1253                                                    % Y coordinate of
1254                                                    % the intersection
1255     ray_intersections_em(z,4,i,p) = z;           % Stores the section
1256                                                    % of the reflection
1257     ray_intersections_em(z,5,i,p) = n_wall_refl_em;
1258
1259     ray_intersections_em(z,6,i,p) = ...
1260         ray_intersections_em(z,4,i,p) ray_intersections_em(z,5,i,p);
1261
1262     x_or = xint_true;
1263     y_or = yint;
1264
1265     a     = centre(row,1);
1266     b     = centre(row,2);
1267
1268     % Generation of a random angle gamma in the range 0 180 degrees
1269     gamma = pi*rand;
1270     % Calculation of the angle alpha between the intersection point
1271     % and a horizontal line that goes across the center of the
1272     % circle
1273     alpha = mod(atan2(yint - b, xint_true - a), 2*pi);
1274
1275     beta = alpha - (pi/2);
1276
1277     % Calculation of the final random point that the ray will be
1278     % reflected towards
1279     x_r = xint_true + k_length*cos(gamma+beta);
1280     y_r = yint      + k_length*sin(gamma+beta);
1281
1282     % Line parameters for the equation of the reflected ray:
1283     m2 = (y_r - yint)/(x_r - xint_true);
1284     n2 = (x_r*yint - xint_true*y_r)/(x_r - xint_true);
1285
1286     rays_em(z+1,1,i,p) = m2;
1287     rays_em(z+1,2,i,p) = n2;
1288
1289     % Plotting of the rays
1290     if z==1

```

```

1291         plot([ points_origin_em(i,1,p) true_xint_em(z,i)], ...
1292              [points_origin_em(i,2,p) true_yint_em(z,i)], 'r')
1293     hold on
1294 else
1295     plot([ true_xint_em(z 1 ,i) true_xint_em(z,i)], ...
1296          [true_yint_em(z 1 ,i) true_yint_em(z,i)], 'r')
1297     hold on
1298 end
1299 prev_refl_in_part_em = 1;
1300 elseif C==0 % There is no intersection
1301     if z==1
1302         xor_c0_em = points_origin_em(i,1,p);
1303         yor_c0_em = points_origin_em(i,2,p);
1304         xdest_c0_em = points_destination_em(i,1,p);
1305         ydest_c0_em = points_destination_em(i,2,p);
1306     elseif z~=1
1307         xor_c0_em = true_xint_em(z 1 ,i);
1308         yor_c0_em = true_yint_em(z 1 ,i);
1309         if prev_refl_in_part_em==1
1310             if yreflection_point < yimpossible_point
1311                 ydest_c0_em = 0.030;
1312                 xdest_c0_em = (ydest_c0_em rays_em(z,2,i,p))/ ...
1313                             rays_em(z,1,i,p); %x=(y n)/m
1314             elseif yreflection_point > yimpossible_point
1315                 ydest_c0_em = 0.030;
1316                 xdest_c0_em = (ydest_c0_em rays_em(z,2,i,p))/ ...
1317                             rays_em(z,1,i,p); %x=(y n)/m
1318             end
1319             elseif prev_refl_in_part_em==0
1320                 xdest_c0_em = 0.030;
1321                 ydest_c0_em = rays_em(z,1,i,p)*xdest_c0_em+rays_em(z,2,i,p);
1322             end %y=mx+n
1323         end
1324     if xdest_c0_em>xor_c0_em
1325         x_wall = xdest;
1326         y_wall = rays_em(z,1,i,p)*x_wall + rays_em(z,2,i,p);
1327
1328         true_xint_em(z,i) = x_wall;
1329         true_yint_em(z,i) = y_wall;
1330
1331         ray_intersections_em(z,1,i,p) = 100; % Stores the number
1332                                             % of the particle
1333                                             % intersected (100:
1334                                             % reflection in wall)
1335         ray_intersections_em(z,2,i,p) = x_wall; % Stores the
1336                                             % X coordinate of the
1337                                             % intersection
1338         ray_intersections_em(z,3,i,p) = y_wall; % Stores the
1339                                             % Y coordinate of the
1340                                             % intersection
1341         ray_intersections_em(z,4,i,p) = z; % Stores the number
1342                                             % of the reflection
1343
1344         n_wall_refl_em = n_wall_refl_em+1; % Increase of 1 because

```



```

1345                                     % the reflection is in
1346                                     % the back wall
1347 ray_intersections_em(z,5,i,p) = n_wall_refl_em;
1348
1349 ray_intersections_em(z,6,i,p) = ...
1350 ray_intersections_em(z,4,i,p) ray_intersections_em(z,5,i,p);
1351
1352 x_or = x_wall; % This will be the origin of the ray for the
1353 y_or = y_wall; % next iteration of z
1354
1355 gamma1 = pi*rand;
1356 beta1 = (pi/2);
1357
1358 % Calculation of the final random point that the ray will be
1359 % reflected towards
1360 x_r = x_wall + k_length*cos(gamma1+beta1);
1361 y_r = y_wall + k_length*sin(gamma1+beta1);
1362
1363 m2 = (y_r - y_wall)/(x_r - x_wall);
1364 n2 = (x_r*y_wall - x_wall*y_r)/(x_r - x_wall);
1365
1366 rays_em(z+1,1,i,p) = m2;
1367 rays_em(z+1,2,i,p) = n2;
1368
1369 plot([xor_c0_em x_wall],[yor_c0_em y_wall], 'r')
1370 hold on
1371 prev_refl_in_part_em = 0;
1372 elseif xdest_c0_em < xor_c0_em
1373 plot([xor_c0_em xdest_c0_em],[yor_c0_em ydest_c0_em], 'r')
1374 hold on
1375 end
1376 end % from if C==1
1377
1378 if C==0 && xdest_c0_em < xor_c0_em % If there is not a reflection ,
1379 break % finish the corresponding ray
1380 end
1381 end
1382 end
1383 end
1384 axis ([ xaxismin_area xaxismax_area yaxismin_area yaxismax_area ])
1385
1386 % Calculation of the emitted energy
1387 emission_radiation = zeros(n_rays_em, n_particles);
1388 for p = 1:n_particles
1389 for i=1:n_bars
1390 node1 = boundary_nodes(i,1);
1391 node2 = boundary_nodes(i,2);
1392
1393 temp_node1 = vsol(node1,p);
1394 temp_node2 = vsol(node2,p);
1395
1396 temp_med_line = (temp_node1+temp_node2)/2;
1397
1398 emission_radiation(i,p) = e*s_b*(temp_med_line+273.15)^4;

```

```

1399     end
1400 end
1401
1402 % Storage of the emitted energy INCIDENT in the boundary lines
1403 particle_intersections_em = zeros(DV3,6,n_particles);
1404 for particle=1:n_particles % Studied particle
1405     counter = 0;
1406     for p=1:n_particles % Particle by particle , studying their emitted
1407         % rays
1408         for i=1:n_rays_em % Ray by ray emitted by the corresponding
1409             % particle
1410             % If the ray i emitted by particle p hits the particle "particle"
1411             if ismember(particle , ray_intersections_em(:,1,i,p))==1
1412                 indices = find(ray_intersections_em(:,1,i,p)==particle);
1413                 reps    = numel(find(ray_intersections_em(:,1,i,p)==particle));
1414                 for j=1:reps
1415                     counter = counter+1;
1416                     particle_intersections_em(counter,1,particle) = i;
1417                     particle_intersections_em(counter,2,particle) = p;
1418                     particle_intersections_em(counter,3,particle) = ...
1419                         ray_intersections_em(indices(j),4,i,p);
1420                     particle_intersections_em(counter,4,particle) = ...
1421                         emission_radiation(i,p)*arc_length(p,1); % W
1422
1423                     % Calculation of the affected boundary line
1424                     distance_to_intersection = zeros(n_bn,1);
1425                     x_int = ray_intersections_em(indices(j),2,i,p);
1426                     y_int = ray_intersections_em(indices(j),3,i,p);
1427
1428                     % Storage of the distance from every boundary node to the
1429                     % intersection point
1430                     for jj = 1:n_bn
1431                         distance_to_intersection(jj,1) = sqrt((x_int ...
1432                             vcorg_scaled_boundary(jj,1,p))^2 + (y_int ...
1433                             vcorg_scaled_boundary(jj,2,p))^2);
1434                     end
1435
1436                     % Calculation of the two nodes closest to the reflection
1437                     % point: node_number1 and node_number2
1438                     [min_distance1 , node_number1]= min(distance_to_intersection);
1439                     distance_to_intersection(node_number1) = Inf;
1440                     [min_distance2 , node_number2]= min(distance_to_intersection);
1441
1442                     % Finding of the boundary line where the reflection occurs
1443                     [row , column] = find(boundary_nodes==node_number1);
1444                     if boundary_nodes(row(1),column(2))==node_number2
1445                         particle_intersections_em(counter,5,particle)=row(1);
1446                     elseif boundary_nodes(row(2),column(1))==node_number2
1447                         particle_intersections_em(counter,5,particle)=row(2);
1448                     end
1449                     particle_intersections_em(counter,6,particle) = ...
1450                         ray_intersections_em(indices(j),6,i,p);
1451                 end
1452             end

```

```

1453     end
1454   end
1455 end
1456
1457 emission_radiation_incident = zeros(n_bars, n_particles);
1458 for p = 1:n_particles
1459   for i = 1:n_bars
1460     repetitions = numel(find(particle_intersections_em(:,5,p)==i));
1461     [row, column] = find(particle_intersections_em(:,5,p)==i);
1462     total_abs_em = 0;
1463     for j=1:repetitions
1464       ray_n = particle_intersections_em(row(j,1),1,p);
1465       part_n = particle_intersections_em(row(j,1),2,p);
1466       n = particle_intersections_em(row(j,1),6,p);
1467       abs_en = (particle_intersections_em(row(j,1),4,p)/
1468               ...
1469               arc_length(p,1))*e*((1 e)^n); % W/m^2
1470       total_abs_em = total_abs_em + abs_en;
1471     end
1472     emission_radiation_incident(i,p) = total_abs_em; % W/m^2
1473   end
1474 end
1475
1476 =====
1477 % PART 5.2 HEAT TRANSFER RESOLUTION WITH THE FEM
1478 =====
1479
1480 n_BC_matrix = zeros(nelt,1,n_particles);
1481 vkg_particles = zeros(ndlt,ndlt,n_particles);
1482 vmg_particles = zeros(ndlt,ndlt,n_particles);
1483 vfg_particles = zeros(ndlt,1,n_particles);
1484 incident_sun = zeros(n_bars,1,p);
1485
1486 for p = 1:n_particles
1487   n_BC_matrix(:, :, p) = n_BC;
1488 end
1489 if set_rays==1
1490   emission_radiation = zeros(n_rays_em, n_particles);
1491   emission_radiation_incident = zeros(n_bars, n_particles);
1492   particle_intersections_em = zeros(DV3,5, n_particles);
1493 end
1494
1495 % Change of the BC vector according to the rays reflections
1496 for p = 1:n_particles
1497   for i = 1:n_intersections(1,p)
1498     n_BC_matrix(particle_intersections(i,5,p),p) = 12;
1499   end
1500 end
1501
1502 % Assembling of vmg, vkg and vfg
1503 for p = 1:n_particles
1504   vkg = zeros(ndlt);
1505   vmg = zeros(ndlt);
1506   vfg = zeros(ndlt,1);

```

```

1507 ndle = 3;
1508 kloce= 0*(1:ndle);
1509
1510 for ie = 1:nelt
1511     inel = 2;
1512     itype = mod(floor(n_BC_matrix(ie ,1,p)/10),10); % Number of tens
1513     iclass = mod(floor(n_BC_matrix(ie ,1,p)),10); % Number of units
1514     if(itype == 3)
1515         inel = 3;
1516     end
1517     vcore = vcorg_scaled(kconec(ie , 1:inel) :,p);
1518     if ie<=n_bars
1519         for ii = 1:n_sections_ray
1520             n = ii - 1;
1521             incident_sun(ie ,1,p) = incident_sun(ie ,1,p) + ...
1522                                     nrays_l_z(ii ,ie ,p)*(1 - absp)^n;
1523         end
1524     end
1525     switch itype
1526     case 1
1527         data_boundaryconditions_lines
1528         vprel = vprel_Neumann(iclass ,:);
1529         barre_neumann;
1530     case 2
1531         data_boundaryconditions_lines
1532         vprel = vprel_Cauchy(iclass ,:);
1533         barre_cauchy;
1534     case 3
1535         data_boundaryconditions_triangles
1536         vprel = vprel_T3(iclass ,:);
1537         ther_T3;
1538     end
1539     kloce = [];
1540     for in = 1:inel
1541         kloce = [kloce ,(kconec(ie , in) - 1)*ndln+(1:ndln)];
1542     end
1543     % Assembling of vke
1544     vkg(kloce ,kloce) = vkg(kloce ,kloce) + vke;
1545     % Assembling of vme
1546     vmg(kloce ,kloce) = vmg(kloce ,kloce) + vme;
1547     % Assembling of vfe
1548     vfg(kloce ,1) = vfg(kloce ,1) + vfe;
1549     clearvars vcore
1550 end
1551 vkg_particles (: ,: ,p) = vkg;
1552 vmg_particles (: ,: ,p) = vmg;
1553 vfg_particles (: ,: ,p) = vfg;
1554 end
1555
1556 vkt = zeros(ndlt ,ndlt , n_particles);
1557 for p = 1:n_particles
1558     vkt (: ,: ,p) = vmg_particles (: ,: ,p) + (scheme*dt)*vkg_particles (: ,: ,p);
1559     vkt (: ,: ,p) = sparse(vkt (: ,: ,p)); % sparse
1560 end

```

```

1561
1562 vsol_stored = zeros(nnt,1,(nsteps/10),n_particles); % Stores the solution
1563 % every 10 timesteps
1564 for istep = 1:nsteps
1565     time = time_previous_iteration + istep*dt;
1566     for p = 1:n_particles
1567         vres = vfg_particles(:, :, p) - vkg_particles(:, :, p)*vsol(:, p);
1568         % Residue for time control
1569         vdu = vkt(:, :, p)\(dt*vres);
1570         vsol(:, p) = vsol(:, p) + vdu; % The solution is updated
1571
1572     end
1573     % Display of the solution every 10 timesteps
1574     if(mod(istep,10)==0)
1575         count_fig = count_fig + 1;
1576         figure(count_fig)
1577         for p = 1:n_particles
1578             vsol_stored(:, 1, istep/10, p) = vsol(:, p);
1579             caxis([20 500])
1580             femplot(vcorg_scaled(:, :, p), kconec, vsol_stored(:, :, istep/10, p), 1)
1581             shading interp;
1582             set(gca, 'fontSize', 16);
1583             set(gca, 'FontName', 'Times New Roman');
1584             title_plot = ['Time: ' num2str(time), ' s'];
1585             title(title_plot)
1586             colorbar
1587
1588             rectangle('Position',[xorig, yorigmin, 0.000001, ...
1589                 abs(yorigmax - yorigmin)], 'EdgeColor', 'y', 'LineWidth', 1.5, ...
1590                 'LineStyle', '')
1591
1592             rectangle('Position',[xdest, ydestmin, 0.000001, ...
1593                 abs(ydestmax - ydestmin)], 'EdgeColor', 'b', 'LineWidth', 1.5, ...
1594                 'LineStyle', '')
1595             hold on
1596             title(colorbar, ' C ')
1597             xlabel('Depth (m)')
1598             ylabel('Window length (m)')
1599             axis equal
1600             axis ([ xaxismin_area xaxismax_area yaxismin_area yaxismax_area ])
1601         end
1602         time_axis(1, set_rays+1) = time;
1603         for p=1:n_particles
1604             average_temp(p, set_rays+1) = sum(vsol(:, p))/nnt;
1605         end
1606     end
1607 end
1608 time_previous_iteration = time;
1609 end
1610
1611 [radius_ascend, indexes] = sort(radius);
1612 sorted_average_temp = average_temp(indexes, :);
1613 radius_ascend_mm = radius_ascend * 10^3;
1614

```

```
1615 figure(200)
1616 for p=1:n_particles
1617     title('Temporal evolution of the average temperature of the particles')
1618     xlabel('Time (s)') % x axis label
1619     ylabel('Temperature ( C)') % y axis label
1620     plot(time_axis ,sorted_average_temp(p,:))
1621
1622     hold on
1623 end
1624
1625 legend(strcat('r = ', num2str(radius_ascend_mm), ' mm'),'Location', ...
1626         'northwest')
```

\*Note: The symbols - have not been properly displayed.

